Studies on Photocatalysis by Nano Titania Modified with Non-Metals

Thesis Submitted to the
Cochin University of Science and Technology
in partial fulfillment of the requirements
for the award of the degree of
Doctor of Philosophy
in Chemistry
Under the Faculty of Science

By

Rajesh K. M.

Department of Applied Chemistry
Cochin University of Science and Technology
Cochin-682 022, Kerala, India.

May 2011

Department of Applied Chemistry
Cochin University of Science and Technology
Cochin – 682 022, Kerala, India.

Dr. S. Sugunan
Professor

Date :.....

Certificate

This is to certify that the research work presented in the thesis entitled **"Studies on Photocatalysis by Nano Titania Modified with Non-Metals"** is an authentic record of research work carried out by Mr. Rajesh K. M. under my supervision at the Department of Chemistry, Cochin University of Science and Technology, in partial fulfillment of the requirements for the degree of Doctor of Philosophy in Chemistry and that no part thereof has been included for the award of any other degree.

Dr. S. Sugunan
(Supervising Guide)

Declaration

I hereby declare that the thesis entitled **"Studies on Photocatalysis by Nano Titania Modified with Non-Metals"** is the bonafide report of the original work carried out by me under the supervision of Dr. S. Sugunan at the Department of Applied Chemistry, Cochin University of Science and Technology, and no part thereof has been included in any other thesis submitted previously for the award of any degree.

16-05-2011 **Rajesh K. M.**
Cochin-22

To My Family and Friends…

Acknowledgement

I begin my hearty gratitude towards God for his amazing grace of blessing in my life which cannot be expressed or limited to a single word. I am proud to express my warm and sincere gratitude to my guide, Prof. Dr. S. Sugunan, for his valuable guidance, supervision, strong motivation, advices and constant encouragement during the course of research work.

I am much indebted to Dr. K. Sreekumar, present HOD, Dr. K. Girish Kumar and Dr. M. R. Prathapachandra Kurup the former HODs for their timely help, support and co-operation during the period of this work. Dr. S. Prathapan deserves special thanks as my doctoral committee member. I also wish to express my sincere thanks to Dr. N. Manoj for his valuable suggestion in the area of my research work and extend my wishes to other faculty members for their supports and suggestions. I wish to express my thanks to the non-teaching staffs of the Department of Applied Chemistry for their valuable advices and assistance during the period of research.

I give my special thanks to my seniors and friends of CUSAT, especially Dr. Sanjay, Murukesan, Jayakumar for their valuable tips in the initial stage of my research work. I express my sincere gratitude to my labmates Ajitha miss, Joyes miss, Rosephilo miss, Bolie, Resmi, Ambili, Dhanya, Sathish, Jofrin, Temi, Reni, Cimi, Nissam, Mothi Krishnamohan, Soumini, Sandhya for their support, cooperation, advices and lovely discussions. I extend my thanks to friends of other labs and department of CUSAT.

I gratefully acknowledge to Dr. Babu Philip and Mr. Hari Sankar, Department of Marine Biology, Microbiology and Biochemistry, CUSAT in collaboration with antibacterial studies, Dr. Mrinal R. Pai and co-wrokers, BARC in collaboration with

water splitting reaction, Dr. K Tripathi and Dr. Jagannath, BARC in collaboration with XPS analysis.

I am thankful to the technical assistance by the staffs of STIC, CUSAT and SAIF IIT Chennai. I also express my special thanks to Leon Prasanth, IICT Hyderabad, Hanosh, Coir board, Arun, Robinson, Anoop, Maheshkumar, Jomon DAC, CUSAT and Aneesh DOP, CUSAT for their valuable help during the research period. I also gratefully acknowledged to Board of Research in Nuclear Science, BRNS for their financial support for this work.

I take this opportunity to convey my hearty thanks to all my teachers from my school days to post graduation level. Especially Dr. Ravi Divakaran for building up my research career in science. I wish to express my warm thanks to staffs from Chemistry and other department of S.N. College Kannur for their support and encouragement for completion of this research within the time bound. I would like to thank all the people who have directly or indirectly helped me in connection with my research. I express my apology that I could not mention personally one by one. Last not the least, my deepest gratitude goes to my family for their everlasting love and support throughout my life.

Rajesh K. M.

PREFACE

Chemical pollutants are harmful substances for human beings and for the environment. Conventional methods of water and air decontamination, even if effective, are often chemically, energetically and operationally intensive and suitable only for large systems; moreover, the residuals coming from intensive chemical treatments can add to the problems of contamination. Research and development on various systems and technologies have extensively been performed worldwide to find solutions for energy and environmental problems. Among this, Photocatalysis by semiconducting materials, an advanced oxidation processes developed in recent decades, has proven to be a promising technology for environmental remediation.

Photocatalysis is the catalysis of a spontaneous chemical reaction where light is required for the catalyst to function. A photocatalyst can transform light energy into chemical energy by creating strong oxidative and reductive species which greatly enhance the rate of the spontaneous reaction. Studies related to photocatalysis have increased immensely over the past few years and currently well over 1000 research papers are published annually. Titanium dioxide (TiO_2) is usually the material of choice for photocatalytic applications because it has been frequently found to possess the best activity and stability when compared to other materials. Buts its activity limited to UV irradiation based on bandgap. Lot of modification is still progressing to attain visible light irradiation with very high photocatalytic activity.

During the last years the main goal of research on photocatalysis was to find the best photocatalyst. This was pursued by trial and error methods. In present study we prepare a modified titania with nonmetal through tried a trail and error method to attain its application in visible light region. The prepared

catalysts are characterized by various techniques and correlated it with its activity. The visible light performance of the prepared catalysts is evaluated by degradation of some aqueous dyes and organic pollutants, production hydrogen through water splitting reaction and an antibacterial study.

This thesis is entitled as “Studies on photocatalysis by nano titania modified with non-metals" based on experimental work carried out during the years 2007-2011 in the laboratory of Department of Applied Chemistry, Cochin University of Science and Technology.

CONTENTS

…..ஜ۞ஜ…..

PAPERS PRESENTED IN INTERNATIONAL / NATIONAL CONFERENCES

- High visible light responsive modified nano titania for the degradation of Organic pollutants – RAJESH K. M. AND SUGUNAN S. (C-Tric 2011: National Seminar on Current Trends in Chemistry – Applied Chemistry, CUSAT, 4-5 March 2011).
- Photocatalytic degradation of herbicide monolinuron by nano crystalline NS co-doped titania: synthesis and characterization - RAJESH K. M. AND SUGUNAN S. (MATCON 2010: International Conference on Materials for the Millennium - Applied Chemistry, CUSAT, 11-13 January 2010).
- Photocatalysis by N and both N S co-doped nano titania on degradation of herbicide 2,4,5- trichlorophenoxyacetic acid - RAJESH K. M. AND SUGUNAN S. (APTChem 2009: - National Conference on Advances in Physical and Theoretical Chemistry - Department of Chemistry Calicut, 19- 20 March 2009).
- Synthesis of nano crystalline non-metal doped titania with high photocatalytic activity on dyes degradation – RAJESH K. M. AND SUGUNAN S. (Catsymp 19: Catalysis for sustainable Energy and Chemicals - NCL Pune, 18-21 January 2009).
- Photocatalytic degradation of Dyes by anion doped nano crystalline titania: Synthesis and Characteristation – RAJESH K. M. AND SUGUNAN S. (Cochin Nano 2009: Second International Conference on Frontiers in Nano science and Technology, Department of Physics CUSAT, 3-6 January, 2009).
- Sulphur and nitrogen co-doped nano crystalline titania with high photocatalytic activity – RAJESH K. M. AND SUGUNAN S. (7th National Seminar on Current Advances in Chemical Science -Sacred Heart College Thevara, kerala, 26- 27th November 2008).
- Photocatalytic degradation of herbicide 2.4-dichlorophenoxy acetic acid by nano crystalline non-metal doped titania – RAJESH K. M. AND SUGUNAN S. (Indian Analytical Science Congress 2008: Analytical Sciences for Substainable Development - Munnar, Kerala, 21-23 November 2008).
- Synthesis, characterization and photocatalytic activity of nitrogen doped titania – RAJESH K. M. AND SUGUNAN S. (CATWORKSHOP 2008 - National conference in catalysis - IMMT Bhubaneswar, 18- 20 February 2008)

WORKSHOP ATTENDED

- Orientation Programme in Catalysis Research held at National Centre for Catalysis Research, IIT Madras, December 2007.

…..ꕥ…..

Chapter 1

Photocatalysis by Titania - Introduction

Contents

Photocatalysis and related phenomena are now well known and well recognized. Recently the photo catalytic activity of material with titania and its modified forms become a leading compound due to the significant positive results on its major application in various fields. Few of them are solar cell efficient producer of electrical energy, environmental clean up – removal or degradation of organic pollutants, antimicrobial activity, energy production- hydrogen generation etc. (1). These facts are indicated by doubling or redoubling of scientific research papers on photo chemistry of titania based compounds on last decades (2).

The enormous efforts to the research on TiO_2 material begins with the discovery of photocatalytic splitting of water on a TiO_2 electrode under ultraviolet (UV) light by Fujishima and Honda in 1972. It led to many promising applications in the areas ranging from photovoltaics and photocatalysis to photo-/electrochromics and sensors. These applications can be roughly divided into "energy" and "environmental" categories. Many of them depend not only on the properties of TiO_2 material itself but also on the modifications of TiO_2 host material and its interaction with the environment (3).

1.1 Catalysis and Photocatalysis

Catalysis is the action of a catalyst on a reaction; and a catalyst is a substance that increases the rate of reaction without modifying the overall standard Gibbs energy change in the reaction. Catalysis was not a process which developed in recent years. It is a natural process associated with the beginning of life itself. The favorability of a catalytic reaction compared to other processes in the fact that it takes place at low temperature, gives highly selected targets of our interest, less expensive, easily controllable, environmentally clean etc.

Catalysis can be two types: homogeneous and heterogeneous. In homogeneous catalysis, reactant and catalyst are in the same phase. Acid base catalysis, enzyme catalysis etc. are examples of homogeneous catalysis. In heterogeneous catalysis reactant and catalyst are in the different phase. Catalysis by metals and semiconductors are examples. Here reactions occur at the interface between the phases.

The conversions of waste and raw materials into energy, reduction of green house gases, conversion of monomers into polymer, production of material from cheap source etc. are the key roles of catalyst. Thus there is a tremendous pressure exerted on chemical manufacturing industry to develop new synthetic methods that are environment friendly and more acceptable by the catalysis field for the production of economic products. Photocatalysis plays a key role in this situation.

In 1930 onwards the term “photocatalysis” was introduced and often used in the scientific literature. The IUPAC recommended definition for photocatalysis as “a catalytic reaction involving light absorption by a catalyst or a substrate”. Salomon in 1980s subdivided photocatalysis into two main classes: (i) photon generated catalysis, which is catalytic in photons and

(ii) catalyzed photolysis, which is non-catalytic in photons. In photo generated catalysis, ground states of the catalyst and the substrate are involved in the thermodynamically spontaneous (exoergic) catalytic step. By contrast, in catalyzed photolysis either the nominal catalyst or the substrate or both are in an excited state during the catalytic step (4).

A photocatalyst (or catalyst) is a solid material, need to satisfy the following events: (i) the molecule is adsorbed on the particle surface; (ii) the molecule undergoes chemical transformation while visiting several reaction surface sites by surface diffusion and (iii) the intermediate or product molecule is subsequently desorbed to the gas phase or to the condensed phase (5). The interactions between the reactant molecule and the photo catalyst's surface site must be such (not too strong or not too weak) that bond breaking and bond making can take place within the residence time of the intermediate(s), and that desorption/adsorption can occur.

There are two different approaches for photocatalysis. These are, (i) from chemistry to catalysis to photocatalysis (i.e. equation 1.1→ 1.2→ 1.4) and (ii) from chemistry to photochemistry to photocatalysis (i.e. equation 1.1→ 1.3→ 1.4). So we can define a photocatalysis based on these approaches. Thus in a broad sense, the term photocatalysis describes a photochemical process in which the photocatalyst accelerates the process, as any catalyst must do according to the definition of catalysis.

$$A \rightarrow B \quad \text{.....(1.1)}$$

$$A + \text{Catalyst} \rightarrow B + \text{Catalyst} \quad \text{.....(1.2)}$$

$$A + h\upsilon \rightarrow B \quad \text{.....(1.3)}$$

$$A + h\upsilon \ \text{Catalyst} \rightarrow B + \text{Catalyst} \quad \text{.....(1.4)}$$

The catalyst may accelerate the photoreaction by interacting with the substrate(s) either in its ground state or in its excited state or with the primary product (of the catalyst), depending on the mechanism of the photoreaction. Thus photocatalysis is a catalytic process occurring on the surface of semiconductor materials under the irradiation of light. Photocatalysis involves three processes: the excitation, bulk diffusion and surface transfer of photo induced charge carriers. These processes are influenced by the bulk structure, surface structure and electronic structure of the semiconductor photo catalysts (6).

1.2 Titania – a Semiconductor Photocatalyst

Semiconductors act as catalysts for many chemical reactions. Oxidation, hydrogenation, hydroxylation etc are examples. The catalytic properties of semiconductors are very closely related to the electronic processes occurring inside and on the surface of them. It is determined by its nature and electronic state. Impurities introduced into the semiconductors also influence the activity. Heterogeneous photo catalysis by semiconductors is an emerging field of study. The only difference of photo catalytic reaction with conventional catalysis is the mode of activation. In photocatalysis the thermal activation is replaced by photonic activation.

A question arises why the semiconducting materials acts as very good photo catalysts. The explanation is as follows, semiconductors are materials with conductivity between that of metals and insulators. Their band gap (E_{bg}), which is the energy gap between the valance band (highest occupied band) and conduction band (lowest unoccupied band), is between that of metals and insulators are shown in Fig. 1.1.

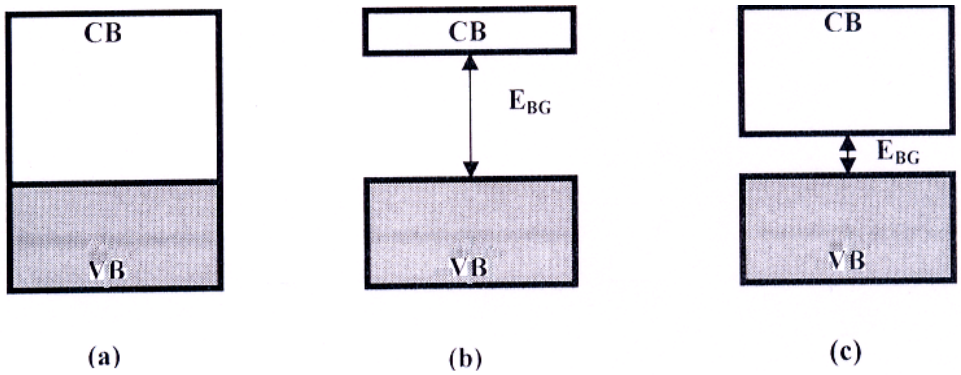

Fig.1.1. Band structure of (a) metals, (b) insulators and (c) semiconductors

A photocatalytic reaction proceeds through the excitation of electron from the valance band to conduction band by absorption of light. In metals the valance band and conduction bands are merged together, as a result there is no bandgap. So either reduction or oxidation happened depends upon band position. But insulators need a high energy for excitation process because the bandgap is very large. Thus, compared with metals and insulators, semiconducting materials act as vey good photocatalysts because of their medium band gap. There are lots of semiconducting materials available as photocatalyst. A few of them with band gap structure are shown in Fig. 1.2.

An ideal semiconductor photocatalyst should be chemically and biologically inert, photo catalytically active, non-photo corrode, easy to produce and use, activated by sunlight, environmentally and economically acceptable etc. It was surprisingly noted that, among the various semiconductors, none of them become an ideal photocatalyst by satisfying all conditions. Thus only a few of them are effectively termed as very good semiconductor photo catalysts. Titania becomes one such of candidate. Because it displays the features of an ideal semiconductor photocatalyst with the exception that it does not absorb visible light. The bandgap of titania is 3.2 eV, which corresponds to the UV range of electromagnetic spectrum. Thus the

activity of titania is limited to UV region, which is around 5-10% of solar spectrum. Despite this limitation, the other positive features to titania make it a prominent semiconductor material and widely studied in the field of semiconductor photochemistry. Most of the early works in semiconductor photocatalysis focused mainly on the photo mineralization of organics dissolved in aqueous solution and semiconductors are employed in the form of a powered dispersion. As a result, a number of commercial devices currently in market utilize titania in the form of powder dispersion.

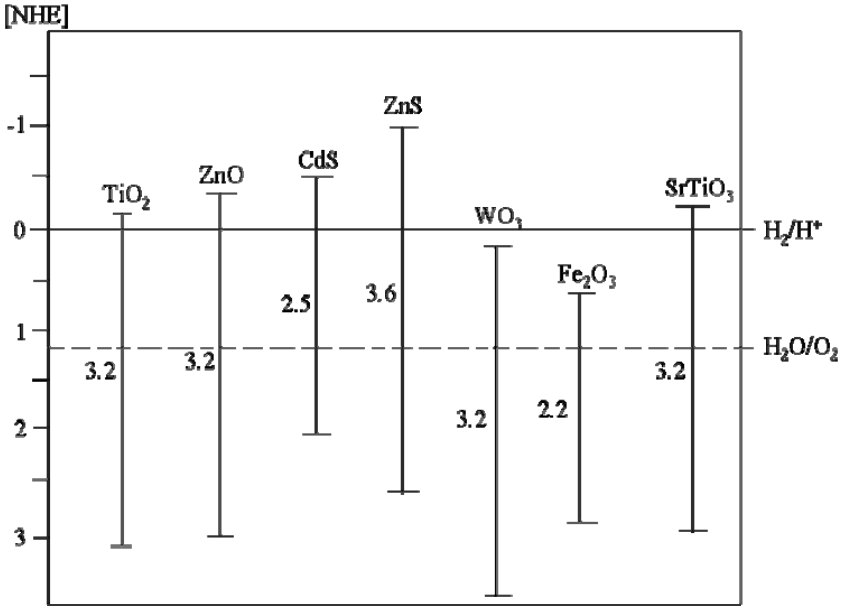

Fig.1.2. Schematic representation of various semiconductors with its band gap

ZnO has characteristics similar to that of TiO_2 and seems to be a suitable alternative to TiO_2. But it dissolves in acidic solutions and therefore cannot be used for technical applications. Other semiconductor particles (for example, CdS or GaP) absorb larger fractions of the solar spectrum than TiO_2 and can form chemically activated surface-bond intermediates, but unfortunately, such catalysts get degraded during the repeated catalytic cycles usually involved in heterogeneous photocatalysis(7).

Compared with other semiconductor photo catalysts, TiO_2 based photo catalysts have been most widely investigated in the past decades. So far, many comprehensive review articles have reported the advances made in the field of TiO_2-based photocatalyst (6).

Titania has following advantages over others. These are

- Non photocorrsive
- High redox ability
- High efficiency
- Low cost
- Chemically inert
- Non toxic
- Eco friendly

1.3 Structure of titania

Titanium dioxide can exist in the crystalline and amorphous forms. The amorphous forms of titania is photo catalytically inactive. It mainly exist in three crystalline forms - Anatase, Rutile and Brookite (Fig.1.3), in which brookite structure is less important in the field of photocatalysis, because it is very difficult to obtain it in the pure form.

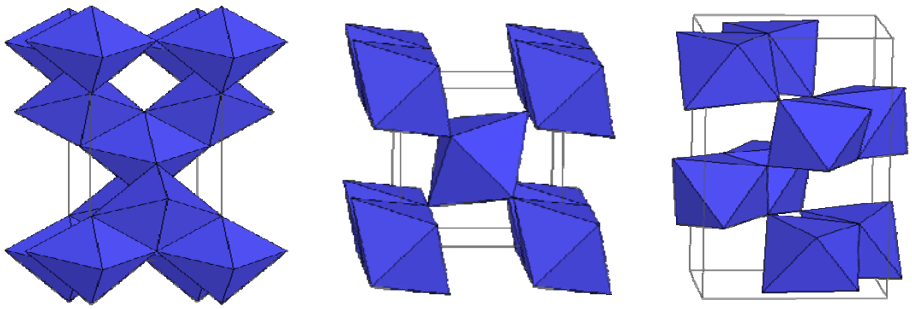

Fig.1.3. Bulk structures of (a) anatase, (b) rutile and (c) brookite

Figure 1.4 shows the unit cell structure of the titania crystal where the grey spheres are oxygen atoms and black spheres are Ti**.** The structure of rutile and anatase can be described in terms of chain of TiO_6 octahedra. The two crystal structures differ by the distortion of each octahedra and by the assembly pattern of the octahedral chain. Each Ti^{4+} ion is surrounded by an octahedron of six O^{2-} ions. The octahedron in rutile is not regular, showing a slight orthorhombic distortion. The octahedron in anatase is significantly distorted so that its symmetry is lower than orthorhombic. In rutile structure each octahedron is in contact with 10 neighbours (two sharing edge oxygen pairs and eight sharing corner oxygen atoms) while in the anatase structure each octahedron is in contact with eight neighbours (four sharing an edge and four sharing a corner) (1).

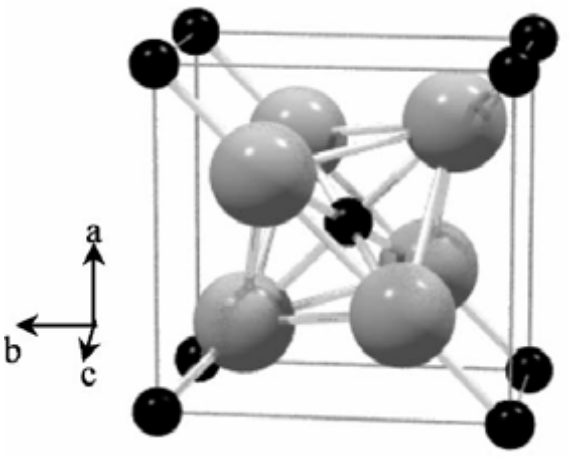

Fig.1.4. Unit cell of TiO_2

Usually, amorphous titania crystallizes into anatase around 400 ^{O}C, which is further converted into rutile from 600 to 1100 ^{O}C. The temperature for transition can vary from 400 to 1100 ^{O}C depending on the type and amount of additives, methods of preparation, reaction atmosphere, oxygen to metal coordination, particle size, morphology, degree of agglomerization and so on. At atmospheric pressure, the transformation mainly depends on treating time, temperature and is also function of impurity concentration (8).

In general, anatase (E_{bg} = 3.2 eV) gives better photocatalytic results than rutile (E_{bg} = 3.0 eV). This is because in anatase, the bottom of the conduction band is located more negative than that of rutile, which results in the production of photo generated electrons with higher reduction potential (9). Another fact related to lower activity of rutile is attributed to its preparation temperature. Normally rutile is obtained by the calcination of amorphous titania to the temperature higher than that for anatase. At higher temperature, there was a possibility of agglomeration of the particles. This results in the increase of particle size though decreasing the surface area. These are the crucial criteria for the better activities of a photocatalyst.

The titanium has no electrons in its valence shell when it is in the oxidation state of +4, resulting in an empty t_{2g} band. The bandgap is the gap between the filled p-band (valence band) and the empty t_{2g} band (conduction band). Molecular orbital diagram is shown below. (Fig. 1.5)

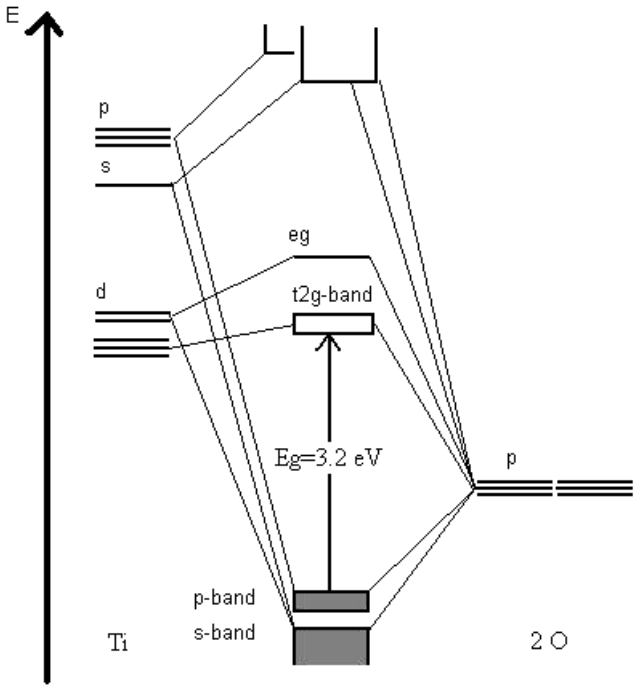

Fig.1.5. Energy level diagram of titania

1.4 Mechanism of Photocatalysis

Upon irradiation of titania semiconductor with light energy greater than its band gap (E_{bg}) generates photo excited species such electrons and holes on conduction band (CB) and valance band (VB) of semiconductor material respectively. These can be diffused and/or migrated to the semiconductors surface (Fig. 1.6.). The promotions of electrons are also related to the thermally activated production of defects within the materials as the time and/or temperature of the calcination process increases. This process is sometimes referred to as metallization of the semiconductor (1).

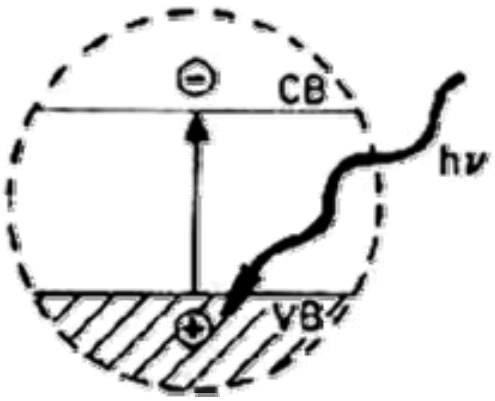

Fig.1.6. Schematic representation of light irradtion on semiconductor material

The photo excited species such as electrons and holes may undergo following events (a) recombination in the bulk, (b) recombination at the surface, (c) reduction of a suitable electron acceptor (A) adsorbed on the surface by the photo generated electron and (d) oxidation of a suitable electron donor (D) adsorbed on the surface by the photo generated hole which can shown on Fig. 1.7 (10).

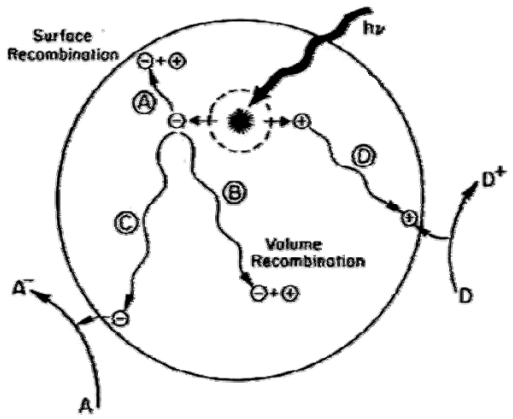

Fig.1.7. Events of photo excited species takes place on semiconductor Surface and Bulk

Electron–hole recombination is promoted by defects in the semiconductor material. So most amorphous semiconductor materials show little photo catalytic activity. No photo catalytic activity was observed when the recombination of electron-hole pair takes place and it generates heat. In other circumstances, if an electron donor molecule (D) is present at the surface, then the photo generated hole can react with these molecules to generate an oxidized product, D^+. Similarly, if there is an electron acceptor molecule (A) present at the surface, then the photo generated electrons can react with them to generate a reduced product, A^- (Equ. 1.5) (11). The overall reaction can be summarized as follows and it can be schematically represented on Fig. 1.6

$$A + D \xrightarrow{\text{Seminconductor/h}\upsilon} A^- + D^+ \quad \text{.....(1.5)}$$

Thus a generalized mechanism for the mineralization of organic pollutants as follows

$$\text{Organic Pollutant} + \text{Semiconductor} / h\upsilon \rightarrow CO_2 + H_2O \quad \text{.....(1.6)}$$

Fig 1.8 shows the schematic representation of redox reaction taking place on the photocatalyst materials. The description is as follows: The photo generated

holes on the surface can react with surface hydroxyl groups to generate adsorbed hydroxyl radicals ($OH^{\bullet}$) which in turn can oxidise the pollutant molecules. Where as the photo generated electrons on the surface can react with adsorbed oxygen to generate superoxide anion ($O_2^{\bullet-}$) which can be subsequently reduced to hydrogen peroxide and then water. The intermediate species hydroperoxide ($OH_2^{\bullet}$) produced can act as a further source of hydroxyl radicals ($OH^{\bullet}$). The process appears to involve the initial oxidation of surface hydroxyl groups on the TiO_2 to hydroxyl radicals which are then oxidised the organics and any subsequent intermediate/s. The reductions of oxygen by photo generated electrons generate superoxide anion ($O_2^{\bullet-}$) as an initial reduction product. The latter species can be further reduced to hydrogen peroxide, which is intermediate in the overall reduction of oxygen to water. Some of the mineralization of the organic pollutant is brought about by oxidising species such as hydroxyl radicals generated via the reduction of oxygen by photo generated electrons (7,11-13,). The efficiency of a photocatalyst depends on the competition of different interface transfer processes involving electrons and holes and their deactivation by recombination. The semiconductor photocatalytic process is a complex sequence of reactions that can be expressed by the following set of equations (Equ. 1.7-1.18) (14,15).

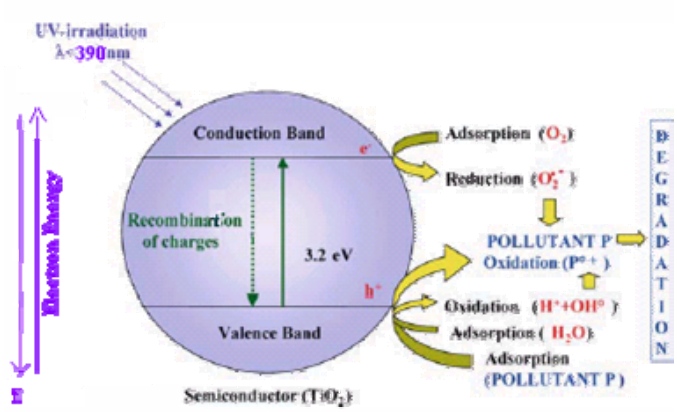

Fig.1.8. Photocatalytic redox reactions on titania surface

$$TiO2 \xrightarrow{\text{Semiconductor / h}\upsilon} e^- + h^+ \longrightarrow \text{Recombination} \quad .....(1.7)$$

$$h^+ + H_2O_{ads} \longrightarrow TiO_2 + O\dot{H}_{ads} + H^+ \quad .....(1.8)$$

$$h^+ + OH^-_{ads} \longrightarrow TiO_2 + O\dot{H}_{ads} \quad .....(1.9)$$

$$TiO_2 + D_{ads} \longrightarrow TiO_2 + D^+_{ads} \quad .....(1.10)$$

$$O\dot{H}_{ads} + D_{ads} \longrightarrow D_{oxide} \quad .....(1.11)$$

The oxidative pathway leads, in many cases, to complete mineralization of an organic substrate to CO_2 and H_2O. In reductive path, generally, A is dissolved O_2, which is transferred in superoxide radical anion ($O_2^{\bullet -}$) and can lead to the additional formation of $HO^{\bullet}$.

$$e^- + A_{ads} \longrightarrow A^-_{ads} \quad .....(1.12)$$

$$e^- + O_{2\,ads} + H^+ \longrightarrow H\dot{O}_2 \longleftrightarrow O_2^{\bullet -} + H^+ \quad .....(1.13)$$

$$H\dot{O}_2 + e^- + H^+ \longrightarrow H_2O_2 \quad .....(1.14)$$

$$2H\dot{O}_2 \longrightarrow H_2O_2 + O_2 \quad .....(1.15)$$

$$H_2O_2 + h\upsilon \longrightarrow O_2^{\bullet -} \longrightarrow O\dot{H} + O_2 + OH^- \quad .....(1.16)$$

$$H_2O_2 + h\upsilon \longrightarrow 2O\dot{H} \quad .....(1.17)$$

$$2O_2 + e^- \longrightarrow O\dot{H} + OH^- \quad .....(1.18)$$

In general, the electron-hole recombination on most semiconductor materials is usually very fast, e.g. typically less than l0 ns for TiO_2. However, if a hole scavenger is added to this, it is possible to remove some of the photo generated holes and effectively trap the photo generated electrons for a sufficient time to allow their transient absorption spectrum to be recorded. Similarly, if an electron scavenger is added, the transient absorption spectrum of trapped photo generated holes can be determined.

The rate of both oxidation and reduction reactions should be equal. If the rate of reduction is slow, the excess electron will be accumulated in the conduction band, which favours the recombination of electron-hole pair. In the other case, the excess holes will be accumulated in the valence band, resulting in a similar situation. In this situation, the addition of sacrificial agents (electron donor or acceptor) is necessary to increase the efficiency of the process. The choice of the sacrificial agents depends on the nature of the process.

In addition to light absorption, the other parameters like band gap, surface area, crystallite nature, crystallite size, crystal phase, crystal purity, morphology, calcination temperature, rate of interfacial charge transfer, carrier density and stability are also essential for photocatalytic activity. In addition to all, method of preparation play a key role on photocatalytic activity. The exact mechanism behind it is still not clear with solid proof.

1.5 Different methods of preparation

There are various methods available for the preparation titania with varying degree of photocatalytic activity. They are Sol-gel method, Sol method, Micelle and inverse micelle method, Hydrothermal method, Solvothermal method, Direct oxidation method, Chemical vapour deposition method, Physical vapour deposition method, Electodeposition method, Sonochemical method, Microwave method etc.

In sol-gel process, a colloidal suspension, or a sol, is formed from the hydrolysis and polymerization reactions of the precursors, which are usually inorganic metal salts or metal organic compounds such as metal alkoxides. Complete polymerization and loss of solvent leads to the transition from the liquid sol into a solid gel phase. It can be further converted into thin film, wet gel, or powder in nano scale on further drying and heat treatment using

proper techniques. An aerogel, highly porous and extremely low-density material is obtained if the solvent in a wet gel is removed under a supercritical condition (3, 16-19).

Micelles are the aggregates of surfactant molecules dispersed in a liquid colloid when the concentration of surfactant exceeds the critical micelle concentration (CMC). In micelles, the hydrophobic hydrocarbon chains of the surfactants are directed toward the interior of the micelle, and the hydrophilic groups of the surfactants are directed toward the surrounding aqueous medium. Reverse micelles are formed in non aqueous media, and the hydrophilic head groups are oriented toward the core of the micelles while the hydrophobic groups are oriented outward toward the non aqueous media. The sol method refers to the non-hydrolytic sol-gel processes and usually involves the reaction of titanium chloride with a variety of different oxygen donor molecules, e.g., a metal alkoxide or an organic ether. Surfactants have been widely used in the preparation of a variety of nano particles with better size distribution and dispersity. (3, 20-27).

Hydrothermal synthesis is normally conducted in steel pressure vessels called autoclaves with or without Teflon liners under controlled temperature and/or pressure with the reaction in aqueous solutions. It is a method that is widely used for the production of small particles with different morphologies. If we use non-aqueous solvent instead of water in hydrothermal process, then it is called solvothermal method. The solvothermal method normally has better control of the size, shape distributions and the crystallinity of the TiO_2 nanoparticles than hydrothermal methods. Oxidation of titanium metal using oxidants or under anodization gives titania nano-materials. The formation of crystalline titania occurs through a dissolution precipitation mechanism. Addition of inorganic salts control the crystalline phases of titania nano rods (3,28-34).

Deposition of any material in a vapour state are condensed to form a solid phase are called vapour deposition. The process carried without any chemical reaction is called physical vapour deposition (PVD) otherwise; it is called chemical vapor deposition (CVD). CVD methods such as electrostatic spray hydrolysis, diffusion flame pyrolysis, thermal plasma pyrolysis, ultrasonic spray pyrolysis, laser-induced pyrolysis, and ultronsic assisted hydrolysis etc. are sued for the preparation of titania nano materials. Methods like thermal deposition, ion plating, ion implantation, sputtering, laser vaporization, and laser surface alloying etc. are used in PVD for the preparation of nano titania materials. In electrodepostion, a metallic coating is produced on a surface by the action of reduction at the cathode. The substrate to be coated is used as cathode and immersed into a solution which contains a salt of the metal to be deposited. The metallic ions are attracted to the cathode and reduced to metallic form (3).

In sonochemical method an ultrasound has been used for the synthesis of a wide range of nano structured materials with high-surface area. It arises from acoustic cavitations: the formation, growth and collapse of bubbles in a liquid. Cavitational collapse produces intense local heating (~5000 K), high pressures (~1000 atm.), and enormous heating and cooling rates (>109 K/s). In Microwave radiation method a dielectric material can be processed with energy in the form of high-frequency electromagnetic waves. The principal frequencies of microwave heating are between 900 and 2450 MHz. The major advantages of using microwaves for industrial processing are rapid heat transfer, volumetric and selective heating (3).

These methods have their own advantages and disadvantages for the preparation of titania with varying degree of photocatalytic activity. Among this sol-gel gets some advantage over others as follows.

- Preparation normally carried out at room temp
- Chemical conditions are mild
- Gives better surface area
- Gives better pore sized particles
- Gives better nano scaled particles
- Gives high purity products

Despite all these advantages, it has some disadvantages also. The precursors are often expensive and sensitive to moisture, the process is little time consuming, required careful attention for ageing and drying, dimensional change on densification, shrinkage and stress cracking on drying etc. These significant limitations are not sufficient to avoid this method with comparing their advantage over others.

Sol-gel process can be classified as colloidal and polymeric based on the starting materials and the precursor (metal organic compound or an aqueous solution of an inorganic salt). One fundamental difference between them is that in colloidal path(precipitation-peptisation), the sol-gel transition is caused by physiochemical effect without the creation of a new chemical bonding in contrast to a chemical reaction, a polymerization or a poly condensation reaction as in the case of polymeric path (35,36). Synthesis of titania nano materials using sol-gel method normally proceeds via an acid-catalyzed hydrolysis of titanium (IV) alkoxide, as titanium precursor followed by condensation (37,38). The formation of Ti-O-Ti chains is favoured with low content of water, low hydrolysis rates, and excess titanium alkoxide in the reaction mixture which results in the three dimensional polymeric skeletons with close packed structure. It was noted that the average titania nano particle radius increases linearly with time, in agreement with the Lifshitz-Slyozov- Wagner model for coarsening (38). Modifying the precursor characteristics by involving different solvents and by using gel modifiers, we can prepare titania of specific properties.

1.6 Drawbacks and modifications

The wide spread application of titania as a photocatalyst began from the discovery of photodecomposition of water on titania, which extents its application in the area of photo catalytic degradation of organic and inorganic pollutants.

The presence of defects such as oxygen vacancies play an important role in photocatalytic activity imposed by titania surface. The presence of these defects changes the electronic structure of material. These defects also cause the electron-hole recombination process which depends on charge transfer and which occurs when the substrate material is exposed to photon energy higher than the bandgap (1).

The high efficiency of titania is limited to the absorption of light in the UV region based on its wide band gap. The band gap of bulk titania lies in the UV regime (3.2 eV for anatase). Our solar system consist around 4- 8 percent UV light and 40-50 percent of visible light

Even though it acts as a very good photocatalyst, it has got some drawback. Among this the two important ones are

- Easy recombination of photo excited species
- Poor activity in visible region.

There are number of ways in which the recombinations of charge carriers are possible. The concentration of charge carriers upon UV excitation in any semiconductor is decreased by recombination process, leading to the destruction of active electron-hole pair. Shockley-Read-Hall model is one of such non-radiative recombination process widely used in the case of titania. In the Shockley-Read-Hall mechanism, four transition processes may occur, These are (i) electron capture (ii) electron emission (iii) hole capture or (iv) hole emission. This model assumes that the semiconductor is non-degenerate and

that the density of trap sites is relatively small compared to the majority carrier density present in the material. This model describes the capture of mobile electrons and/or holes at trap sites within the semiconductor. The electron (or hole) is trapped by elimination via recombination with holes from the valence band (or electrons from the conduction band). The active sites for electron or hole trapping may vary and are usually described as defect states within the crystal due to interstitial atoms, defect states, or grain boundaries etc (1,39,40).

Most studies of the photochemical filling of trap states have concerned electron trapping. When an electron trap becomes filled, the Fermi level crosses the energy level of the trap and the trap becomes inactivated for further electron capture. This trap saturation effect can enhance the lifetime of photo generated charge carriers and can improve the quantum yield of carriers at higher light intensities. The electrons from these trap sites can be observed by various methods following thermal excitation into the conduction band (1,41).

The reaction rate for any photochemical process that occurs on the substrate is directly affected by the rate of recombination of photo excited electrons and holes. The rate of recombination depends on factors such as charge trapping, the chemisorption or physorption of target molecules, the incident light intensity etc. Sometimes a sacrificial electron or holes scavengers is used to decrease the recombination rate which leads to increase the lifetime of the other charge carrier. Anpo et al. reported that adsorbed molecular oxygen is, most frequently, referred as electron scavenger used to prolong the lifetime of photo generated holes. The adsorbed oxygen molecule readily accepts an electron to become the superoxide ion, which are detected by IR spectroscopy (42-44) and/or EPR (20). For photo produced holes, commonly employed scavenger molecules are methanol (21, 45-49), propanol (50), ethanol (47), glycerol (51) and surface hydroxyl groups (52).

The second limitation was modified by various research groups in different ways with different degree of success. Modifications employed are i) coupled with other semiconductors or sensitized with dyes, ii) doped with metals (called second generation photocatalysis) and iii) doped with non-metals (called third generation of photocatalysis).

In the method of modification coupled with other semiconductors or sensitized with dyes, (Fig.1.9) the absorption wavelength region of semiconductor is extended to higher region by absorption by dye or other semiconductor associated with it. The light absorption by these species excites electron from ground state to excited state then the excited electrons transferred to the conduction band of the titania semiconductors. In order to achieve the electron transfer process from excited state to conduction band the potential of conduction band should be more positive than the excited state. Some species which are used for this purpose includes $Ru(bpy)_3^{2+}$, porphyrin, merocyanine, CdS, CdSe, GaAs etc. The solubility of the dye/coupled semiconductors in water and other solvents and their stability are major disadvantages of the process. Some times the coupled semiconductors undergo photo corrosion and affect the photocatalytic activity of the semiconductor (53-56).

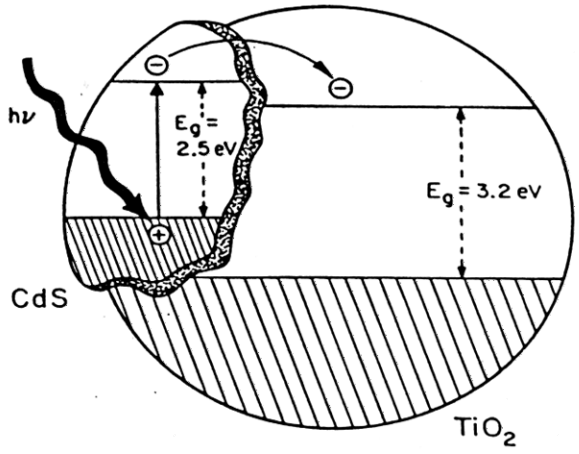

Fig. 1.9. Titania coupled with CdS semiconductor

In metal doped titania (Fig. 1.10), a metal ion inserted on the titania structure, which significantly enhance the photocatalytic efficiency either by widening the light absorption range or by modifying the redox potential of the photo excited species. The doped ions produce additional energy levels between the valence band and conduction band on the titania semiconductor, which enhances the light absorption in visible light by decreasing the bandgap of titania. There are lots of reports available in literature with both positive or negative results of titania modified with different metal ions with different amount of dopant. Though, the doping of metal ion increases the activity significantly, none of them shows stable activity after certain time due to the instability of doped metal ion against photo corrosion. Most times the doped metal ions itself act as electron-hole recombination centers (13,57-63).

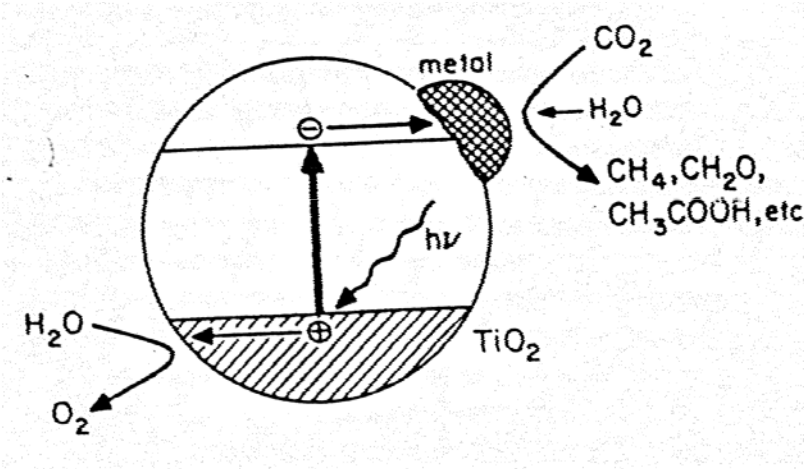

Fig. 1.10. Titania doped with metal ion

Titania doped with non-metals (Fig. 1.11) such as C, N, S, P, B, halogens etc, called the third generation of photocatalyst. They got greater attention during the last decade due to their higher photocatalytic activity in visible region. Asahi et al. first reported the idea of doping with non-metal such as N on titania and also reported theoretical results from the substitution

of C, N, F, P or S for oxygen atoms in the titania lattice. The great success of anion doped titania with high activity in visible region is due to decrease of their band gap either by mixing p orbital of the dopant with O 2p orbital and generate a state just above the valence band or generate a mid-gap level of dopants between the valence band and conduction band. Lot of theoretical calculations has also been reported for the band gap alteration using anion doped titania. Later the chemical state and composition of the dopants were well studied using modern techniques. The incorporation of these impurities on titania network generates some defects, which retard the easy recombination of the photo excited species and enhance the greater photocatalytic activity (1,64-76).

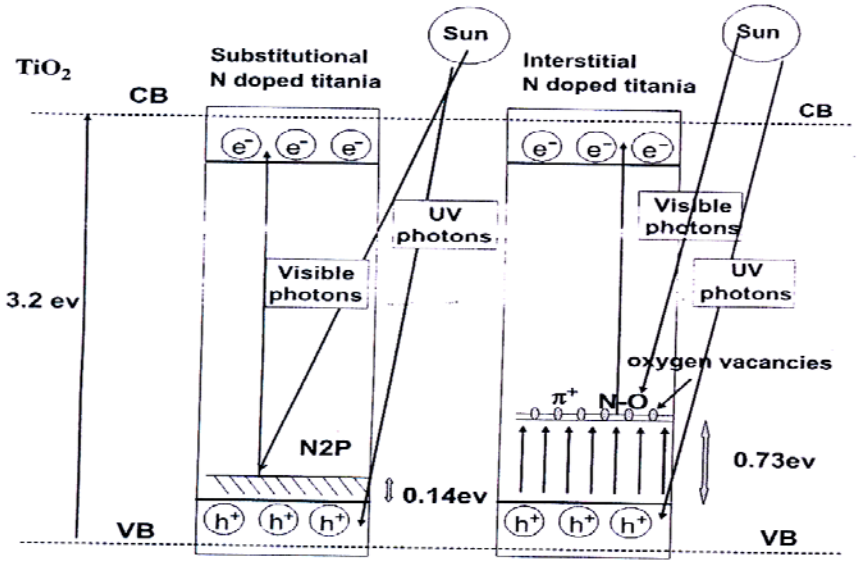

Fig. 1.11. Non-metal(N) doped titania

The density functional theory calculations showed that for anatase samples, N doping results in a decrease in the photon energy necessary to excite the material whereas for rutile samples, the opposite effect is observed and is attributed to the contraction of the valance band and the stabilization of the N 2p state, thus causing an overall increase in the effective band gap (77-82).

1.7 Scope of present study

The current area of interest in this field of photocatalysis by titania is the modification of TiO_2 sensitive to visible light. The present work aims to prepare visible light responsive anion doped titania via sol-gel precipitation method. The prepared catalysts were characterized by various techniques. The photocatalytic abilities of the prepared catalyst were measured by the degradation of dyes, pesticides, hydrogen production through water splitting reaction and antibacterial study. We also compared the activities of prepared catalysts with pure titania prepared in the laboratory and one of the commercial anatase titania samples.

The objectives of present study involves

- Prepare N doped and N S co-doped nano titania through sol-gel precipitation method.
- Prepare modified catalysts with different amount of dopant source and pure titania.
- Physico chemical characterization of the prepared catalysts via. XRD, UV-Vis DRS, BET surface area, SEM-EDX, TEM, RAMAN, XPS, TG etc.
- Photocatalytic efficiency of the prepared catalysts to be evaluated by the degradation of dyes like Methylene Blue, Rhodamine B, Crystal Violet and Acid Red 1.
- To evaluate the degradation of organic pollutants (Collectively called pesticides) like 2,4-Dichlorophenoxyacetic acid, Monolinuron, 2,4,5-Trichlorophenoxyacetic acid and Aldicarb.
- Hydrogen production through photocatalytic water splitting in visible region
- Anti bacterial study using Escherichia coli (E.Coli) bacteria.

References

[1] Tracy L.; Thompson; John T. Y.; Jr., Chem. Rev. 106 (2006) 4428.

[2] www.isiknowledge.com

[3] Xiaobo C.; Samuel S. M., Chem. Rev. 107 (2007) 2891.

[4] Parmon V.; Emeline A.V.; Serpone N., Int. J. Photoenergy 4 (2002) 91.

[5] Somorjai G.; "Photocatalysis - Fundamentals and Applications", Chapt. 9. N. Serpone and E. Pelizzetti (eds.), Wiley-Interscience, New York, (1989).

[6] Gang L.; Lianzhou W.; Hua G. Y.; Hui-Ming C.; Gao Q. L., J. Mater. Chem. DOI: 10.1039/b909930a

[7] Matsunaga T.; Tomoda R.; Nakajima T.; Wake H., FEMS Microbiol. Lett. 29 (1985) 2.

[8] Ocana M.; Garcia Romos J. V.; Sema C. J., J. Am. Ceram. Soc., 75 (1992) 201.

[9] Kavan L.; Gra¨zel M., Gilbert S. E.; Klemenz C; Scheel H. J., J. Am. Chem. Soc. 118 (1996) 6716

[10] Mills A.; Hunte S. L.; J. Photochem. Photobiol. A: Chem. 108 (1997) 1.

[11] Prashant V. K.; Dan Meisel, C. R. Chimie. 6 (2003) 999.

[12] Fujishima T.; Rao N.; Tryk D., J. Photochem. Photobiol. C: Photochem. Rev. 1 (2000) 1.

[13] Hoffmann M. R.; Martin S. T.; Choi W.; Bahnemann D. W., Chem. Rev. 95 (1995) 69.

[14] Hufschmidt D.; Liu L.; Seizer V.; Behnemann D., Water Sci. Technol. 49 (2004) 135.

[15] Martin. S. T.; Herrmann. H.; Choi. W.; Hoffmann. M. R., Trans. Faraday Soc. 90 (1994) 3315.

[16] Pierre, A. C.; Pajonk, G. M., Chem. ReV. 102 (2002) 4243.

[17] Hench, L. L.; West, J. K., Chem. ReV. 90 (1990) 33.

[18] Lu Z. L.; Lindner E.; Mayer H. A., Chem. ReV. 102 (2002) 3543.

[19] Wight A. P.; Davis M. E., Chem. ReV. 102 (2002) 3589.

[20] Anpo M.; Che M.; Fubini B.; Garrone E.; Giamello E.; Paganini M. C., Top. Catal. 8 (1999) 189.

[21] Thompson T. L.; Yates J. T.; Jr., J. Phys. Chem. B 109 (2005) 18230.

[22] Niederberger M.; Bartl M. H.; Stucky G. D.. Chem. Mater. 14 (2002) 4364.

[23] Parala H.; Devi A.; Bhakta R.; Fischer, R. A., J. Mater.Chem. 12 (2002) 1625.

[24] Tang J.; Redl F.; Zhu Y.; Siegrist T.; Brus L. E.; Steigerwald M. L., Nano Lett. 5 (2005) 543.

[25] Arnal P.; Corriu R. J. P.; Leclercq D.; Mutin P. H.; Vioux A., J Mater. Chem. 6 (1996) 1925.

[26] Hay J. N.; Raval H. M., J. Sol-Gel Sci. Technol. 13 (1998) 109.

[27] Lafond V.; Mutin P. H.; Vioux A., Chem. Mater. 16 (2004) 5380.

[28] Wu, J. M., J. Cryst. Growth 269 (2004) 347.

[29] Peng X.; Chen A., J. Mater. Chem. 14 (2004) 2542.

[30] Li X. L.; Peng Q.; Yi J. X.; Wang X.; Li Y. D., Chem. Eur. J. 12 (2006) 2383.

[31] Xu J.; Ge J. P.; Li Y. D., J. Phys. Chem. B 110 (2006) 2497.

[32] Wang X.; Zhuang J.; Peng Q.; Li Y. D., Nature 437 (2005) 121.

[33] Wen B.; Liu C.; Liu Y., J. Phys. Chem. B 109 (2005) 12372.

[34] Yang S. W.; Gao L., Mater. Chem. Phys. 99 (2006) 437.

[35] Shi L.; Wong N. B.; Tin K. C.; Chung C. Y., J. Mat. Sci. Lett, 16 (1997) 1284.

[36] Uhihom R. J. R.; Keizer K.; Burggraaf A. J., J. Membrane Sci, 66 (1992) 1023.

[37] Bessekhouad Y.; Robert D.; Weber J. V., J. Photochem. Photobiol. A 157 (2003) 47.

[38] Moritz T.; Reiss J.; Diesner K.; Su D.; Chemseddine A., J. Phys. Chem. B 101 (1997) 8052.

[39] Li S. S., Semiconductor Physicals Electronics; Plenum Press: NewYork, (1993).

[40] Shockley W.; Read Jr. W. T., Phys. Rev. 87 (1952) 835.

[41] Schwarzburg K.; Willig F., Appl. Phys. Lett. 58 (1991) 2520.

[42] Berger T.; Sterrer M.; Diwald O.; Knozinger E.; Panayatov D.; Thompson T. L.; Yates J.T.; Jr., J. Phys. Chem. B 109 (2005) 6061.

[43] Szczepankiewicz S. H.; Colussi A. J.; Hoffmann M. R., J. Phys. Chem. B 104 (2000) 9842.

[44] Xiao-e L.; Green A. N. M.; Haque S. A.; Mills A.; Durrant J. R., J. Photochem. Photobiol. A 162 (2004) 253.

[45] Micic O. I.; Zhang Y. N.; Cromack K. R.; Trifunac A. D.; Thurnauer M. C., J. Phys. Chem. 97 (1993) 13284.

[46] Yoshihara T.; Katoh R.; Furube A.; Tamaki Y.; Murai M.; Hara K.; Murata S.; Arakawa H.; Tachiya M., J. Phys. Chem. B 108 (2004) 3817.

[47] Tan T.; Beydoun D.; Amal R., J. Photochem. Photobiol. A 159 (2003) 273.

[48] Du Y. K.; Rabani J., J. Phys. Chem. B 107 (2003) 11970.

[49] Nakamura R.; Nakato Y., J. Am. Chem. Soc. 126 (2004) 1290.

[50] Goto H.; Hanada Y.; Ohno T.; Matsumura M., J. Catal. 225 (2004) 223.

[51] Shkrob I. A.; Sauer M. C., J. Phys. Chem. B 108 (2004) 12497.

[52] Lana-Villarreal T.; Bisquert J.; Mora-Sero I.; Salvador P., J. Phys. Chem. B 109 (2005) 10355.

[53] Abe R.; Sayama K.; Arakawa H., Chem. Phys. lett. 362 (2002) 441.

[54] Boschloo G.; Hagfeldt A., J. Phy. Chem. B 109 (2005) 12093.

[55] Cho Y.; Choi W.; Lee C. H.; Hyeon T.; Lee H. I., Enviro. Sci. Tech. 35 (2001) 966.

[56] Tae E. L.; Lee S. H.; Lee J. K.; Yoo S. S.; Kang E. J.; Yoon K. B., J. Phys.chem. B 109 (2005) 22513.

[57] Choi W.Y.; Termin A.; Hoffmann M. R.; J. Phys. Chem. 98 (1994) 13669.

[58] Karvinen S.; Hirva P.; Pakkanen T. A., J. Mol. Struct- Theochem, 626 (2003) 271.

[59] Anpo M., Studies in Sur. Sci. And Catl. 130 (2000) 157.

[60] Lin J.; Yu J. C.; Lo D.; Lam S. K., J. Catalysis 183 (1999) 368.

[61] Beydoun D.; Tse H.; Amal R.; Low G.; McEvoy S., J. Mol. Cat. A: Chem.. 177 (2002) 265.

[62] Pal B.; Hata T.; Goto K.; Nogami G., J. Mol. Catal. A: Chem. 169 (2001) 147.

[63] Wu J. C. S.; Chen C. H., J. Photochem. Photobiol. A 163 (2004) 507.

[64] Asahi R.; Morikawa T.; Ohwaki T.; Aoki K.; Taga Y., Science, 293 (2001) 269.

[65] Umebayashi T.; Yamaki T.; Itoh H.; Asai K., Appl. Phys. Lett. 81 (2002) 454.

[66] Hattori A.; Yamamoto M.; Tada H.; Ito S., Chem. Lett. 27 (1998) 707.

[67] Yamaki T.; Sumita T.; Yamamoto S., J. Mat. Sci. Lett. 21 (2002) 33.

[68] Sato S., Chem. Phys. Lett. 123 (1986) 126.

[69] Moon S. C.; Mametsuka H.; Tabata S.; Suzuki E., Cat. Today, 58 (2000) 125.

[70] Morikawa T.; Asahi R.; Ohwaki T.; Aoki A.; Taga Y., Jap. J. Appl. Phys. 40 (2) (2001) 561.

[71] Umebayashi T.; Yamaki T.; Tabata S.; Asai K., Chem. Lett. 32 (2003) 330.

[72] Sakthivel S.; Kisch H., Chem.Phys.Chem. 4 (2003) 487.

[73] Irie H.; Watanabe Y.; Hashimoto K., J. Phys. Chem. B. 107 (2003) 5483.

[74] Gole J. L.; Stout J. D.; Burda C.; Lou Y.; Chen X., J Phys. Chem. B 108 (2004) 1230.

[75] Chen X.; Burda C., J. Phys. Chem. B 108 (2004) 15446.

[76] Valentin C. D.; Pacchioni G.; Selloni A.; Livraghi S.; Giamello E., J. Phys. Chem. B. 109 (2005) 11414.

[77] Diwald O.; Thompson T. L.; Goralski E. G.; Walck S. D.; Yates J. T; Jr., J. Phys. Chem. B 108 (2004) 52.

[78] Di Valentin C.; Pacchioni G.; Selloni A, Phys. Rev. B 70 (2004) 15446

[79] Di Valentin C.; Pacchioni G.; Selloni A.; Livraghi S.; Giamello E, J. Phys. Chem. B 109 (2005) 11414

[80] Howe R. F.; Gratzel M., J. Phys. Chem. 91 (1987) 3906.

Chapter 2

Experimental and Characterization Techniques

Contents

A suitable technique is needed to assess the structure and properties of materials, which are also related to the nature of material under investigation. Some techniques are qualitative, which provide information such as appearance, presence, morphology, whereas some other techniques are quantitative and provide the information about chemical composition, exact size, concentration etc. The recent technological developments assist to obtain two or three dimensional information about the materials. Therefore characterisation techniques are powerful tools to bring out the invisible information of the samples into the light.

2.1 Introduction

The world of catalysis is nothing without its characterisation. It gives a better understanding of the relationship between catalyst properties and performance. The physiochemical characteristic of a semiconductor catalyst highly depends on the experimental conditions used for its synthesis. During the characterisation, the sample is treated with suitable agents like photon, electrons, or ions and we obtain lot of data which are related to the surface of the catalyst. And these data are converted to suitable information about the samples such as size, shape, phase, crystallinity, type of surface structure, chemical composition (quantitative and qualitative) and the information required to realize the mechanism of the processes proceeding on the surface of the solid etc with proper software using computers. Spectroscopy, microscopy, X-ray analyses are some of the important tools to obtain data from the samples (1).

The important characterisation techniques to understand the different physiochemical features of the materials are:

- X-ray Diffraction(XRD)
- UV-Visible Diffuse Reflectance Spectroscopy (UV-Vis. DRS)
- Transmission Electron Microscopy (TEM)
- X-ray Photoelectron Spectroscopy (XPS)
- Scanning Electron Microscopy (SEM)
- Thermo Gravimetric Analysis (TG)
- Raman Spectroscopy

2.2 Chemicals and Reagents Used

Chemicals	Company
Titanium tetraisopropoxide	Sigma Aldrich
Isopropy alcohol	SRL (99.5%)
Urea	Merck (99.0%)
Thiourea	Merck
Commericial anatase titania	Sigma Aldrich
Methylene Blue	Sigma Aldrich
Rhodamine B	Sigma Aldrich
Crystal violet	Sigma Aldrich
Acid Red 1	Sigma Aldrich
2,4-Dichlorophenoxy acetic acid	Sigma Aldrich
2,4,5-Tichlorophenoxy acetic acid	Sigma Aldrich
Monolinuron	Sigma Aldrich
Aldicarb	Sigma Aldrich
Methanol	Merck
Acetonitrile	Merck
Trifluoroacetic acid	Sigma Aldrich

2.3 Catalyst Preparation

The Catalytic activity strongly depends on the methods of preparation. Small deviation in the preparation conditions sometimes gives large variation in their activity. Therefore intense care should be taken for selection of methods, with suitable experimental conditions for the preparation catalyst (2,3). Fig. 2.1 shows the schematic representation of the catalyst preparation. A novel sol-gel precipitation method is used for the preparation of catalyst. In this method titanium tetraisopropoxide is taken as precursor for titanium, isopropyl alcohol as solvent medium, aqueous solution of urea as the source of dopant N and aqueous solution of thiourea as the source dopants N and S.

Preparation of Nitrogen doped catalyst (N-TiO_2): Take 1:10 ml volume ratio of titanium tetraisopropoxide in isopropyl alcohol. To this solution, add

aqueous solution of 10% urea dropwise and it was stirred mechanically for 12 hours. The obtained gel was aged for one day and dried at temperature 70 ^{0}C. The dried sample was calcined at 400^{0}C for four hours.

Preparation of Nitrogen Sulphur co-doped catalyst (NS- TiO_2): The experimental conditions are same as the above except the source of dopant. In this case aqueous solution 1% thiourea was taken.

To compare the amount of dopant against activity we also prepared catalyst with dopant source amount above and below the amount mentioned in the procedure. For this we prepare nitrogen doped catalyst with 5% and 12.5% aqueous solution of urea and nitrogen sulphur co-doped titania with 0.5% and 2.0% aqueous solution of thiourea respectively. Also prepare pure titania in the same method except the dopant source. All the chemicals were used as such without any further purification.

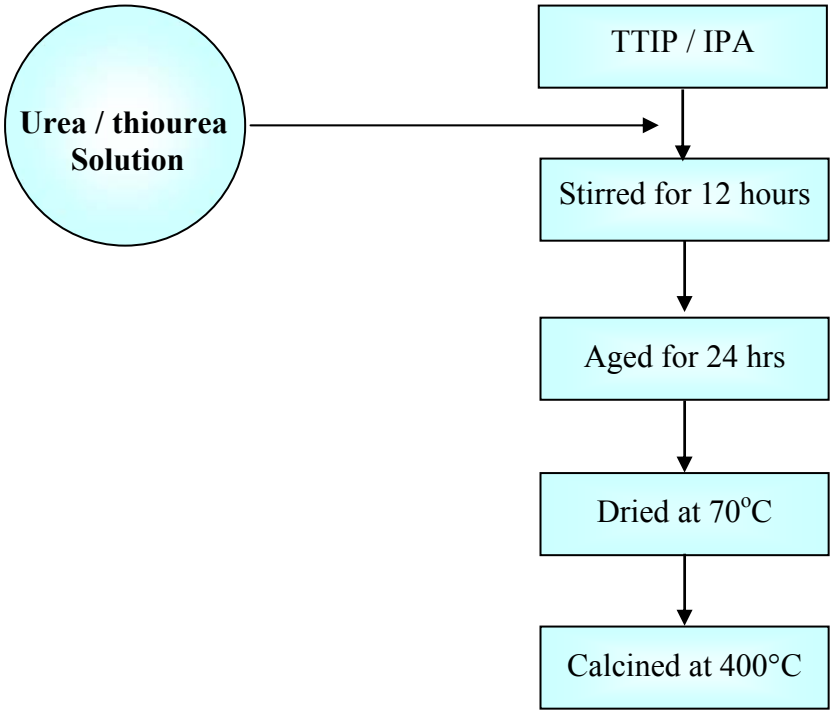

Fig. 2.1. Schematic representation of catalyst preparation

2.4 Catalyst Notations

N doped titania (5 % Urea)	N-TiO_2 (l)
N doped titania (10 % Urea)	**N-TiO_2**
N doped titania (12.5 % Urea)	N-TiO_2 (h)
N S co-doped titania(0.5% Thiourea)	NS-TiO_2 (l)
N S co-doped titania(1.0% Thiourea)	**NS-TiO_2**
N S co-doped titania(2.0% Thiourea)	NS-TiO_2 (h)
Undoped titania (prepared in lab.)	L-TiO_2
Commercial Anatase titania	A-TiO_2

2.5 Material Characterisation

The technique such X-ray diffraction, spectroscopy, nitrogen adsorption-desorption, electron microscopy, thermo gravimetric analysis etc are used to find the active nature of the prepared catalysts. These techniques are utilized to interpret the structure and properties of the catalyst.

2.5.1 X-ray Diffraction (XRD)

X-ray diffraction is the one of most powerful tools used to determine crystallinity, crystallite size, phase purity, phase composition, lattice parameters, geometry, and identification of impurities, lattice defects etc of a solid material. It is also used for both qualitative and quantitative analysis of solid phases. It is a nondestructive technique and a standard method for the characterisation of polycrystalline solids (4,5).

In this method X-rays interact with crystalline matter and undergoes diffraction, produced by the reticular planes that form the atoms of the crystal (5,6). When there is constructive interference from X-rays scattered by the atomic planes in a crystal, a diffraction peak is observed. From the diffraction patterns, the phase purity (7), degree of crystallinity and unit cell parameters of the semiconducting materials can be determined (8, 9). From the Bragg's relation, $n\lambda = 2d\sin\theta$, we can calculate the distance between two

(hkl) planes d by knowing the angle of diffraction (2θ). Where λ = wavelength of X-rays, n = an integer known as the order of reflection (h, k and l represent Miller indices of the indices of the respective planes) (8).

The porous nature of the material also obtained from the XRD techniques. The wide angle spectra (peaks in the 2θ range of 10-70) give the micro porous nature whereas the low angle (small angle, peaks in the 2θ range of 1.0-10) gives mesoporous nature of the materials.

XRD analysis can also be used to calculate the average crystallite or grain size of the catalyst using the Scherrer equation as follows,

$$\mathbf{D = K\lambda / \beta \ Cos\ \theta}$$

Where θ and λ are the Bragg angle and the wavelength of the X-ray used. K is a constant approximately equal to 0.89; β is the full width half maximum of the intense peak at θ value.

One of the most important applications of X-ray diffraction is the phase identification. Each crystalline powder gives a unique diffraction diagram, called characteristic finger print, which enables the determination of phase purity and the degree of crystallinity by comparing with a standard (a pattern), taken from any X-ray powder data file catalogues, published by the American Society for Testing Materials (JCPDS).

The X-rays are produced by bombarding either copper (Cu) or molybdenum (Mo) with high energy electrons. The emitted X-rays are then filtered or passed through a monochromater to produce Kα radiation from the respective metal. CuKα possesses a wavelength of 1.541 Å and MoKα possesses a wavelength of 0.709 Å. Once the X-rays impinge on the sample, they diffract from each of the exposed planes and a detector rotates around the sample recording the intensities of diffraction at each angle. The angles at which the peaks

are observed can be used to determine the interplanar spacing of atoms (periodicity) or d-spacing for each crystal plane using Bragg's Law (1).

The poweder X-ray diffraction analysis is performed by using Bruker AXS D8 advance X-Ray Diffractometer with Ni filtered Cu Kα radiation source(λ = 1.5406 A^{o}) by recording 2θ in the range of 10-70 ^{0}at a scan rate of 0.5 ^{O} /min.

2.5.2 UV-Visible Diffuse Reflectance Spectroscopy

Electronic transition in materials, most preferably in liquid state, is studied by UV-visible spectroscopy. This method is applicable to the materials which are soluble in suitable liquids. But in the case of insoluble solids this method is not applicable. In such cases UV-Vis. Reflectance or diffuse reflectance methods are used. The former is suitable for highly reflective materials whereas later is applied for powdered samples and roughened solids.

UV-Visible diffuse reflectance spectroscopy is a non-destructive technique which provides the information about the structure and composition of materials. In this method, the samples interact with light energy, absorption and scattering takes place, producing a reflecting spectrum. It is performed with the electronic excitation by the absorption of light. Electronic excitations are two types, d-d transition and charger transfer (CT) transition. d-d transition gives the information about the oxidation state and the co-ordination environment of the samples, whereas CT transitions are intense and are sensitive to the nature of donor and acceptor atoms.

The band gap of the semiconducting materials can be calculated from UV-Vis. DRS spectrum using the equation,

$$E = h\nu = hc / \lambda = 1240 / \lambda \text{ (nm)}$$

One of the simple version of Kubelka-Munk equation where λ is the wavelength from which reflection taken place (10-12).

The UV Vis reflectance spectra were obtained in the range of 200-900 nm on Labomed UV-VIS Double Beam UVD-500 spectrophotometer equipped with an integrating sphere assembly, using $BaSO_4$ as reflectance standard with a CCD detector.

2.5.3 Surface area measurements

Surface area measurements are commonly carried out by gas physisorption method. Normally nitrogen gas is used for this purpose because it is less expensive, easily available, inert and is able to penetrate even the finest pores. The nitrogen physisorption measurements are performed at liquid nitrogen temperature (77 K).

BET method has been widely adopted as a standard method for the determination of surface area. This was introduced by Brunauer, Emmett and Teller. In this method, adsorption is characterized by an isotherm, represents the equilibrium amount of gas adsorbed on a solid at a given temperature as a function of time. This theory assumes that materials possess uniform, localized sites in which adsorption at one site is independent by others, adsorption is multilayer, and the heat of adsorption at each layer is a constant and equal to the liquefaction of the adsorbate. This theory is extended to Langmuir model to multilayer adsorption. The BET equation can be represented as

$$\frac{P}{V(P_0 - P)} = \frac{1}{V_m C} + \frac{(C-1)P}{CV_m P_0}$$

Here C is a constant for at a given temperature and is related to the heat of adsorption, V is the volume adsorbed at equilibrium pressure P, V_m is the volume of adsorbate necessary to form a monolayer on the surface and Po is the saturation vapour pressure of the adsorbate.

The BET equation holds a linearity between P / V (Po – P) and P / P_o with slope is equal to (C-1) / C V_m and y intercept is equal to 1 / V_m C. From the slope and y intercept V_m can be calculated. The specific surface area is then obtained by following relation

$$S.A_{(BET)} = V_m \, Am \, N_A / V_{mol}$$

According to equation, the specific BET surface area ($S.A_{BET}$) can be calculated by knowing V_m(calculated from BET method), Am= cross sectional area of adsorbed gas (0.162 nm^2 for N2), N_A = Avagadro number and V_{mol} molar volume of adsorbate gas at STP (2.414 mol^{-1}) (7, 13).

The BET surface area was measured using Micromeritics Tristar 3000 surface area analyzer. The samples were activated at 90 ^{0}C for 1 hour before the analysis and then degassed at 350^0 C for 3 h under nitrogen flow.

2.5.4 CHNS Elemental Analysis

The CHNS elemental analysis is mainly applicable for organic compounds and inorganic complexes. It gives both qualitative and quantitative information about the percentage of the elements present in the sample. These elements in the samples were oxidized to their oxides and amount of oxides are calculated using proper techniques. From which the percentage of elements are calculated.

In our case we are interested only on the qualitative information about the presence of dopant elements N and S in the samples and the CHNS elemental analysis was performed on a Elementar Vario EL III apparatus.

2.5.5 Scanning Electron Microscopy

Scanning electron microscopy is one of the most widely used electron microscopic techniques for the morphological analysis of the samples. It

produces a high resolution image of the sample surface by measuring the emitted electrons from the specimen. The interaction of a beam of electrons with the specimen results in the generation of secondary electrons, back scattered electrons, auger electrons, characteristic X-rays and photons of various energies. Secondary electrons and back scattered electrons can form images as well as supply atomic information about the sample. The secondary electrons are originating from the surface, whereas the back scattered electrons arise from the bulk, a three dimensional image of the material obtained from SEM analysis with a resolution lower than that of TEM.

In SEM analysis, a thin coating of powdered samples on carbon tape placed on a metal stub. A beam of electrons (primary electrons) is focused on a spot volume of the specimen, resulting in the transfer of energy to the spot. The emitted electrons, also known as secondary electrons are attracted and collected by a positively biased grid or detector and then translated into a signal. To produce the SEM image, the electron beam is swept across the area being inspected, producing many signals. These signals are then amplified, analyzed, and translated into images of the topography being inspected. Finally, the image is shown on a cathode ray tube. X-rays are also produced during the interaction of electrons with samples, which results in the compositional information about the sample through energy dispersive X-ray spectroscopy (EDX) equipped with SEM instrument (14-16).

The scanning electron micrographs of the samples were taken using JEOL Model JSM-6390LV scanning electron microscope with a resolution of 1.38 eV

2.5.6 Energy Dispersive X-ray analysis (EDX)

Energy dispersive X-ray analysis is a technique used to get the information about the elemental composition of the samples. The energy of the X-ray emitted

from the material by the interaction with beam of electrons depends on the material under examination. By moving the electron beam across the material an image of each element in the sample can be obtained. Lithium drifted silicon is used as detector in EDX, which operated at liquid nitrogen temperature. When the X-rays strike the detector, it will generate photoelectron, which causes the generation of electron-hole pairs, which in turn generate the current pulses as signal depending on the energy of incoming x-rays. EDX is always in conjunction with the SEM analysis, because the X-rays are also produced during the interaction of electrons with samples during the SEM analysis. EDX spectra of the samples were recorded in a JEOL Model JED-2300 instrument (12,17).

2.5.7 Transmission Electron Microscopy

Transmission electron microscopy is another electron microscopic technique with high resolution for the structural analysis. It resembles optical microscopy, except electromagnetic radiations instead of optical lenses are used to focus an electron beam on the sample. The transmission mode measures the intensity from an electron source after it has passed through a transparent sample. TEM also provides real space image on the atomic distribution in the bulk and surface of a nano crystal. A combination of topographic and crystallographic information gives particle size distribution based on the assumption that the size of the imaged particle is truly proportional to the size of the actual particle, independent of their dimensions. It involves the irradiation of thin samples with high energy electron beam and measure the imaging and angular distributions analysis of the forward scattered electrons. It also gives useful information for the characterisation and identification of various morphological phases of the materials like cubic, hexagonal etc.

In Transmission electron microscopy, the sample is bombarded with a highly-energetic beam of electrons in vacuum. Black and white images are

formed by the passage of some electrons through the sample. The optics bring the scattered electrons from the same point in the sample to the same point in the image (the so-called bright-field image), in contrast, selection of strongly diffracting regions of the sample, which would appear brighter than the transmitted beam, is known as dark-field imaging. The magnified images are recorded by hitting a fluorescent screen, photographic plate, or light sensitive sensor such as a CCD camera and displayed in real time on a monitor or computer.

By applying a selected area aperture and using parallel incident beam illumination, we get an electron diffraction pattern from a selected area around 100 nm. Because a selected area diffraction pattern can be recorded from almost every grain in poly crystalline materials, reciprocal lattices and mutual crystal orientation relationship can be easily obtained. The high resolution TEM images also provide the actual morphology with accurate particle size and phase purity (1, 18-20).

The TEM analysis of the sample was carried out in ultrahigh resolution analytical electron microscope JEOL 3010. A sonicated solution of the sample in alcohol which evaporates on the TEM grid to from a dry film was prepared.

2.5.8 X-ray Photoelectron Spectroscopy

X-ray photoelectron spectroscopy is one of characterisation tools for the determination of elemental composition of the material under investigation. It is also one of the surface analysis techniques under ESCA (electron spectroscopy for chemical analysis). In this method, core electrons are excited by X-rays through photoelectric effect and the kinetic energy of the emitted electrons is measured and their spectra are reported in terms its binding energy. Depending on the chemical environment of atoms, the binding energy of core

electrons varies slightly, which helps to get the information about the chemical nature of elements present in the materials. It gives quantitative information about the sample.

The binding energy of the ejected photoelectron depends on the final state configuration after photoemission. The shakeup peaks may occur when the outgoing photoelectron simultaneously interacts with a valence electron and excites it to a higher energy level. The element with higher binding energy shows its higher oxidation state, whereas the lower binding energy is the evidence for an increased electron density around the element.

The binding energy of the photoelectron is characteristic of the orbitals from which the photoelectron originates which undergoes full relaxations of all atomic orbitals towards the hole in the core level. There exists a coupling between orbit and spin angular momentum and is given by the spin-orbit interaction. The spin-orbit interaction is very large for core holes and in general two peaks or structures will be visible in the spectrum, separated by the core hole spin-orbit splitting. The intensity ratio of $2p_{1/2}$ and $2p_{3/2}$ is 1:2 and that of $3d_{3/2}$ and $3d_{5/2}$ is 2:3. This rule breaks down if there are other interactions which mix with spin-orbit splitting. The emitted photoelectrons are collected by an electron energy analyzer such as a hemispherical mirror analyzer to produce a spectrum of the number of electrons versus their binding energy, which provides the quantitative information about the composition of the near surface region of the sample (21-25).

XPS spectra were recorded in an indigenously developed electron spectrometer equipped with Thermo VG Clamp-2 Analyser and a Mg Kα X-ray source (1253.6 eV, 30mA × 8 kV). A thin sample wafer of 12 mm in diameter was used in these studies. As an internal reference for the absolute binding energy of C 1s peak at 284.6 eV was used.

2.5.9 Raman Spectroscopy

Raman spectroscopy is spectroscopic technique, named in honors of Sir C. V. Raman, based on his valuable discovery of theory behind it. It is used to study the vibrational, rotational and other lower frequency modes in condensed matter physics and chemistry. It also provides the information about the phase purity of the solid material under investigation. Raman effect occurs when light impinges upon a molecule and interacts with the electron cloud of the bonds of that molecule. The incident photon excites the molecule into a virtual state. For the spontaneous Raman effect, the molecule will be excited from the ground state to a virtual energy state, and relax into a vibrational excited state, which generates Stokes Raman scattering. If the molecule was already in an elevated vibrational energy state, the Raman scattering is then called anti-Stokes Raman scattering. A change in the molecular polarization potential or amount of deformation of the electron cloud with respect to the vibrational coordinate is required for the molecule to exhibit the Raman effect. The amount of the polarizability change will determine the Raman scattering intensity, where as the Raman Shift is equal to the vibrational level that is involved.

The Raman spectra of the sample were collected on UV-Vis. Raman spectrometer system (Horiba Jobin Yvon LabRam HR) and scattered photons were measured with UV sensitive liquid nitrogen cooled CCD detector

2.5.10 Thermal Analysis

The thermal stability of a solid material is determined by the technique called thermo gravimetric analysis and is reported as change in weight loss as function of time. In addition to the stability, it gives the information about drying range, hydration, decomposition temperature, phase change etc. Its derivative mode of weight loss curve (DTG) can be used to tell the point at which weight loss is most prominent. Some instruments also perform the

recording of the temperature difference between the specimen and one or more reference pans (differential thermal analysis or DTA) or the heat flow into the specimen pan compared to that of the reference pan (differential scanning calorimetry or DSC). A plot of the differential temperature, ΔT, against the programmed temperature, T, indicates the transition temperatures with its exothermic or endothermic nature. When an endothermic change occurs, the sample temperature lags behind the reference temperature because of the heat in the sample. Exothermic behaviour is associated with the decrease in enthalpy of a phase or a chemical system. DTA and thermo gravimetric analyses are often run simultaneously on a single sample.

The thermo gravimetric measurement is normally carried out in air or in an inert atmosphere, such as Helium or Argon. The analyzer usually consists of a high-precision balance with a pan (generally platinum) loaded with the sample. The pan is placed in a small electrically heated oven with a thermocouple to accurately measure the temperature. The atmosphere may be purged with an inert gas to prevent oxidation or other undesired reactions (26-29).

TG/DTA were done on a Perkin Elmer Pyris Diamond thermo gravimetric / Differential thermal analyzer instrument under nitrogen atmosphere at a heating rate of 10 ºC/min from room temperature to 700 ºC with samples mounted on a Platinum sample holder.

2.6 Photocatalytic activity study

The experiments were carried in Oriel Arc lamp system designed to produce uniform illumination (Oriel Uniform Illuminator). This system delivers a 1.0 inch (2.54 cm) diameter collimated beam. The work plane is 2.6 inches (6.65 cm) from the bottom of the beam turning assembly. Uniform illuminator contains a fan cooled lamp housing that offers a temperature controlled, stable environment for the lamp. The light source used in this

system is 100 W Xe ozone free lamps with an average life of 500 hours. The various filers used in this system are i) dichoric mirror of wavelength in between 200 nm- 30 micron full reflector with irradiance of 163 mW/cm^2 for complete reflection, ii) 280-400 nm dichoric mirror with irradiance of 29.9 mW/cm^2 for UV irradiation and iii) 420-630 nm dichoric mirror (cold mirror) with irradiance of 64.7 mW/cm^2 for visible irradiation.

Studies involve a 10 ml of 10^{-4} M aqueous solution of sample taken in beaker placed below the beam turning assembly unit which holds the dichoric mirrors under room temperature. The mixture was stirred for 30 minute to achieve the adsorption equilibrium before the lamp was turned on for the photocatalytic reaction to begin. After the irradiation, the sample solution was taken out, centrifuged to remove the catalyst particles and properly diluted to measure its absorbance/ concentrations at characteristic wavelength. From this its percent of degradation is calculated. In the case of dyes the absorbance /concentrations were measured using UV-Visible Spectrophotometer (Spectrascan UV 2600 – Chemito) and for other pollutants were analysed by HPLC (Dionex Ultimate 3000) with photo diode array UV detector and a 5μm Thermo Hypersil ODS-2 C-18 reverse phase column (150 X 4.6mm). The experiments were repeated and its average value was reported.

Percent of degradation is calculated as follows:

Percent of Degradation = **{Co – C} x 100 / Co**

Where Co and C are the concentration of sample before and after irradiation

In the case of dyes such as methylene blue, rhodamine B and crystal violet the degradation studies were conducted using dichoric mirror filters with 280-400 nm for UV source and a full reflector of 200nm- 30 micron white light source for visible light. While in the case of dye the acid red 1 and all other pesticides such as 2,4-dichlorophenoxyacetic acid [2,4-D], 2,4,5-trichlorophenoxy

acetic acid[2,4,5-T], monolinuron[3-(4-Chlorophenyl)-1-methoxy-1-methylurea.] and aldicarb [2-methyl-2(methylthio)propionaldehyde-O-methyl carbamoyl-oxime] the degradation studies were conducted using dichoric mirror filters with 280-400 nm, 420-630 nm respectively for UV and visible light. For antibacterial studies dichoric mirror of 420-630 nm was used as the source of visible light.

References

[1] Reshmi R., "Physicochemcial and biochemical characterisation of enzymes immobilized on inorganic matrices" Ph. D thesis (2009).

[2] Xiaobo C.; Samuel S. M., Chem. Rev. 107 (2007) 2891.

[3] Antonelli D. M.; Ying J. Y., Angew. Chem. Int. Ed. Engl. 34 (1995) 315.

[4] Wang Z. L., "Characterisation of nanophase materials", Wiley-VCH, Chapter 2, Weinheim (2000).

[5] Whiston C., "X-ray methods", ACOL, Tmames Plytech, London (1991).

[6] Lipson H.; Steeple H., "Interpretation of X-ray Powder Diffraction Patterns", Macmillan, London (1970) 261.

[7] Hodnett B. K., "Heterogeneous catalytic oxidation: fundamental andtechnological aspect of selective and total oxidation of organic compound", John Wiley, New York, (2000).

[8] Bragg W. H.; Bragg W. L., "The Crystalline State, McMillan", New York Vol. 1 (1949).

[9] Biz S.; Occelli M., Catal. Rev. Sci. Eng., 40 (1998) 329.

[10] Hecht H. G., "Modern aspects of reflectance spectroscopy", W. W. Wendlandt (Eds.), Plenum press, Newyork (1968).

[11] Kubelka P.; Munk F., Tech. Phys., 12 (1931) 593.

[12] Joyes J., "Studies on Catalysis by titania", Ph. D thesis (2009).

[13] Brunauer P.; Emmett P. H.; Teller E., J. Am. Chem. Soc. 60 (2) (1938) 309.

[14] Goldstein J. I.; Newbury D. E.; Echlin P.; Joy D. C.; Fiori C.; Lifshin E., 'Scanning Microscopy and X-Ray Microanalysis', Plenum Press, New York (1981).

[15] Charles N. S., "Heterogeneous catalysis in Industrial Practice" 2nd edn., McGraw-Hill International (Edn.), (1993).

[16] Wachs I. E., "Characterisation of Catalytic Materials", Butterworth-Heinemann: Manning (1992).

[17] Matta J.; Courcot D.; Abiaad E.; Aboukais A., Chem. Mater. 14 (2002) 411.

[18] Thomas J. M.; Lamber R. M., "Characterisation of catalysis". John Wiley (1980).

[19] Brent F.; James H., "Transmission electron microscopy and diffractometry of materils", 3rd edn., Springer Verlag Berlin Heidelberg (2008).

[20] Leonid A. B.; Frank W. G., J. Res. Natl. Inst. Stand. Technol. 106 (2001) 997.

[21] Thomas J. M.: Gai P.L., Adv. Catal. 48 (2004) 171.

[22] Kung H. H., J. Solid state Chem. 52 (1984) 191.

[23] Kung M. C.; Kung H. H., Catal. Rev. Sci. Eng. 27 (1985) 425.

[24] Shirley D. A., Phys. Rev. B 5 (1972) 4709.

[25] Sherwood, P. M. A.; Briggs D.; Seah M. P., "Practical surface analysis" Wiley, Newyork (1990).

[26] Wendlandt W. M., "Thermal methods of analysis", Wiley, New York (1974).

[27] Dodd J.W.; Tonge K. H., "Thermal methods: analytical chemistry by open learning" Wiley, Chichester (1987).

[28] Maciejewski M.; Baiker A., J. Therm,. Anal. 48 (1997) 611.

Chapter 3

Results and Discussions

Contents

Synthesis of a compound with desired properties depends on its method of preparation and its characterisation. These are functionalized by various qualitative, quantitative, sensitive and specific techniques. Quantitative determination of composition and structure on the atomic scale is one of the major advantages of characterisation techniques. The research work behind the area of photocatalysis is mainly focused on the synthesis and characterisation of titania and its modified material with variety of applications. The main aim of characterisation is to correlate between structure and physiochemical properties with its the photocatalytic activities.

3.1 Introduction

In heterogeneous catalysis, the reactions most probably occur on its surface. Therefore it is necessary to characterize the catalyst to get a correct correlation between its physio-chemical properties and catalytic performance (1). In this chapter we discuss the results of characterisation techniques carried out on the prepared catalysts. The techniques are X-ray diffraction analysis (XRD), UV-Visible Diffuse reflectance spectroscopy (UV-Vis. DRS), CHNS elemental analysis, Scanning electron microscopy (SEM), Energy dispersive X-ray analysis (EDX), Transmission electron microscopy (TEM), High resolution TEM analysis (HRTEM), Selected area electron diffraction (SAED), X-ray photoelectron spectroscopy (XPS), Raman spectra analysis (RAMAN), and thermo gravimetric analysis(TG).

3.2 Optimization of catalyst

In the initial stages of the research focused on the preparation of pure titania and non-metal doped titania. In this purpose we used titanium tetraisopropoxide as the precursor for titania with isopropyl alcohol as the solvent source. We used several dopants sources such as urea, thiourea, ammonium chloride, liquid ammonia, triethylamine, diphenylamine, triethanolamine, orthophenylene diamine, aniline, ammonia etc for the preparation of non-metal doped titania. All the prepared catalysts were characterized by CHNS elemental analysis for the presence of dopant content, UV-Vis. DRS for the calculation of band gap and XRD analysis for the phase purity and crystallite nature. From these, we selected nitrogen doped titania catalyst obtained from urea and nitrogen sulphur co-doped titania catalyst obtained from thiourea as the dopant source for further studies. The preparations are repeated with same experimental conditions for the selected catalysts. The same characterisation techniques are also repeated and show a very good correlation results.

We also prepared different pure and modified catalyst with variations in amount of dopants concentration, amount of precursor concentration and different calcination temperature. The photocatalytic ability of all the prepared catalysts was evaluated by studying the degradation of aqueous solution of methylene blue in sunlight. From the activity studies we optimized nitrogen doped and nitrogen sulphur co-doped titania catalyst calcined at 400 ^{O}C by using 1:10 volume ratio of titanium isopropoxide to isopropy alcohol with 10% aqueous solution of urea and 1 % aqueous solution of thiourea respectively. And these are denoted as N-TiO_2 and NS-TiO_2. For the comparative study we also selected two other catalysts, for each optimized doped system with higher and lower amount of dopant source. Thus for nitrogen doped titania we used 5 % and 12.5 % aqueous urea solution, and for nitrogen sulphur co-doped titania we used 0.5 % and 2.0 % aqueous thiourea solution respectively. These are denoted as N-TiO_2 (l), N-TiO_2 (h), NS-TiO_2 (l) and NS-TiO_2 (h). For the preparation of pure titania same experimental conditions are repeated without adding the dopant source and it is denoted as L-TiO_2.

The physical appearance such as colour of the pure titania, nitrogen doped titania, nitrogen sulphur co-doped titania are white, yellow and slight less deep yellow respectively. The colour change in modified catalyst compared to pure titania indicates that the presence of some impurities incorporated into the network of titania. Later it is confirmed from other characterisation techniques that nitrogen and sulphur are these impurities.

3.3 X-ray Diffraction Analysis (XRD)

The crystallographic phases present in a sample are well understood from its X-ray diffraction pattern. X-ray diffraction analysis provides a powerful tool to understand the phase purity of the samples. It is widely used for determining the three dimensional structure of solid materials. It also provides the information such as crystallite nature, crystallite size, unit cell

dimensions etc. (2). Fig. 3.1 shows the XRD pattern obtained for the samples of nitrogen doped titania (N-TiO_2), nitrogen sulphur co-doped titania (NS-TiO_2), pure titania (L-TiO_2) and commercial anatase titania (A-TiO_2) using Bruker AXS D8 advance X-Ray Diffractometer with Ni filtered Cu Kα radiation source (λ = 1.5406 A^o) by recording 2θ in the range of 10-70 ^{O}at a scan rate of 0.5 ^{O}/min.

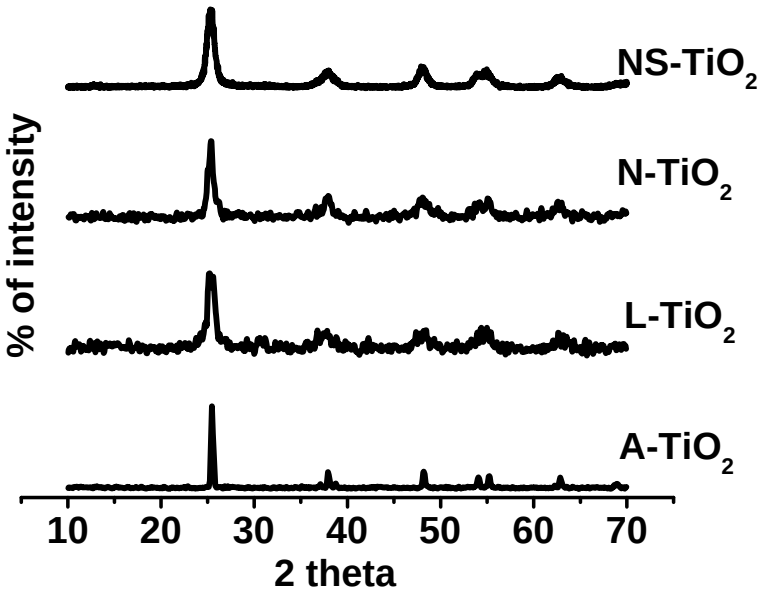

Fig. 3.1. XRD spectra of pure and modified titania

The spectra showed that all the prepared catalyst give peaks at 2θ values around 25.4, 37.8, 55.1 and 62.8. These values correspond to the peaks of anatase phase (compared with standard value obtained from JCPDS data). Thus it is clear from the spectrum that all the prepared catalysts are in purely anatase with main peak at 2θ value of 25.4 corresponding to the (101) plane. The absence of peaks corresponding to the other phases indicated that all the prepared catalysts are purely anatase. There are no characteristic peaks corresponding to dopants due to their very small concentration. This reveals that the incorporation of dopants in the titania lattice do not make change on the its structure.

It is also noted from the spectra that all the prepared catalysts are well crystalline in nature. Crystallite size is determined by measuring the broadening of a major peak in a diffraction pattern associated with a particular planar reflection within unit cell of the crystal. It is inversely related to the FWHM (full width at half-maximum) of an individual peak. If the crystallite sizes are small then it can be randomly arranged or have low degrees of periodicity which results in the broadening of peak. If the crystallites are big, the periodicities of the individual crystallite domains reinforced resulting in a tall narrow peak (3). Thus larger the crystallite size, narrower the peak.

Crystallite size is a measure of the size of a coherently diffracting domain. The presence of poly crystallite aggregates show that crystallite size is not generally the exactly same as particle size. The average crystallite size is calculated from the broadening of the (101) XRD peaks of anatase using the Scherrer* equation and are reported in Table 3.1. It is clear from the Table that prepared samples are the nano sized particles with in the range of 10-12 nm. The broadening of the peaks in the prepared samples indicated that the particles size is decreased compared to commercial sample, having sharp peak (4,5). It was worth to note that the crystallite size in the range of 11-13 nm contributed to the optimum for photocatalytic activity mentioned by Wang et. al. This is because a very small crystallite size causes a blue shift in the absorption spectrum and favours surface recombination of the photo-excited holes and electrons while a larger crystallite size exhibits lower surface area and thus a smaller number of catalytic active sites per unit mass of catalyst (6-9).

* Scherrer equation, $\mathbf{D = K\lambda / \beta \ Cos\ \theta}$

Where **D** is the crystallite size, **θ** and **λ** are the Bragg angle and the wavelength of the X-ray used. **K** is a constant approximately equal to 0.89; **β** is the full width half maximum of the strongest peak at θ value.

Table 3.1. Crystallite size, bandgap and surface area of the prepared catalysts
a- Crystalline size calculated from XRD
b-Band gap calculated from UV-Visible DRS spectrum

Catalyst	Crystallite size (nm)[a]	Band gap (eV)[b]	S.A $_{BET}$ (m^2/g)
NS-TiO2	10.0	2.3	100.9
N-TiO2	9.6	2.3	122.9
L-TiO2	11.6	3.1	85.7
A-TiO2	36.2	3.2	12.7

3.4 UV-Visible Diffuse Reflectance Spectroscopy (UV-Vis.DRS)

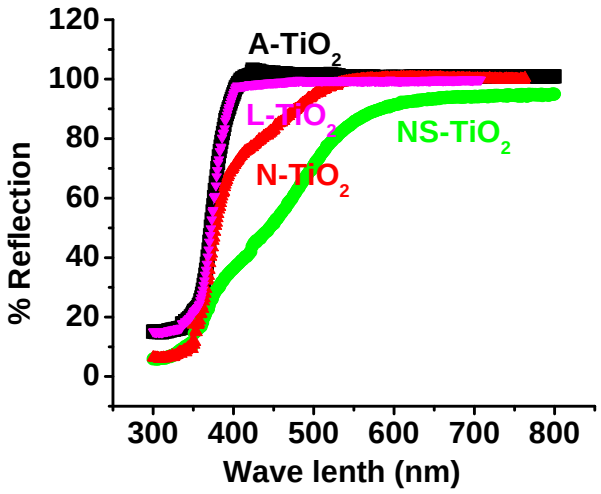

Fig. 3.2. UV-Vis. DRS spectra pure and modified titania

UV-Vis Diffuse reflectance spectroscopy is one of the spectroscopic techniques used for the insoluble solid materials. This technique allows the analyst to take advantage of the reflection of the incoming beam rather than using standard absorption configuration. Since only the surface of the sample is responsible for reflection and absorption of the incident radiation, it is used in the surface science of chemistry and physics. The most appropriate theory behind the diffuse reflections and transmission of light scattering layers is

developed by Kubelka and Munk (9-11). For an infinitely thick, opaque layer the Kubelka-Munk equation can be written as

$$F(R\alpha) = (1-R\alpha)^2 / 2R\alpha = k/s$$

Where **Rα** is the diffuse reflectance of the layer relative to a non absorbing standard such as $BaSO_4$, **k** is molar absorption coefficient of sample and **s** is the scattering coefficient.

A classical semiconductor exhibits minimal optical absorption for photons with energies smaller than the bandgap and high absorption for photons with energies greater than the bandgap. As a result, there is a sharp increase in absorption at energies close to the bandgap that manifests itself as an absorption edge (or reflection threshold) in the UV-Vis. absorption spectrum. For titania which has a bandgap between 3.0-3.2 eV, this absorption edge occurs at about 385-400 nm (see Fig 3.3). That is charge transfer from the valence band (mainly formed by 2p orbitals of the oxygen anions) to the conduction band (mainly formed by 3d orbitals of titanium cation) (12, 13).

The band gap of catalyst is calculated using following equation.

$$\mathbf{E = hv = hc / \lambda} \quad \text{or}$$

$$\mathbf{E = 1240 / \lambda\ (nm)}$$

E is the band gap in eV and **λ** is the wavelength from which reflection taken place

(This relation is called one of the simple version of KM (Kubelka-Munk) equation. The **λ** value obtained from the spectrum as shown in Fig.3.3).

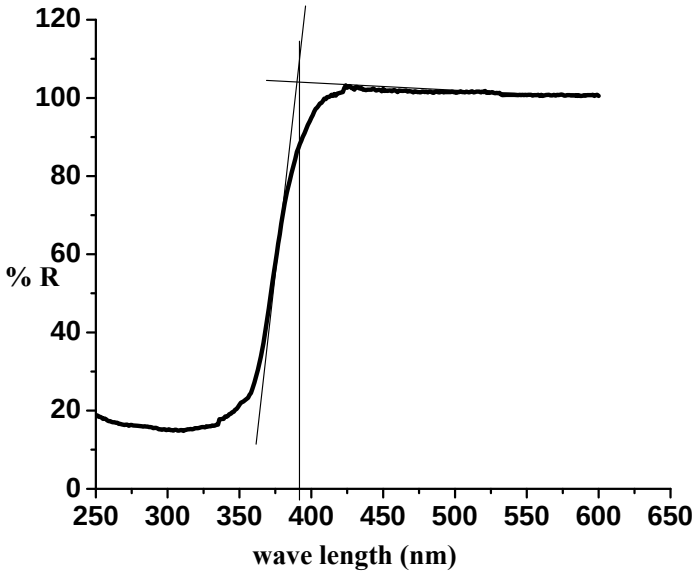

Fig.3.3. UV-Vis. DRS of pure titania

Fig.3.2 shows the UV-Vis diffuse reflectance spectra of the samples measured in the range of 200-900 nm using on Labomed UV-VIS Double beamUVD-500 spectrophotometer equipped with an integrating sphere assembly, using $BaSO_4$ as reflectance standard with a CCD detector.

From the figure it is clear that both the modified catalyst (N-TiO_2 and NS-TiO_2) gives a shift in absorption in the visible region compared to the pure samples. This indicated that the incorporation of impurities such as N and S in titania system, which responsible for the visible light absorption of the catalyst. The calculated values of band gap of all the catalysts are shown in Table 3.1. The decrease of bandgap may be attributed to the incorporation dopants energy states between the energy states of titania. That is the energy states of dopants such as 2p level of Nitrogen and 3p level of sulphur creates an intermediate energy level within the valence band and conduction band of pure titania. The two absorption edges in the modified catalyst are attributed to the pure titania and impurities such as nitrogen and sulphur are incorporated states of titania.

3.5 CHNS Elemental analysis

The presence of dopants elements in the modified catalyst were also confirmed from their elemental analysis. The CHNS elemental analysis was performed using a Elementar Vario EL III apparatus.

Table 3.2. CHNS elemental analysis of pure and modified titania

Catalyst	% Nitrogen	% Sulphur
N-TiO_2 (l)	0.41	--
N-TiO_2	0.69	--
N-TiO_2 (h)	0.73	--
NS-TiO_2 (l)	0.12	0.88
NS-TiO_2	0.18	1.14
NS-TiO_2 (h)	0.19	1.28

The results are shown in Table 3.2. The results indicated that the dopants such as nitrogen and sulphur are incorporated in the modified catalysts. It also noted that the percentage of dopant increases with increase in the dopant source concentration. At higher concentration of dopants source, the increase of dopant incorporated in the catalyst is not much significant. From the initial activity study we selected N-TiO_2 and NS-TiO_2 for further studies.

3.6 Scanning Electron Microscopy

The catalytic morphology can affect the transport of reactants and products to or from its active sites, its light absorption power and generation of photo excited species (9). Studies of the catalytic morphologies are an important parameter for interpreting the photocatalytic activity. The morphologies are noticeably dependent on the preparation procedure and the composition. Surface morphology of the catalysts is also observed from its TEM images.

The scanning electron microscopic images of the nitrogen doped and nitrogen sulphur co-doped titania are shown in Figure 3.4 and 3.5 respectively. The images show that the particles are somewhat spherical in nature and some are rectangular in shape. Most of them are shapeless due to the agglomerated crystallite powder morphology.

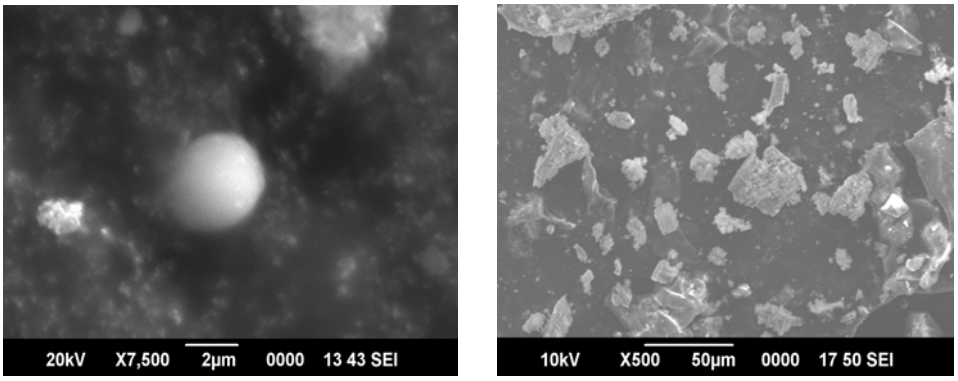

Fig. 3.4. SEM images of N-TiO_2

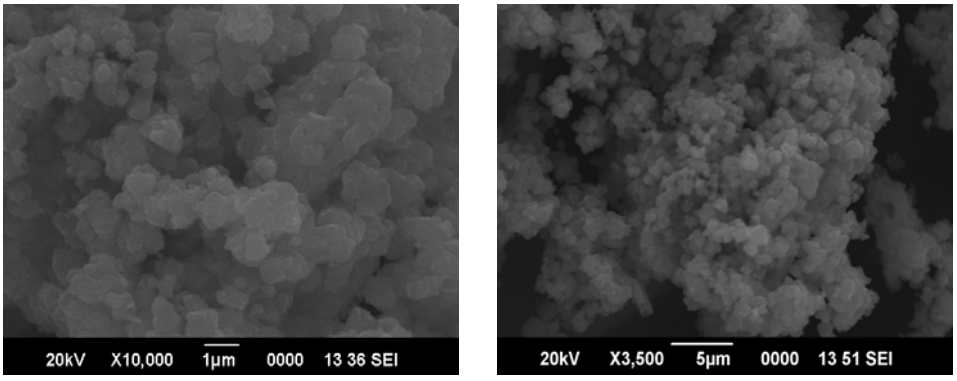

Fig. 3.5. SEM images of NS-TiO_2

3.7 Energy Dispersive X-ray analysis

The energy dispersive X-ray analysis gives both qualitative and quantitative information about the elemental composition of the materials. From the EDX spectra we can conclude that the presence other materials such as impurities or adducts in the samples. These impurities occur either accidently with the reagents molecules or added for modification of the

basic materials. The intensity of the spectra correlates with the amount of elements present in it. The EDX spectra of catalysts nitrogen doped titania and nitrogen sulphur co-doped titania are shown in fig. 3.6 and 3.7 respectively. The presence of doped elements such as nitrogen and sulphur in modified samples are clearly shown in the spectra of these catalysts. This indicates the incorporation of dopants such as nitrogen and sulphur in the titania network. As per the in efficiency of the instrument for the quantification elements of atomic number less than eleven, we can only give the qualitative information (not shown here) about the elemental composition of catalysts. The chemical compositions of the catalysts were obtained from JEOL Model JED-2300, energy dispersive X-ray analyzer used in conjunction with SEM.

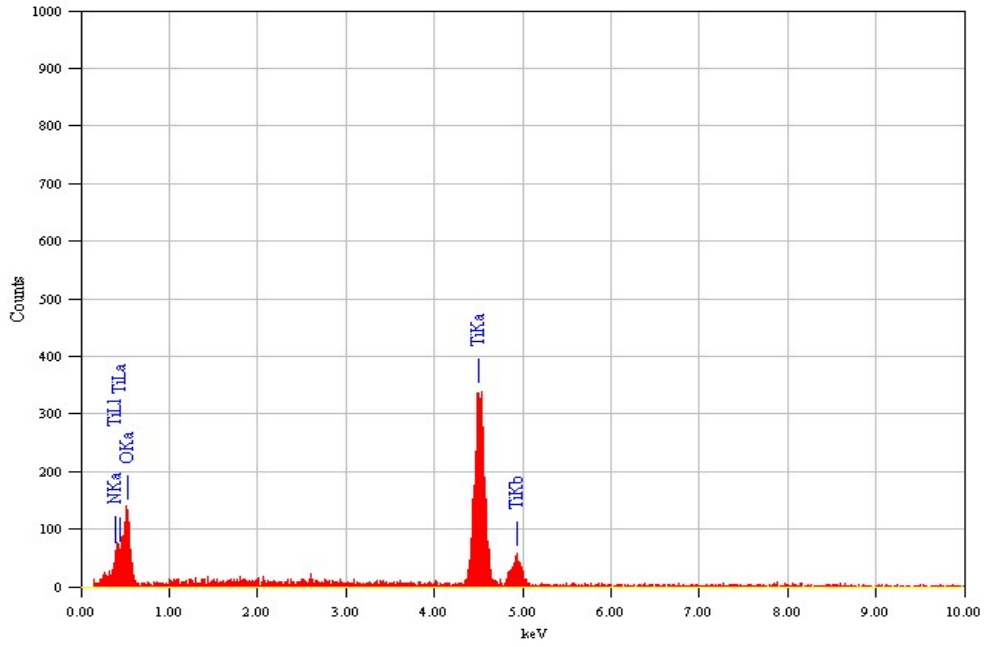

Fig. 3.6. EDX spectra of N-TiO_2

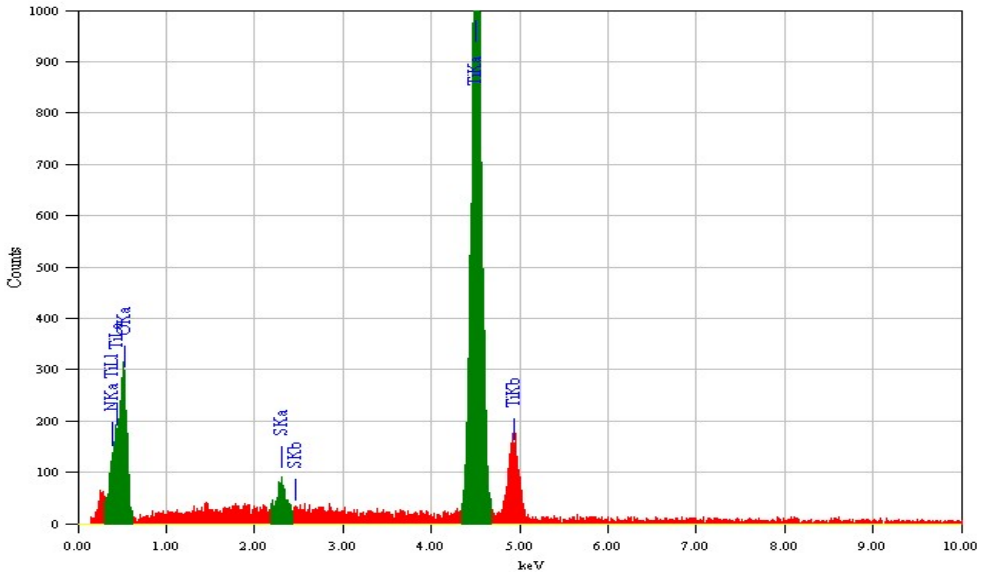

Fig. 3.7. EDX spectra of NS-TiO_2

3.8 Transmission Electron Microscopy

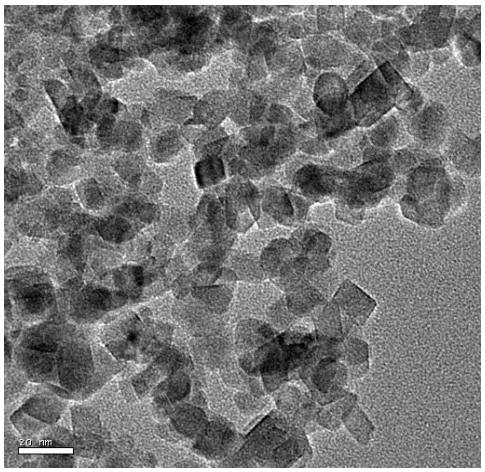

Fig. 3.8. TEM image of N-TiO_2

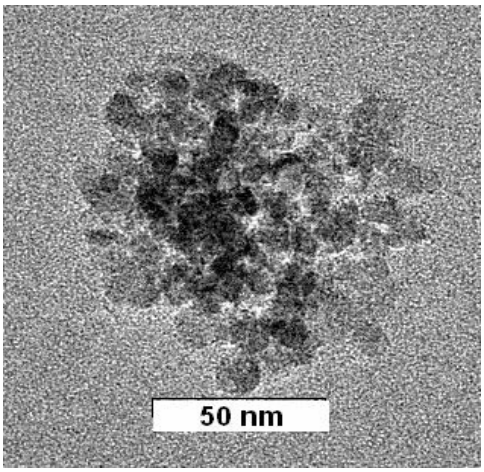

Fig. 3.9. TEM image of NS-TiO_2

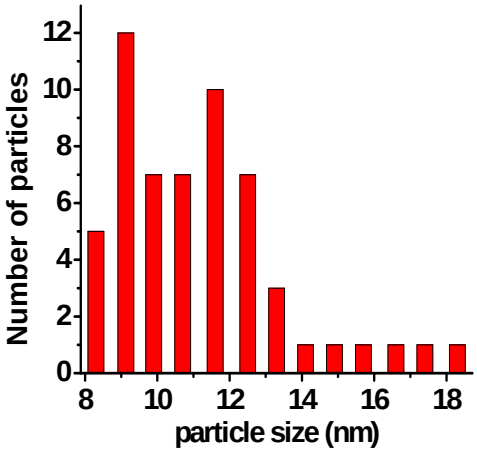

Fig. 3.10. Particle size histogram of N-TiO_2

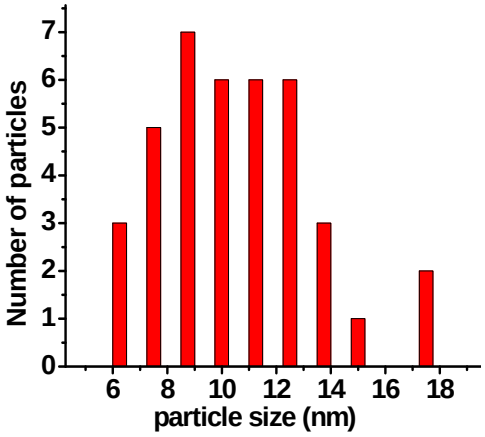

Fig. 3.11. Particle size histogram of NS-TiO_2

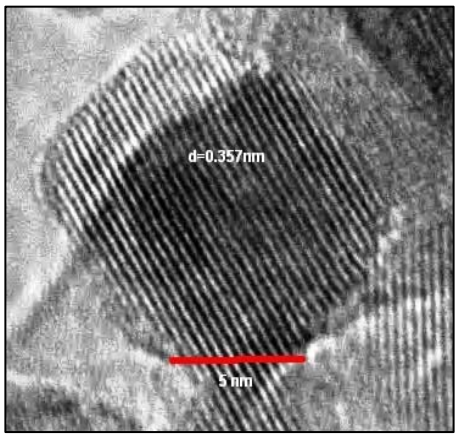

Fig. 3.12. HRTEM image of N-TiO_2

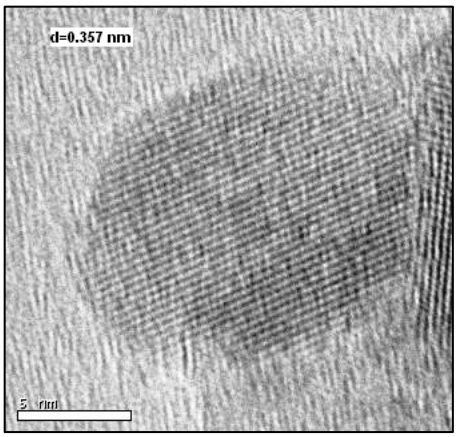

Fig. 3.13. HRTEM image of NS-TiO_2

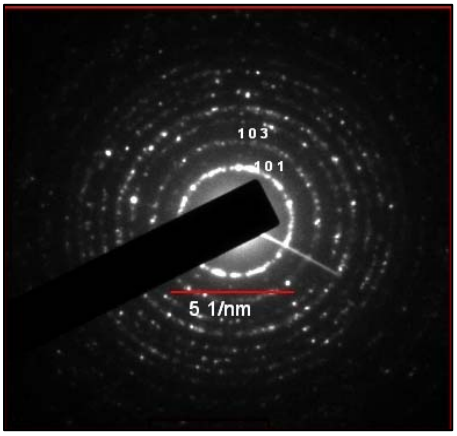

Fig. 3.14. SAED image of N-TiO_2

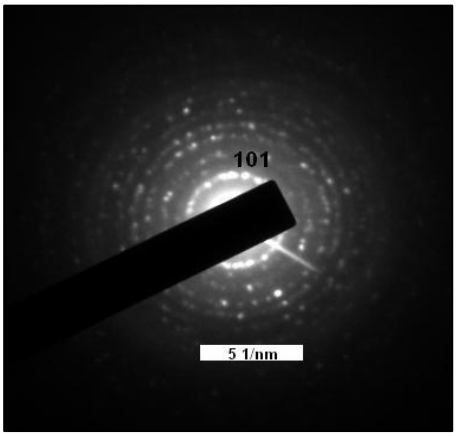

Fig. 3.15. SAED image of NS-TiO_2

The Transmission Electron Microscopic (TEM) images of the modified catalysts N-TiO_2 and NS-TiO_2 are shown in Fig. 3.8 and 3.9 respectively. It can be noted from the images that the particles are agglomerated and exhibit both spherical and rectangular shapes. These are also in agreement with results of SEM images. Further observations indicate that the morphology of modified TiO_2 powders is very rough and may be beneficial for enhancing the adsorption of reactants due to its great surface roughness and high surface area.

Fig. 3.10 and 3.11 indicates the particle size histogram of the modified catalysts N-TiO_2 and NS-TiO_2 respectively. The results showed that both the catalysts give an average particle size of 7-13 nm. This result roughly indicated very good correlation of crystallite size obtained from XRD analysis. This crystallite size is believed to be correlated with the optimum size for better photocatalytic results (6).

The High resolution TEM images of the both catalysts are shown in Fig. 3.12 and 3.13. Particles in nano size range are clearly observed from the images. Both catalysts give around the same d value (d=0.357nm) obtained from their respective HRTEM images. These values give very good correlation with the d value obtained from the XRD spectrum of the respective catalyst, and this corresponds to the major anatase 101 planes. This result once again confirms the formation of purely anatase phase of the prepared samples. The images also indicated that the particles are well ordered and highly crystalline nature.

Fig. 3.14 and 3.15 show the selected area electron diffraction (SAED) pattern of the modified catalyst N-TiO_2 and NS-TiO_2 respectively. Electron diffraction reveals that each particle is composed of many small crystal nuclei, which is a convincing proof that the particles grow in aggregation model. The

well clarified electron diffraction pattern (used for the identification of crystallographic spacing) indicates that those particles are highly crystalline and well ordered. The d value corresponding to each pattern is calculated using the following equation.

d = L h / R √(2ME). Where

L = Camera constant

h = Plank's constant

E = Energy of electron beam

M = Mass of electron

R = Radius of the diffraction circle.

Thus the d value obtained from the main diffraction circle is approximately equal to 0.357 nm, which corresponds to the anatase 101 plane. Thus this result indicates that the prepared catalysts are purely anatase with major 101 planes, which is also good agreement with that obtained from the XRD results.

3.9 X-ray Photoelectron Spectroscopy (XPS)

The atomic concentration values derived from the XPS data are presented in Table 3.3–3.6. For oxygen the 1s XPS spectra was de-convoluted using Gaussian multi-peak fitting program and peak area of 529.3 eV peak was taken for atomic ratio calculation purpose. Peak areas for corresponding peaks were divided by the sensitivity factors in these calculations. The values of sensitivity factors used in these calculations are given in Table 3.7. It may be noted that at some places C 1s peak with binding energy value of 284.8 eV is referred as standard value for the surface adventitious carbon. Thus if we include this correction the B.E. values observed in present study will be shifted to higher side by 0.2 eV.

Fig. 3.16 and 3.17 represents the Ti 2p XPS spectra of catalyst N-TiO_2 and NS-TiO_2 respectively. In each case there are two peaks. For N-TiO_2 peaks appear at 458.2 and 464.7 eV and for NS-TiO_2 peaks appear at 458.4 and 464.1 eV respectively. These are assigned to the Ti $2p_{3/2}$ and Ti $2p_{1/2}$ states. These doublet peaks are due to the spin-orbit splitting of Ti 2p (14). The above value indicates that titanium exists as Ti^{4+} with stable Ti-O bond in the prepared catalysts. There is no evidence for the existence of Ti^{3+} states. But for the pure titania (from literature) these peaks are observed at 458.9 and 464.7 eV respectively, which are contributed by O-Ti-O in TiO_2 (4,15,16). Compared with this, the Ti 2p peaks for both modified catalysts show a smaller shift in the binding energy. These shifts of Ti $2p_{3/2}$ and Ti $2p_{1/2}$ core level signals suggesting the successful incorporation of the dopant into the titania lattice, which are attributed to Ti 2p peaks of N-Ti-N or O-Ti-N in modified titania (17).

Table 3.3. Atomic ratio derived from XPS data of Ti $2p_{3/2}$

Catalyst	Ti $2p_{3/2}$ peak			Ti:O:N/ Ti:O:N:S
	B.E. (eV)	FWHM (eV)	Peak Area	
N-TiO_2	458.2	1.07	977.9	1 : 1.80 : 0.27
NS-TiO_2	458.4	1.13	7194.8	1 : 1.86 : 0.09 : 0.18

Table3.7. Sensitivity factor obtained from XPS analysis

Element	XPS peak	Sensitivity Factor
Ti	2p3/2	5.22
O	1s	2.85
N	1s	1.74
S	2s	1.25

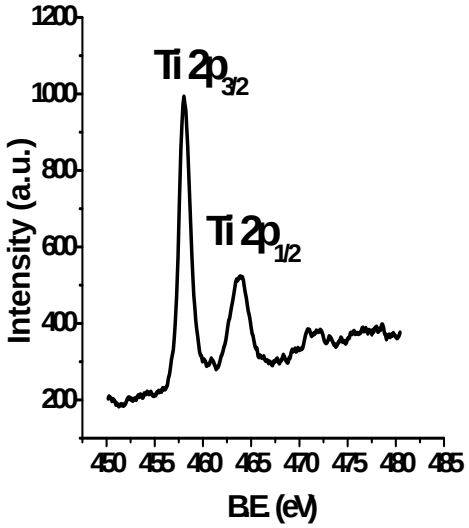

Fig. 3.16. Ti 2p XPS spectra of N-TiO_2

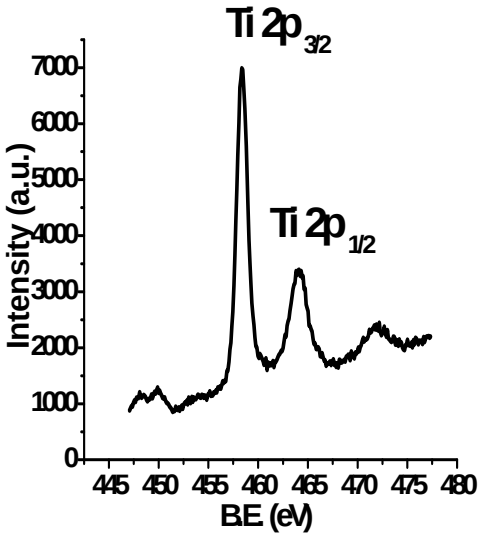

Fig. 3.17. Ti 2p XPS spectra of NS-TiO_2

The O 1s XPS spectrum of catalyst N-TiO_2 and NS-TiO_2 are shown in Fig 3.18 and 3.19. The valence band of titania is mainly constructed with O 2p state, which is hybridized with the Ti 3d states (18,19). It shows a strong peak at 529.3 eV corresponding to bulk oxygen bonded to titanium where as weak band at 531 eV is due to oxygen attached to N. The weak shoulder at higher binding energy is associated with hydroxyl groups or sulphate ions adsorbed on the TiO_2 surface. But in the case of catalyst NS-TiO_2 shows another weak shoulder at higher binding energy of 532.2 eV (not shown here) due to the effect of sulphur which exists as S^{6+} by replacing some of Ti.

Table 3.4. Atomic ratio derived from XPS data of O 1s

Catalyst	O 1s peak			Ti:O:N/ Ti:O:N:S
	B.E. (eV)	FWHM (eV)	Peak Area	
N-TiO_2	529.2	1.07	961.9	1 : 1.80 : 0.27
NS-TiO_2	529.4	1.05	7069.2	1 : 1.86 : 0.09 : 0.18

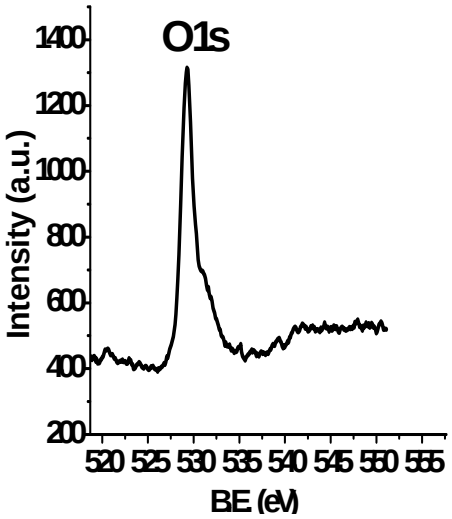

Fig. 3.18. O 1s XPS spectra of N-TiO_2

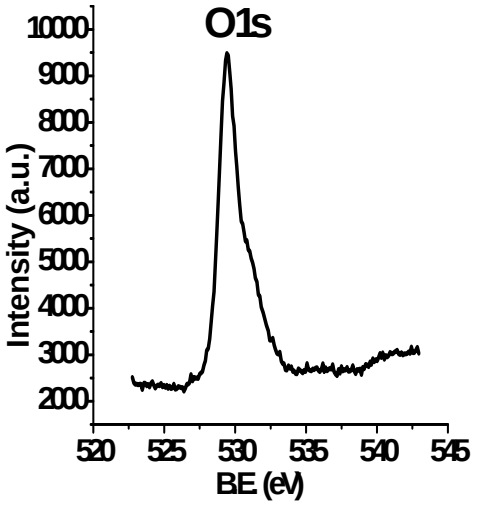

Fig. 3.19. O 1s XPS spectra of NS-TiO_2

The N 1s XPS spectrum of catalyst N-TiO_2 and NS-TiO_2 are shown in Fig. 3.20 and 3.21. The assignment of the XPS peak of N 1s has still been under debate, and controversial hypotheses have been provided. Since the preparation methods and conditions largely affect N XPS spectral features, the peak position may be different for the same compounds prepared by different methods. In addition, the N source is different, which could probably influence the characteristics of the N state. Asahi et.al.(20) assigned the atomic beta N peak at 396 eV to substitutional N, which may be related to the active sites in photocatalysis. Most researchers also agree on N 1s peak at 396.0 - 397.5 eV responsible for substitutional doping of N atoms into the TiO_2 lattice indicates the characteristic peaks of Ti-N-Ti type linkage (4,15,16,21). Both the substitutional and interstitial N could affect the electronic band structure of TiO_2 and improve the photocatalytic activity in visible light region (22). Some researchers attributed the N 1s peaks at binding energies at 400 and 402 eV to molecularly adsorbed nitrogen species. Burda et.al. (15) observed a N 1s core level at 401.3 eV in N-doped titania nano particles and suggested that it is attributed to the N atoms in the environment of O-Ti-N, based on the comparison with the

N 1s electron binding energy of TiN (397.2 eV). Viswanath et.al. and Ma et al. (4, 23) supported the above assignment and they concluded that the observed N 1s core level peak at 398-399 eV attributed to O-Ti-N linkage in the crystalline TiO_2 lattice.

The peak at 399.7 eV is also attributed to N-O bonds (24). It has also been reported that N 1s peak at around 400 eV can be assigned to molecularly chemisorbed gamma Nitrogen (25). Many researchers pointed out that the presence of oxidized nitrogen such as Ti-O-N and/or Ti-N-O linkages should appear above 400 eV (4,15,16,19,20,21). Di Valentin et. al. reported that there are two types of N species in N-TiO2 using electron paramagnetic resonance spectroscopy measurements and DFT calculations (26). Their spin-Hamiltonian parameters were consistent with calculations for both substitutional and interstitial N impurities. The N 1s peak observed at 399.6 – 399.9 eV, may also be attributed to the formation of hyponitite(17,27).

Thus the main peak which appears around 399 eV can be assigned to either substitutional N replaced O atom of the TiO_2 lattice or the interstitial N bound to one lattice oxygen and formed as NO species. None of the catalysts shows the peak at 396-397 eV attributed to atomic nitrogen (18). Therefore, the peak around 399.6 eV in Fig 3.20 is assigned to the O-Ti-N linkage. These can be further evidenced by the positively shifted binding energy of N 1s core level to 400.2 eV in NS-TiO_2 (Fig. 3.21). The shift of binding energy to higher values indicated a decrease in the electron density of N atom. In other words, some N atoms become more positive when the S incorporated. It is likely that nitrogen species coordinate to S in the form of O-S-N linkage, similar to the O-Ti-N as in the case of doped only with nitrogen.

Table 3.5. Atomic ratio derived from XPS data of N 1s

Catalyst	N 1s peak			Ti:O:N/ Ti:O:N:S B.E. (eV)
	B.E. (eV)	FWHM (eV)	Peak Area	
N-TiO_2	399.5	3.0	89.3	1 : 1.80 : 0.27
NS-TiO_2	400.3	2.41	485.9	1 : 1.86 : 0.09 : 0.18

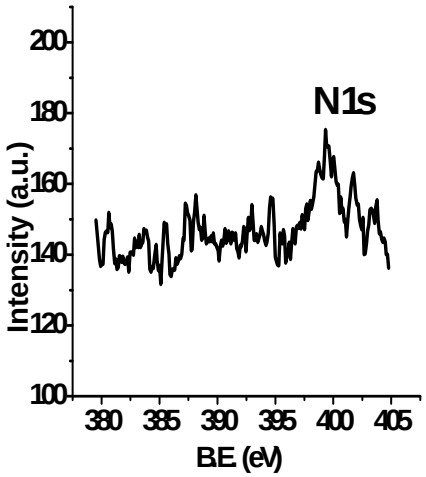

Fig. 3.20. N 1s XPS spectra of N-TiO_2

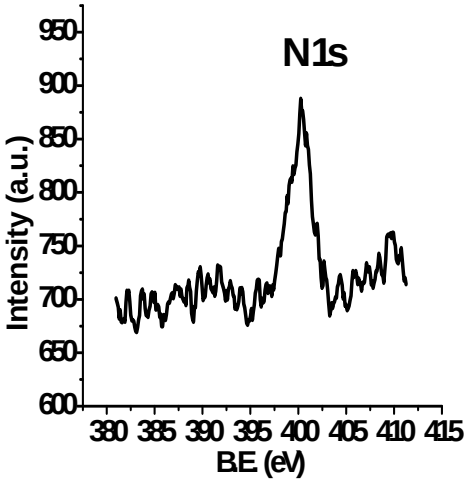

Fig. 3.21. N 1s XPS spectra of NS-TiO_2

Fig.3.22. represents the S 2p XPS spectrum of catalyst NS-TiO_2. T. Ohno and others reported that the peak of S 2p around 168.0 – 170.0 eV corresponds to the S atom incorporated as cation in the form of S^{6+} in titania network and are expected to replace with Ti ions. The peak around 160.0 – 163.5 eV corresponds to S atom in Ti-S state (14,28). Therefore, the absence of peak at 160-163.5 eV indicates that sulphur does not replace oxygen atoms in the TiO_2 lattice. And the peak at 168.5 eV could be assigned to S^{6+} state (as SO_4^{2-}). These sulphate ions can form S=O and S-O-S bonds on the TiO_2 surface, creating unbalanced charge on Ti and vacancies/defects in the titania network (14).

Table 3.6. Atomic ratio derived from XPS data of S 2p

Catalyst	N 1s peak			Ti:O:N/ Ti:O:N:S
	B.E. (eV)	FWHM (eV)	Peak Area	
N-TiO_2	-	-	-	1 : 1.80 : 0.27
NS-TiO_2	168.3	1.70	435	1 : 1.86 : 0.09 : 0.18

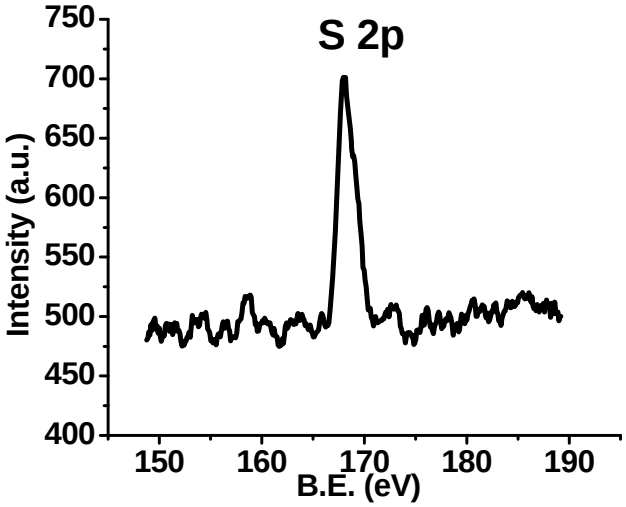

Fig. 3.22. S 2p XPS spectra of NS-TiO_2

3.10 Raman Spectroscopy

Raman spectra of the prepared catalyst are shown in Fig. 3.23. The results show that all the prepared catalysts give the peaks around 145, 397, 515 and 641 cm^{-1} which are the characteristic peaks of anatase. No other peaks correspond to the rutile phase indicating that the prepared catalysts are purely anatase. The absence of more additional bands except those corresponding to anatase also verified that the lattice distortion is minor, since a severe lattice distortion to a lower symmetry usually leads to the splitting of Raman modes.

From a measurement of the maximum of low frequency Raman band, it is possible to determine the nano particle size (not shown here). Since the particle size can cause large shifts in the location of the scattered Raman peaks and their widths, namely the quantum size confinement effect. Consequently,

compared with the lowest frequency peak at 145 of different samples, it can be evidently seen that the intensities of this peak are dramatically increased and its widths are broadened after the dopants introduced (14,29-31). It indicates that the crystallite nature is enhanced, phase purity is retained and the particle size is decreased, which correlates the results obtained from XRD and TEM results.

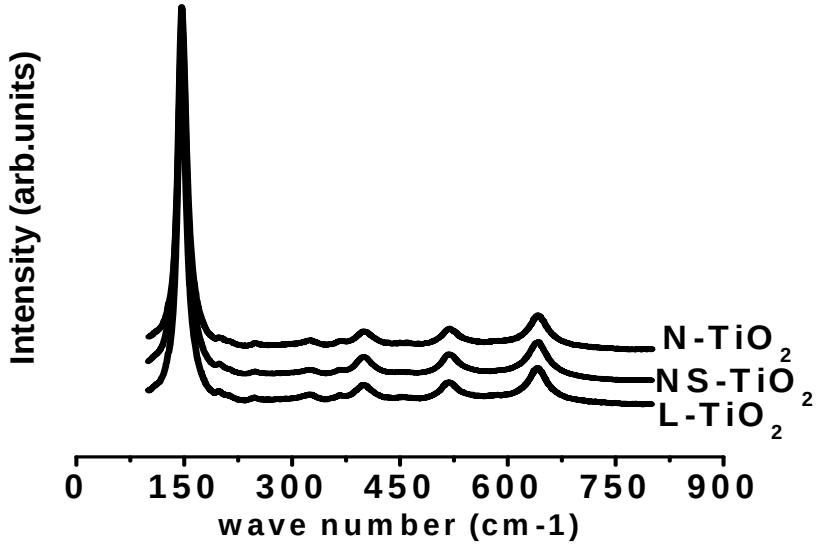

Fig. 3.23. Raman spectra of the prepared catalyst

3.11 Thermal Analysis

The thermo gravimetric analysis is a well established technique for evaluating the thermal stability of the materials. It finds widest applications in the determination of different parameters depending on preparation of catalyst. These are nature and composition of active phase, effect of added promoters or presence of impurities on the catalyst, dispersion of active phase and active phase support interactions, nature and heterogeneity of active sites on catalyst surface, mechanistic aspects of the reaction under investigation, transient chemical changes that occurs on the surface, catalyst deactivation and regeneration etc. This can also be used for quality

control and catalyst characterisation through finger print spectra of different batches of the same catalyst. The techniques involve the pursuit of weight of sample over a period of time while its temperature is raised linearly. Recording analytical data and the temperature curve with provision for controlled heating of sample is carried out. In a thermo gravimetric curve (TG), horizontal portions point out regions where there is no weight change, where as weight loss is indicated by curved portions(9).

Thermo gravimetric analysis was done on a Perking Elmer Pyris Diamond thermo gravimetric/differential thermal analyzer instrument under nitrogen atmosphere at heating rate of 10 ^{o}C/min from room temperature to 700 ^{o}C with samples mounted on a alumina sample holder. The thermo gravimetric analysis of the both modified catalyst N TiO_2 and NS-TiO_2 are shown in Fig. 3.24. The results indicated that both the catalysts give a very good thermal stability above the temperature of 400 ^{0}C . Initially there is a loss of weight due to removal of water molecules and above the temperature of 350 ^{0}C both compounds show no apparent loss of weight. So the catalysts can be prepared at a lower temperature.

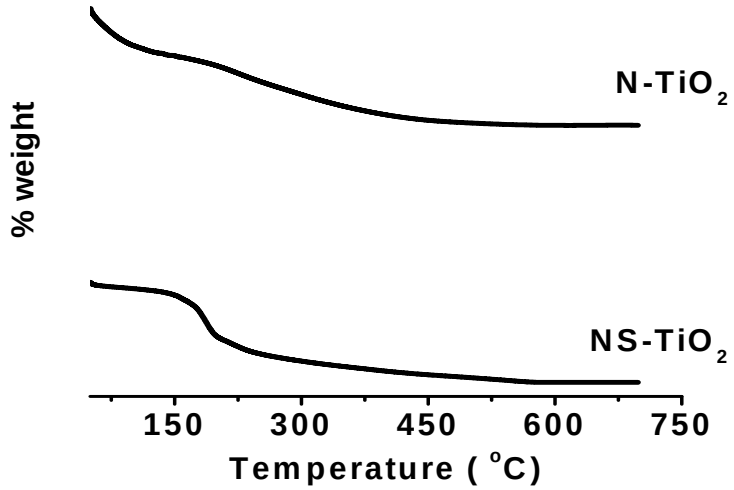

Fig. 3.24. Thermo gram of N TiO_2 and NS-TiO_2

References

[1] Ramaswamy A. V., "Catalysis principles and applications" Narora, New Delhi.

[2] Niemantsverdriet J. W., "Spectroscopy in Catalysis: An introduction" Wiley-VCH Verlag GmbH and Co. Weinheim (2007).

[3] Xiaobo C.; Samuel S. M.,. Chem Rev. 107 (2007) 2891.

[4] Sathish M.; Viswanathan B.; Viswanath R. P.; Gopinath C. S., Chem. Mater. 17 (2005) 6349.

[5] Li H. X.; Li J. X.; Huo Y. I., J. Phys. Chem. B 110 (2006) 1559.

[6] Wang Y. Q.; Ying J. Y., Chem. Mater. 11 (1999) 3113.

[7] Zhang Z.; Wang C. C.; Zakaria R.; Ying J. Y., J. Phys. Chem. B 102 (1998) 10871.

[8] Anpo M.; Shima T.; Kodamo S.; Kubokawa Y., J. Phys. Chem. 91 (1987) 4305.

[9] Joyes J., "Studies on Catalysis by titania" Ph.D thesis (2009).

[10] Sakthivel S.; Kisch H., Angew Chem. Int. Ed 42 (2003) 4908.

[11] Herrera J. E.; Resasco D. E., J. Phys. Chem. B 107 (2003) 3738.

[12] Kormann C.; Bahnemann D. W.; Hoffmann M. R., J. Phys. Chem. 92 (1988) 5196.

[13] Gerischer H.; Heller A., J. Phys. Chem. 95 (1991) 5261.

[14] Ying W.; Yan W.; Yanling M.; Hanming D.; Yougkui S.; Xian Z.; Xiaozhen T., J. Phys. Chem. C 112 (2008) 6620.

[15] Chen X.; Burda C., J. Phys. Chem. B 108 (2004) 15446.

[16] Wong M. S.; Chou H. P.; Yang T. S., Thin solid films 494 (2006) 244.

[17] Feng P.; Lingfeng C.; Hao Y.; Hongjuan W.; Jian Y., J. Solid state Chem. 181 (2008) 130.

[18] Tezuka Y.; Shin S.; Agui A.; Fujisawa M.; Ishii T.; Yagishita A., J. Elect. Spectrosc. Relat. Phenonm. 79 (1996) 195.

[19] Onishi H.; Aruga T.; Egawa C.; Iwasawa Y., Surf. Sci. 199 (1988) 54.

[20] Asahi R.; Morikawa T.; Ohwaki T.; Aoki K.; Taga Y., Science 293 (2001) 269.

[21] Sakthivel S.; Janczarek M.; Kisch H., J. Phys. chem. B 108 (2004) 19384.

[22] Cong Y.; Jinlong Z.; Feng; Masakazu A.; Dannong H., J. Phys. Chem. C. 111 (2007) 10618.

[23] Ma T.; Akiyama M.; Abe E.; Imai I., Nano lett. 5 (2005) 2543.

[24] Xiang-Zhong S.; Jun G.; Zhi-Cheng L.; Shan-Mei X., Appl. Surf. Sci. (2008).

[25] Saha N. C.; Tompkins H. G., J. Appl. Phys. 72 (1992) 3072.

[26] Valentin C. Di.; Pacchioni G.; Selloni A.; Livraghi S.; Giamello E., J. Phys. Chem. B 109 (2005) 11414.

[27] Kisch H.; Sakthivel S.; Janczarek M.; and Mitoraj D., J. Phys. Chem. C 111 (2007) 11445.

[28] Ohno T.; Mitsui T.; Matsumura M., Chem. Lett. 32 (4) (2003) 364.

[29] Shu Y.; Yohei A.; Masakazu K.; Jinshu W.; Qing T.; Tsugio S., J. Mater. Chem. 15 (2005) 674.

[30] Ying W.; Yan W.; Yanling M.; Hanming D.; Yongkui S.; Xian Z.; Xiaozhen T., J. Phys. Chem. C 112 (2008) 6620.

[31] Ye C.; Jinlong Z.; Feng C.; Masakazu A., J. Phys. Chem. C 111 (2007) 6976.

Chapter 4

Photocatalytic Degradation of Dyes

Contents

The development of better catalysts is also going to benefit from recent progress in nano science. Among the advanced oxidation processes, photocatalysis by semiconducting materials has become a leading technology in the field of environmental cleaning. Among the various materials, titania becomes more promising one and its modified forms more suitable for using visible region. In this chapter we discuss the photocatalytic application of our modified catalyst for the degradation of dyes like Methylene blue, Crystal violet, Rhodamine B and Acid red 1. Studies like effect of catalyst amount, time of irradiation, light source and dopant concentrations are also discussed.

4.1 Introduction

By definition, dyes can be said to be coloured, ionizing and aromatic organic compounds which show an affinity towards the substrate to which it is being applied. It is generally applied in aqueous solution. Dyes may also require a mordant to better the fastness of the dye on the material on which it is applied. Both dyes and pigments appear to be colored because they absorb some particular wavelengths of light more than others. In contrast with a dye, a pigment generally is insoluble, and has no affinity for the substrate (1, 2).

Dyes may be classified in several ways, according to their chemical constitution, application, origin and use. They can be natural and synthetic based on their origin. Dyes are classified into acidic, basic, mordant, direct, reactive, vat, disperse, sulfur, azo etc based on their applications. Their exposure to environment generates colouration of natural water, toxicity, mutagenicity, carcinogenicity and causes pollution, eutrophication, and perturbation in aquatic life in eco-system (3-9).

Many industries use dyes in order to colour their products and pour a lot of coloured waste water into the effluent. The discharge of dye-bearing wastewater into natural streams and rivers from the textile, paper, carpet, leather, distillery and printing industries make severe problems. The cleaning of wastewater is one of the most serious environmental problems of the present day. Discharge of dyeing industry wastewater into natural water bodies is not desirable as the colour prevents re-oxygenation in receiving water by cutting off penetration of sunlight. It also increases the BOD, and cause lack of dissolved oxygen to sustain aquatic life. In addition, most of the dyes, even in very low concentration, used as colouring materials are toxic to some micro organisms and also to aquatic life, and may cause direct destruction or inhibition of their catalytic capabilities. Many dyes are difficult to degrade, as they are resistant to aerobic digestion. Dyes can also cause allergic dermatitis

and skin irritation. Some of them have been reported to be carcinogenic and mutagenic. Hence, a contamination due to dyes is not only a severe public health concern but also may causes serious environmental problems because of their persistence. This upsets the biological activities in water bodies. Nowadays research is focused on reactive and other anionic dyes because a large fraction of these dyes are remain in waste water due to low removal efficiency of the conventional wastewater treatment plants (10-14).

There are a lot of physical and chemical techniques such as coagulation, ozonization, membrane filtration, electrolysis; oxidation, active sludge biochemical processes, bio-degradation etc. has been widely used for the removal of dyes from wastewater. These established technologies are often unable to reduce contaminant concentration adequately to a desired level with effectively and economically. Each of them has its own merits and demerits. The water colouration can be removed by chemical treatment through destructing the chromophoric group of the dyes but often they do not offer the complete mineralization. Adsorption and chemical coagulation do not result in dye degradation and create ongoing waste disposal problem. Chlorination and ozonisation may cause the decolouration through chemical reaction. But the by-product in the chlorination and ozonisation process may itself become more toxic than the starting compounds (15-19).

In the field of environmental contamination caused by dyes, the heterogeneous photocatalytic process is an authentic technique, which can be successfully used to oxidize the organic pollutants present in the aqueous system. Experimental observations indicate that almost complete mineralization of organic compounds to carbon dioxide, water and inorganic anions have taken place by photocatalytic process. Semiconductors are the key materials in photocatalytic process, in which titania takes a role model among others. Research works based on titania are emerging techniques related to the

purification of water and air. It is also announced as the most effective and useful photocatalyst due to its wide application in the field of waste water treatment, water and air purification, deodorization, hydrogen production through water splitting reaction, conversion or degradation of most pollutants, removal of micro organisms etc.(20-22). Most of these treatments are based on the technology called advance oxidation process (AOP). During the advance oxidation process the pollutants or organic matters are completely mineralized to carbon dioxide or converted to less or more harmful compounds based on the stability of that intermediates.

The light absorption capacity is an important factor which influences the photocatalytic efficiency of any photocatalyst in a photocatalytic reaction. Even though titania is a very good photocatalyst, one major drawback is lack of its activity in visible region. Pure titania is active only in UV region of the solar spectrum based on its bandgap (3.2eV for anatase). This practically rules out the use of sunlight as energy source because sunlight contains around 5-8% of UV light.

Various modifications are carried out by different research groups. Few of them are catalysts doped with metals, non metals or coupled with other semiconductor materials, encapsulation of dyes, metal complexes or co-doping with metals and nonmetals (23-33). The effect of incorporation of materials on the activity of titania depends on factors such as method of preparation, type of materials, their concentrations, experimental conditions etc (34).

The basic mechanism behind the photocatalysis is as follows. Upon irradiation with suitable light energy the electron from the valence band of the titania catalysts promoted to its conduction band creating holes in valence band and electrons in conduction band. The electrons on the conduction band of the titania catalyst surface are scavenged by the molecular oxygen to produce

reactive oxygen radicals, whereas the holes in the valence band become trapped by the surface bound hydroxyl radicals that at produced on oxidation of either the surface hydroxyl group and/or the surface bound water molecules. These hydroxyl radicals have very high oxidation potential, hence named advanced oxidation process (AOP), which results in the oxidation of the pollutants (35-39).

In this study, we measure the photocatalytic efficiency of the prepared catalysts such as nitrogen doped titania, nitrogen sulphur co doped titania and the pure titania for the degradation of the different dyes in aqueous media under visible light irradiation. The dyes used in these studies are Crystal violet, Methylene blue, Rhodamine B and Acid red 1. The selection of dyes in this study is based on their major application in coir and textile industries and their concentration can be easily monitored using a spectrophotometer. Studies were carried out to demonstrate the effect of catalyst amount, effect of time, effect of light source and effect of dopant concentration on the degradation of dyes. However the qualitative and quantitative analysis of individual by-products is incomplete, due to technical and financial limitations. Thus in present studies we ignore the mechanical pathway behind the degradation of each dye and reports are purely based on the percent of degradation calculated from spectrophotometer data. The dichoric mirror of wavelength range in between 200 nm-30 micron used as the source of white light (and in result it is denoted as full reflector) for the degradation studies of dyes such as Crystal violet, Rhodamine B and Methylene blue and their optimization. And in the rest of the dyes we used dichoric mirror of wavelength range in between 420-630 nm as source of visible light. After the irradiation the sample was centrifuged, filtered and calculated the concentration using spectrophotometer. Then the percent of degradation was calculated using the relation, {Co – C} X 100 / Co., where Co and C are the concentration of dyes before and after irradiation.

4.2 Activity studies

4.2.1 Crystal violet

Crystal violet or Gentian violet (also known as Methyl Violet 10B) is a basic triarylmethane dye. Crystal violet is the deepest blue of all the methyl violets, and is satisfactory for most purposes for which methyl violet is used. When dissolved in water the dye has a blue-violet colour. The colour of the dye depends on the acidity of the solution. Its darker blue shade makes it a choice for use in Gram's stain for the demonstration and primary classification of bacteria

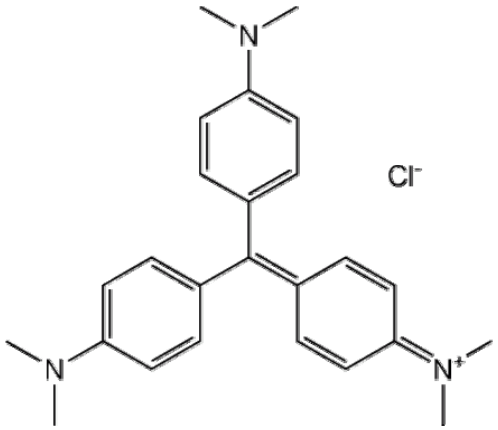

Fig. 4.1. Structure of crystal violet

Crystal violet is used as a textile dye. It also used to dye paper, component of navy blue, black inks for printing, ball-point pens and ink-jet printers. It is also used to colorize diverse products such as fertilizers, anti-freezes, detergents, and leather jackets.

Like malachite green (MG), crystal violet (CV) is readily absorbed into fish tissue from water exposure and is reduced metabolically by fish. Several studies by the National Toxicology Program reported the carcinogenic and mutagenic effects of crystal violet in rodents. It has also been linked to increased risk of human bladder cancer. Its leuco form induces renal, hepatic and lung tumour in mice (1, 40, 41).

The instruments with specification and the experimental setup for the photocatalytic reactions are discussed in chapter 2.

a. Effect of catalyst amount

A 10^{-4} molar aqueous solution of crystal violet was used in this study. About 10 ml of solution with catalyst amount of 1g/L to 5 g/L was added. Before irradiation the system was magnetically stirred for 30 minutes under dark to establish the adsorption-desorption equilibrium between the catalytic surface and the dye. The irradiation time was limited to one hour based on the lamp life. The dichoric mirror of 200 nm-30 micron was used as source for white light. The absorbance of the solution before and after the irradiation was measured using spectrophotometer at 581 nm.

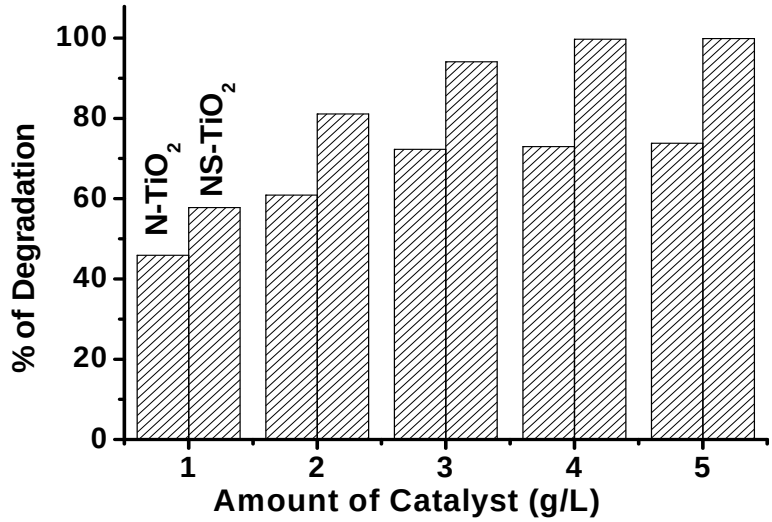

Fig.4.2. % Degradation of crystal violet against amount of catalyst Irradiation time: 1 hour; Dye con. 10 ml of 10^{-4} M

Fig. 4.2 represents the percent degradation of crystal violet against the different amount of catalyst. This shows that the percent degradation of both the modified catalysts increase with increase in the amount of catalyst from 1 g/L to 3 g/L and above this limit there is not much change. This indicated that the active site provided for the adsorption of substrate on the catalyst surface is

limited to catalyst amount of 3g/L and after that no much change in the degradation. At higher dosage the vacant sites are consumed by the intermediate products obtained during the reactions which retard further degradation of the substrate. Hence the percent degradation decreased or retained without a noticeable change (9, 42-47). Moreover, the particle-particle interaction becomes significant as the amount of particles in solution increases, which reduces the active site density for the surface excited holes and electrons. It is also observed that NS-TiO_2 gives better results than N-TiO_2. It may be due to the presence of the both impurities such as N and S which enhance higher activity by narrowing the bandgap. The higher activity is also attributed to the highly ordered nature of the catalyst and its method of preparation.

b. Effect of time

For this study a 50 ml of 10^{-4} molar aqueous solution of crystal violet was used. The catalyst amount of 3 g/L, optimized in the previous experiment, was added. Before irradiation the system was magnetically stirred for 30 minutes under dark to establish the adsorption-desorption equilibrium between the catalytic surface and the dye.

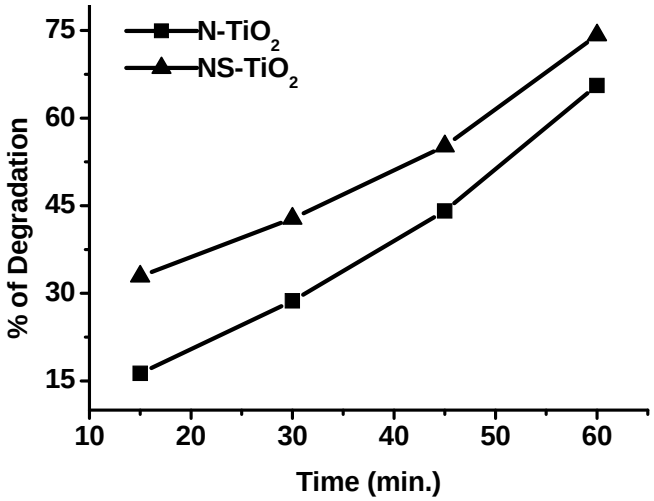

Fig. 4.3. % Degradation of crystal violet against time Amount of Catalyst: 3 g/L; Dye con. 10 ml of 10^{-4} M

The irradiation time was limited to one hour based on the lamp life. The dichoric mirror of 200 nm-30 micron was used as source of white light. After the lamp was switched on, around 10ml of the suspension was pipetted out from the solution at an interval of 15 minutes. The pipetted sample was filtered and measured its absorbance.

From the results (Fig. 4.3) it is noted that both the modified catalysts give a linear increase of percent degradation with the increase of time. Beyond this limit of time (one hour) there is no noticeable change (which is not shown in figure). This result indicates that when the time of irradiation increases the percent degradation increases and reaches a maximum for one hour irradiation. With increase of time more and more light energy falls on the catalyst surfaces which increases the formation of photo excited species and enhances the photocatalytic activity.

c. Effect of light source

Here also studies involve the usage of 10 ml 10^{-4} molar aqueous solution of crystal violet with a light illumination of one hour. The dichoric mirror of 200 nm-30 micron (full reflector), 280-400 nm and 420-630 nm were used as source for white light, UV light and visible light respectively. We also conducted the reaction without catalyst in white light region. In this case we compared the percent degradation of both modified catalyst with pure titania prepared in our laboratory and commercially available 100% anatase titania for their activities in visible light, UV light and white light.

From the results (Table 4.1) it is noted that both the modified catalysts give better activity for the degradation of dyes in visible light irradiation when compared with pure and commercial titania, whereas activity decreased in UV light irradiation. But it is also noted that all the catalysts give good results in white light.

Table 4.1. % of degradation of crystal violet against light source
Irradiation time: 1 hour; Dye con. : 10 ml of 10^{-4} M, Catalyst: 3 g/L

Studies	% of Degradation				
	N-TiO_2	**NS-TiO_2**	**L-TiO_2**	**A-TiO_2**	**Without Catalyst**
Full reflector	72.3	94.1	70.8	99.9	2.0
UV light only	45.1	57.8	60.9	98.6	
Visible light	68.6	87.9	39.8	44.6	
Adsorption	19.3	24.7	21.9	20.3	

The higher activity of modified catalysts in visible light is attributed to the presence of dopant elements such N and S, which helps in narrowing the band gap of titania by introducing their energy levels between the bandgap of titania or by mixing with valence bands of pure titania. Moreover the higher surface area and small particle size of the modified catalysts are also contribute for the higher activity. The higher activity of pure and commercial titania in UV irradiation is based on its band width. The higher activity of all the catalyst in white light is due to the combined contribution of both visible and UV part of lights in full reflector dichoric mirror.

The higher activity of pure and commercial titania in UV irradiation is attributed to its bandgap. It can be noted that pure titania exhibits noticeable activity in visible region which is explained as follows. The actual absorption spectrum of a photocatalyst is an overlapping result of intrinsic and extrinsic absorption bands. The photo excitation of extrinsic absorption bands of a photocatalyst can also lead to surface photoreactions. The extrinsic absorption originates from the photo ionization of original or newly formed defects and the excitation of surface states. Such extrinsic absorption requires less energy to activate. Therefore, it is possible to generate free charge carriers to induce surface chemical reactions by using visible light (40).

d. Effect of dopant concentration

Studies involve 10 ml 10^{-4} molar aqueous solution of crystal violet with a catalyst amount of 3 g/L and light illumination of one hour. The catalysts with higher and lower concentration of dopants were used to evaluate their photocatalytic activity.

Table 4.2. % Degradation of crystal violet against dopant concentration
Irradiation time: 1 hour; Dye con. : 10 ml of 10^{-4} M, Catalyst: 3 g/L

Catalyst	% of degradation
N-TiO_2 (l)	67.1
N-TiO_2	**72.3**
N-TiO_2 (h)	71.6
NS-TiO_2 (l)	88.1
NS-TiO_2	**94.1**
NS-TiO_2 (h)	52.9

The result (Table 4.2) shows that the optimized catalyst labeled such as N-TiO_2 and NS-TiO_2 gives better results than catalysts with dopant concentration higher and lower than that of optimized one. Different loading of the dopant on titania reveals that at higher loading, the space charge region narrows and the efficiency of charge separation is reduced which results in the lower activities of the catalyst. An optimum concentration of dopant ions makes the thickness of space charge layer substantially equal to the light penetration depth. Since the space charge region becomes very narrow when the concentration of doping ions is too high, the penetration depth of light into titania greatly exceeds the space charge layer, it results in the recombination of the photo generated carriers becoming easier (49). To sum up, there is an optimum dopant concentration in titania for the most efficient separation of photo generated carriers and have for photocatalytic activity.

4.2.2 Rhodamine B

Rhodamine B is an amphoteric dye, although usually listed as basic as it has an overall positive charge. It also belongs to the family of Xanthenes dye. Rhodamine B can be used to dye silk, cotton, wool, fibers, nylon, acetate fibers, paper, spirit inks and lacquers, soap, wood stains, feathers, leather and distempers on china clay etc. It has also been used as a drug and cosmetic colour in aqueous drug solutions, tablets, capsules, toothpaste, soap, hair-waving fluids, bath salts, lipsticks and rouges. It is often used as a tracer dye within water to determine the rate and direction of flow and transport. Pollution of water due to the discharge of effluents from dyeing industries affects the environment due to its toxicity (40, 50, 51).

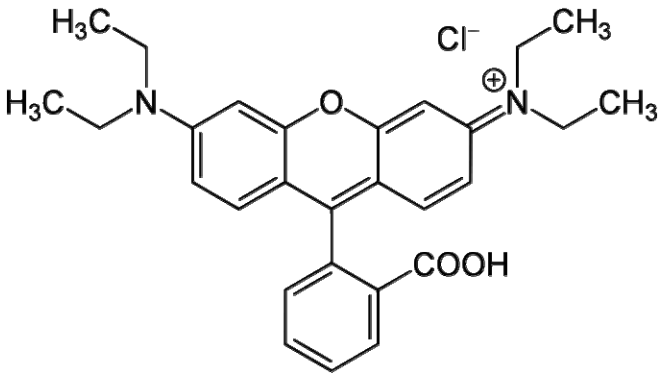

Fig. 4.4. Structure of Rhodamine B

The experimental conditions and setup for the degradation of rhodamine was also similar to that of crystal violet. The dichoric mirror of 200 nm-30 micron was used as source for white light. The absorbance of the solution before and after the irradiation was measured using spectrophotometer at 553 nm.

a. Effect of catalyst amount

Studies contain one hour irradiation to a 10 ml 10^{-4} molar aqueous solution of rhodamine B with a catalyst of amount from 1g/L to 5 g/L was used.

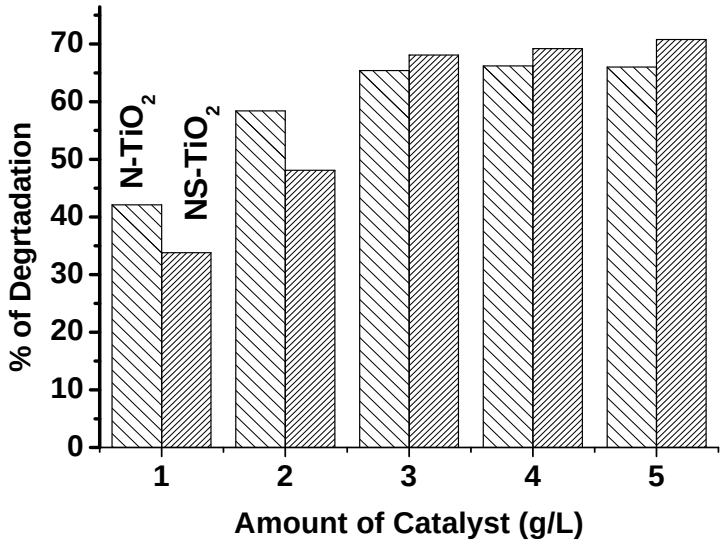

Fig. 4.5. % Degradation of rhodamine B against amount of catalyst
Irradiation time: 1 hour; Dye con. 10 ml of 10^{-4} M

Fig. 4.5 represents the percent degradation of rhodamine B against the different amount of catalyst. Results show that the percent degradation of both the modified catalysts increase with increase in the amount of catalyst and reaches a maximum of 3 g/L and above this limit there is no significant change. This indicated that the active site provided for the adsorption of substrate on the catalyst surface is limited to catalyst amount of 3g/L. The increase in the degradation efficiency of the dye with an increase in the catalyst amount may be due to an increase in the active sites available on the catalyst surface for the reaction, which in turn increases the rate of radical formation. The reduction in the degradation when the catalyst amount is increased beyond 3 g/L is due to light scattering and reduction in light penetration through the solution. With a higher catalyst loading the deactivation of activated molecules by collision with ground state molecules dominates the reaction, thus reducing the rate of reaction. It is also observed that NS-TiO_2 gives better results than N-TiO_2. It may be due to the presence of both the impurities N and S which enhance the activity through narrowing the

bandgap. The higher activity also attributed to the highly ordered nature of the catalyst and its method of preparation.

b. Effect of time

A 50 ml of 10^{-4} molar aqueous solution of rhodamine B with catalyst amount of 3 g/L was used for this study. The catalyst amount was optimized in the previous study. Before irradiation, the system was magnetically stirred for 30 minutes under dark to establish the adsorption-desorption equilibrium between the catalytic surface and the dye. The irradiation time was limited to one hour based on the lamp life. The dichoric mirror of 200 nm-30 micron was used as source of white light. After the lamp was switched on, around 10ml of the suspension was pipetted out from the solution at an interval of 15 minutes. The pipetted sample was filtered and measured its absorbance at 553 nm.

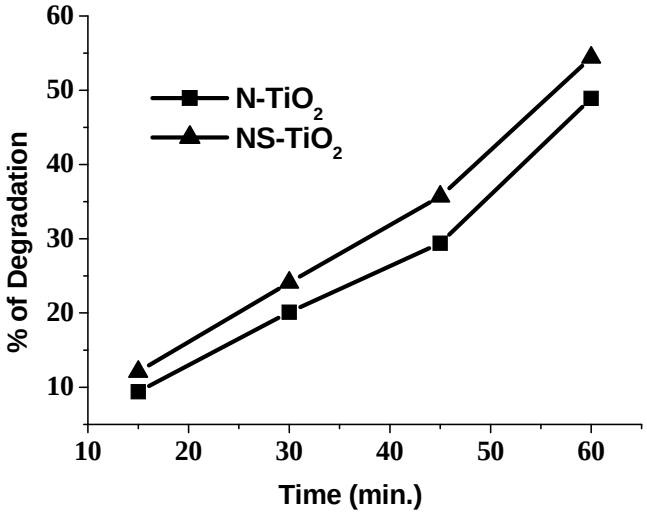

Fig. 4.6. % Degradation of rhodamine B against time
Amount of Catalyst: 3 g/L; Dye con. 10 ml of 10^{-4} M

The photocatalytic percent degradation of rhodamine against the irradiation time is shown in fig. 4.6. Results show that both the modified catalysts give a linear relationship with the increase of time. When time

increases more and more light energy falls on the catalyst surfaces which increases the formation of photo excited species and enhances the photocatalytic activity.

c. Effect of light source

In this study we use 10 ml 10^{-4} molar aqueous solution of rhodamine B with a catalyst amount of 3 g/L and light illumination of one hour. The dichoric mirror of 200 nm-30 micron (full reflector), 280-400 nm and 420-630 nm were used as source for white light, UV light and visible light respectively. We also conducted a blank reaction without catalyst in white light region and blank without light sources. We also compared the percent degradation of both modified catalyst with pure titania prepared in our laboratory and commercially available 100% anatase titania for their activities in visible light, UV light and white light.

Table 4.3. % of degradation of rhodamine B against light source
Irradiation time: 1 hour; Dye con. : 10 ml of 10^{-4} M, Catalyst: 3 g/L

Studies	% of Degradation				
	N-TiO_2	**NS-TiO_2**	**L-TiO_2**	**A-TiO_2**	**Without Catalyst**
Full reflector	65.4	68.1	54.1	98.7	1.1
UV light only	31.1	40.5	44.2	97.5	
Visible light	54.2	61.3	40.5	47.8	
Adsorption	12.8	11.3	16.1	20.5	

From the results (Table 4.3.) it is noted that both the modified catalysts give better activity for the degradation of dye in visible light irradiation when compared with pure and commercial titania whereas activity decreased in UV light irradiation. But it is also noted that all the catalyst give good results in white light. The higher activity of modified catalysts in visible light is attributed to the presence of dopant elements which help to narrow the band

gap of titania by introducing their energy levels between the bandgap of titania or by mixing with valence bands of pure titania. Moreover the higher surface area and small particle size of the modified catalyst also contribute to the higher activity. The higher activity of pure and commercial titania in UV irradiation is based on its bandgap. The higher activity of all the catalyst in white light is due to the combined effects of both visible and UV part of light in full reflector dichoric mirror.

d. Effect of dopant concentration.

In this section we can evaluate the percent of degradation of rhodamine B against various modified catalyst with different dopant concentration. Studies involve 10 ml 10^{-4} molar aqueous solution of rhodamine B with a catalyst amount of 3 g/L and a visible light illumination of one hour.

Table 4.4. % Degradation of rhodamine B against dopant concentration
Irradiation time: 1 hour; Dye con. : 10 ml of 10^{-4} M, Catalyst: 3 g/L

Catalyst	% of degradation
N-TiO_2 (l)	49.6
N-TiO_2	**65.4**
N-TiO_2 (h)	54.7
NS-TiO_2 (l)	58.1
NS-TiO_2	**68.1**
NS-TiO_2 (h)	42.1

Table 4.4 gives the results of all modified catalyst for the photocatalytic removal of rhodamine B on using white light irradiation. It was noted from the results that the activity of modified catalyst increases with increase of dopant concentration and reaches an optimum and above this there is no significant change in the activity. When the concentration of dopant is excessively high, the space charge region became very narrow and the penetration depth of light into titania greatly exceeds the space charge layer. Therefore, the recombination of

the photo generated electron-hole pairs became easier. Thus it is clear from the results that both N-TiO_2 and NS-TiO_2 give higher activity compared to others. To sum up, there is an optimum concentration of dopant in titania for the most efficient separation of photo generated carriers and photocatalytic activity.

4.2.3 Methylene Blue

Methylene blue is a heterocyclic aromatic chemical compound with the molecular formula $C_{16}H_{18}N_3SCl$. At room temperature it appears as a odourless dark green powder, which yields a blue solution when dissolved in water and gives characteristic spectrophotometric absorbance at 653 nm. It has many uses in a range of different field. Methylene Blue (MB) is a cationic dye, extensively used in variety of industrial application with main application in textile and coir industries. It is most commonly used dye for coloring cotton, wood, paper stocks, and silk. It is also utilized in the field of medicine.

Severe exposure to methylene blue releases aromatic amines (e.g., Benzedrine, Methylene) and is a potential carcinogen. It will cause increased heart rate, vomiting, shock, cyanosis, and tissue necrosis in humans. Due to these critical negative effects, methylene blue should be eliminated from the human environment. Its presence, even in very low concentration, is highly visible and will affect aquatic life as well as food web. In water, it causes increase the BOD level and is harmful for aquatic life (50, 52).

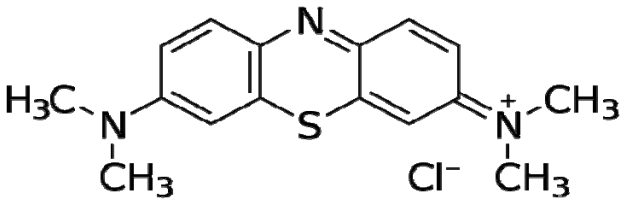

Fig. 4.7. Structure of methylene blue

a. Effect of catalyst amount

A 10^{-4} molar aqueous solution of methylene blue was used in this study. About 10 ml of solution was taken and catalyst amount of 1g/L to 5 g/L was added. Before irradiation the system was magnetically stirred for 30 minutes under dark to establish the adsorption-desorption equilibrium between the catalytic surface and the dye. The dichoric mirror of 200 nm-30 micron is used as source for white light. The absorbance of the solution before and after the irradiation was measured using spectrophotometer at 653 nm

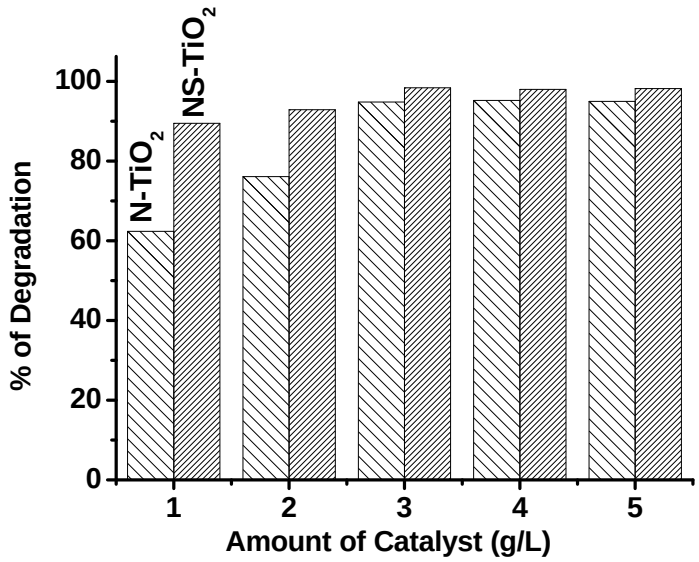

Fig. 4.8. % Degradation of methylene blue against amount of catalyst Irradiation time: 1 hour; Dye con. 10 ml of 10^{-4} M

Fig. 4.8 represents the percent degradation of methylene blue against the different amount of catalyst dosage. It is noted from the results that the percent degradation increases with increase of catalyst amount and reaches a maximum and beyond this the degradation independent of catalyst concentration. Thus the amount of catalyst plays a major role in photocatalytic dye degradation. To avoid the use of excess catalyst, it is necessary to find the optimum loading for the efficient removal of dye. So it is necessary to optimize the amount of catalyst to obtain the highest photocatalytic activity. The optimum catalyst amount in

this case is 3 g/L. At higher amount, the vacant sites are consumed by the intermediate products during the reaction which retards the further degradation of the substrate and hence the percentage degradation decreased or retained without a noticeable change. It is also observed that NS-TiO_2 gives better results than N-TiO_2. It may be due to the presence of the both impurities which enhance more activity through narrowing the bandgap. The higher activity is also attributed to the highly ordered nature of the catalyst and its method of preparation which are favourable factors for photocatalytic activity.

b. Effect of time.

Studies involve a 50 ml of 10^{-4} molar aqueous solution of methylene blue with a catalyst amount of 3 g/L, which was optimized by the above experiment. Before irradiation the system was magnetically stirred for 30 minutes under dark to establish the adsorption-desorption equilibrium between the catalytic surface and the dye. The dichoric mirror of 200nm-30micron was used as source of white light. After switched on the lamp, around 10ml of the suspension was pipette out from the solution at an interval of 15 minutes. The pipetted sample was filtered and measured the absorbance at 653 nm.

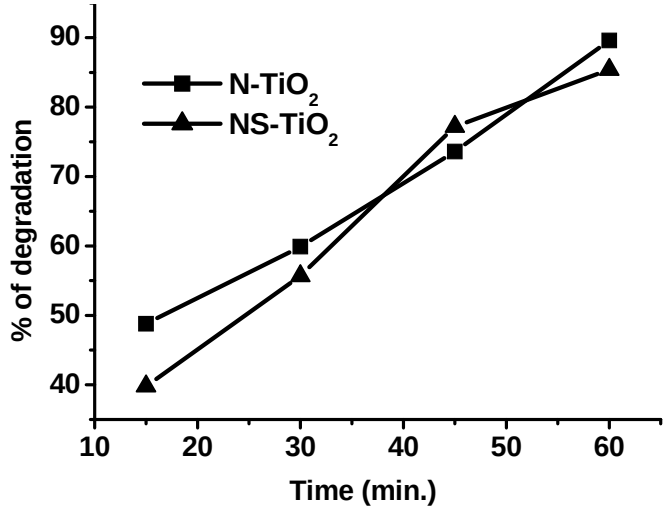

Fig. 49. % Degradation of methylene blue against time
Amount of Catalyst: 3 g/L; Dye con. 10 ml of 10^{-4} M

The photocatalytic degradation of methylene blue against the irradiation time is shown Fig. 4.9. It is clear from the results that both the modified catalysts give a linear increase of percent degradation with the increase of time. Beyond this limit of time (one hour) there is no noticeable change (which is not shown in figure). The result indicates that when the time of irradiation increases the percentage of degradation increases and reaches a maximum at one hour irradiation. As time increases more and more light energy falls on the catalyst surfaces which increases the formation of photo excited species and enhances the photocatalytic activity.

c. Effect of light source

Add a catalyst amount of 3 g/L to a 10 ml of 10^{-4} molar aqueous solution of methylene blue and irradiate the solution for one hour. Before irradiation the system was magnetically stirred for 30 minutes under dark to establish the adsorption-desorption equilibrium between the catalytic surface and the dye. We also conducted a blank reaction without catalyst in white light region and a blank reaction in dark. Percent degradation of catalyst in UV, visible and white light irradiations were compared. The dichoric mirror of 200 nm-30 micron (full reflector), 280-400 nm and 420-630 nm were used for the source of white light, UV and visible light respectively.

Table 4.5. % of degradation of methylene blue against light source
Irradiation time: 1 hour; Dye con. : 10 ml of 10^{-4} M, Catalyst: 3 g/L

Studies	% of Degradation				
	N-TiO_2	**NS-TiO_2**	**L-TiO_2**	**A-TiO_2**	**Without Catalyst**
Full reflector	94.8	98.4	69.8	99.9	16.8
UV light only	58.5	55.5	68.0	98.8	
Visible light	75.2	81.2	41.5	65.6	
Adsorption	24.7	24.5	20.4	57.4	

The percent photocatalytic degradation of methylene blue against modified and pure titania in white light, UV and visible light are shown in Table 4.5. Results show that both the modified catalysts give better activity for the degradation of dye in visible light irradiation when compared with pure and commercial titania whereas activity decreased in UV light irradiation. But it is also noted that all the catalysts give good results in white light. The higher activity of modified catalysts in visible light is attributed to the presence of dopant elements which helps to narrow the band gap of titania by introducing their energy levels between the bandgap of titania or by mixing with valence bands of pure titania. Moreover the higher surface area and small particle size of the modified catalyst also contribute to the higher activity. The higher activity of pure and commercial titania in UV irradiation is based on its bandgap. The higher activity of all the catalyst in white light is due to the combined contribution of both visible and UV part of light in full reflector dichoric mirror.

d. Effect of dopant concentration

Studies involve 10 ml 10^{-4} molar aqueous solution of methylene blue with a catalyst amount of 3 g/L and light illumination of one hour. The catalysts with higher and lower concentration of dopants were used to evaluate their photocatalytic activity

Table 4.6. % Degradation of methylene blue against dopant concentration
Irradiation time: 1 hour; Dye con. : 10 ml of 10^{-4} M, Catalyst: 3 g/L

Catalyst	% of degradation
N-TiO_2 (l)	71.3
N-TiO_2	**94.8**
N-TiO_2 (h)	82.9
NS-TiO_2 (l)	96.2
NS-TiO_2	**98.4**
NS-TiO_2 (h)	92.1

The results shows that the optimized catalyst labeled such as N-TiO_2 and NS-TiO_2 give better results than catalysts with dopants concentration higher and lower than that of optimized one. Different loading of the dopants on titania reveal that at higher loading, the space charge region narrows and the efficiency of charge separation is reduced which results in the lower activities of the catalyst. An optimum concentration of dopant ions makes the thickness of space charge layer substantially equal to the light penetration depth. Since the space charge region becomes very narrow when the concentration of doping ions is too high, and the penetration depth of light into titania greatly exceeds the space charge layer, it results in the recombination of the photo generated carriers becoming easier (49). To sum up, there is an optimum concentration of dopant in titania for the most efficient separation of photo generated carriers and thus photocatalytic activity

4.2.4 Acid Red 1

Acid red 1 (Red 2G) is a synthetic red azo dye. It is a water-soluble dye employed mostly in the form of sodium salts of the sulfonic or carboxylic acids. They are anionic in nature which is attached strongly to cationic groups in the fiber directly. They are applicable to all kinds of natural fibers like wool, cotton and silk as well as to synthetic polyesters, acrylic and rayon. But they are not substantive to cellulosic fibers. They are also used in paints, inks, plastics and leather.

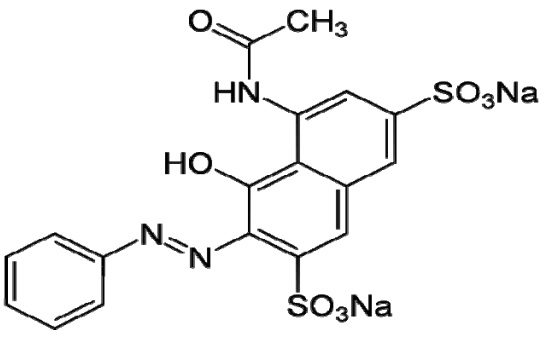

Fig. 4.10. Structure of acid red 1

a. Effect of catalyst amount

In this study a 10 ml 10^{-4} molar aqueous solution of acid red 1 was used. A catalyst amount of1.0 g/L to 5.0 g/L was added to this solution. Before irradiation the system was magnetically stirred for 30 minutes under dark to establish the adsorption-desorption equilibrium between the catalytic surface and the dye. The dichoric mirror of 420-630 nm was used as source for visible light. After the irradiation the sample was centrifuged, filtered and measured its absorbance at 505 nm.

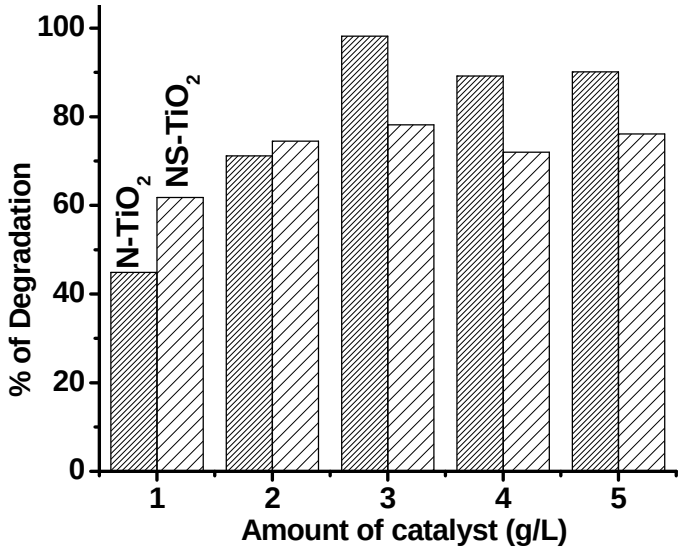

Fig. 4.11. % Degradation of acid red 1 against amount of catalyst
Irradiation time: 1 hour; Dye con. 10 ml of 10^{-4} M

Fig. 4.11 shows the percent degradation of acid red 1 against catalyst amount. It is observed that the initial degradation rate increases proportionally with the catalyst concentration until it reaches a plateau, indicating a progressive saturation of the photonic absorption by the catalyst for a given incident radiation flux. Above this amount, the rate of decrease of acid red 1 concentration is not affected by a progressive increase in catalyst concentration. This phenomenon may be due to the aggregation of catalyst

particles at high concentrations, causing a decrease in the number of surface active sites. The optimized catalyst amount in this case is 3.0 g/L.

b. Effect of time

In this experiment a total of 50 ml 10^{-4} molar aqueous solution acid red 1 was taken and add catalyst amount of 3.0 g/L. Before irradiation the system was magnetically stirred for 30 minutes under dark to establish the adsorption-desorption equilibrium between the catalytic surface and the dye. The dichoric mirror of 420-630 nm was used as source for visible light. After the lamp was switched on, around 10ml of the suspension was pipetted out from the solution at an interval of 15 minutes up to one hour. The collected samples were centrifuged, filtered and measured the absorbance at 505 nm.

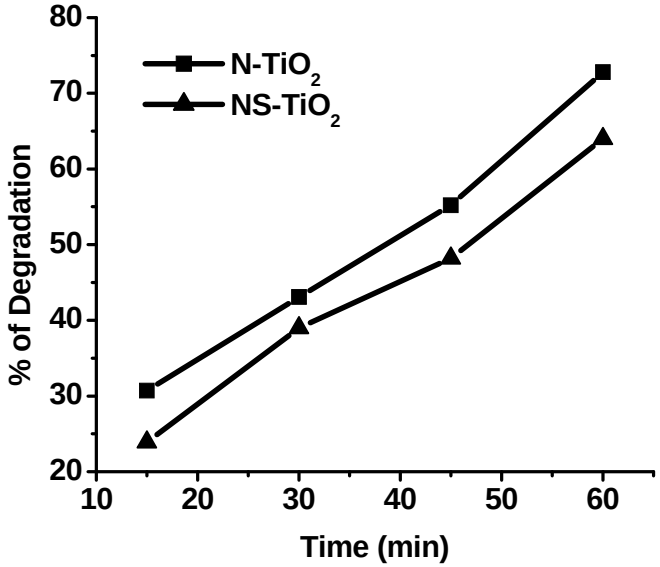

Fig. 4.12. % Degradation of acid red 1 against time
Amount of Catalyst: 3 g/L; Dye con. 10 ml of 10^{-4} M

The photocatalytic degradation of acid red 1 against irradiation time is shown in Fig. 4.12. It is noted from the results that the percent degradation increases with increase of irradiation time. As time of irradiation increases more and more light energy falls on the catalyst surfaces which cause the generation of

higher amount of photo excited species. These are cause to increase the reactive oxygen species which responsible to the degradation of the adsorbed species.

c. Effect of light source

In this study a10 ml 10^{-4} molar aqueous solution of acid red 1 was used with a catalyst amount of 3 g/L and light illumination of 45 minute. The dichoric mirror of 280-400nm and 420-630nm was used for the source of UV light and visible light respectively. Results without catalyst in visible light and also without light source were reported. Study involves a comparison of the percent degradation of both modified catalyst with pure titania prepared in our laboratory and commercially available 100% anatase titania for their activities in UV and visible light irradiation. Remaining parts of experiments were same as in above cases.

Table 4.7. % of degradation of acid red 1 against light source
Irradiation time: 1 hour; Dye con. : 10 ml of 10^{-4} M, Catalyst: 3 g/L

Studies	% of Degradation				
	N-TiO_2	**NS-TiO_2**	**L-TiO_2**	**A-TiO_2**	**Without Catalyst**
Visible light	98.2	78.2	59.4	54.4	7.5
UV light only	75.7	65.7	82.4	99.2	---
Adsorption	3.6	8.5	13.4	15.2	---

The percent of photocatalytic degradation of acid red 1 against the modified catalyst and pure titania in both UV and visible light are shown in Table 4.7. Results show that both the modified catalysts give higher activity in visible and lower activity in UV light for the degradation of acid red 1 when compared with pure and commercial titania. The dark reaction shows significant of adsorption capacity of the catalysts. The little change in the concentration of acid red 1 without catalyst addition was due to leaching property of the material under light. The higher activity of modified catalysts in visible light is attributed to the presence of dopant elements, which

significantly reduces the crystallite size, reduces the band gap and controls the surface property through increase the surface area. The exact reason for the higher activity of N-TiO_2 compared to NS-TiO_2 is not established.

d. Effect of dopant concentration

In this section we evaluated the percent of degradation of acid red 1 against various catalysts includes modified catalyst with different dopant concentration and pure titania. Studies involve 10 ml 10^{-4} molar aqueous solution of acid red 1 with a catalyst amount of 3 g/L and a visible light illumination of one hour

Table 4.8. % Degradation of acid red 1 against various catalyst
Irradiation time: 1 hour; Dye con. : 10 ml of 10^{-4} M, Catalyst: 3 g/L

Catalyst	% of degradation
N-TiO_2 (l)	53.5
N-TiO_2	**98.2**
N-TiO_2 (h)	60.3
NS-TiO_2 (l)	61.3
NS-TiO_2	**78.2**
NS-TiO_2 (h)	63.5
L-TiO_2	68.7
A-TiO_2	62.4

Table 4.8 exhibits the result of all the catalyst for the photocatalytic removal of acid red 1 using visible light irradiation. The results show that the optimized catalyst labeled as N-TiO_2 and NS-TiO_2 gives better result. An appropriate amount of dopant could suppress the recombination of photo-induced electron-hole pairs whereas the excess amount of dopant might cover the surface of titania and decreased the photo quantum efficiency. The higher activity of modified titania compared to pure titania is attributed to the effect of dopants which enhance the activity in visible light region by narrowing the bandgap of the titania semiconductor.

References

[1] http://en.wikipedia.org

[2] http://www.dyespigments.com

[3] Hauming Y.; Jing O.; Aidong T.; Yu X.; Xianwei L.; Xiaodan D.; Yongmei Y., Mat. Resr. Bulln. 41 (2006) 1310.

[4] Vandevivere P.C.; Bianchi R.; Verstraete W., J. Chem. Technol. Bio. Technol. 72 (1998) 289.

[5] Augugliaro V.; Baiocchi C.; Bianco Prevot A.; Garcia-Lopez E.; Loddo V.; Malato S.; Marci G.; Palmisano L.; Pazzi M.; Pramauro E., Chemosphere 49 (2002) 1223.

[6] Li J.; Bishop P.L., Wat. Sci. Techol. 46 (1-2) (2002) 207.

[7] Li J.; Bishop P.L., Wat. Sci. Techol. 49 (11-12) (2004) 237.

[8] Liu Y.; Che X.; Li J.; Burda C., Chemosphere 61 (2005) 11.

[9] Burda C.; Lou Y.; Chen X.; Samia A.C.S.; Stout J.; Gole J. L., Nano Letters 3 (2003) 1049.

[10] Mittal A. K.; Venkobachar C., Indian J. Environ. Health, 31 (1989) 105.

[11] Edwin vasu A., E- J. Chem. 5 (4) (2008) 844.

[12] Muqing Q.; Qiaoling J.; Danli Y.; Kai F., Desalination and Water treatment 24 (2010) 61.

[13] Rasika C. T.; Kavita S. M.; Ashish A. B.; Gayatri S. K.; Rajashree V. K.; Nirmala R. D., Der Pharma Chemica, 2 (3) (2010) 171.

[14] Slimani R.; Anouzla A.; Abrouki Y.; Ramli Y.; El Antri S.; Mamouni R.; Lazar S.; El Haddad M., J. Mater. Environ. Sci. 2 (1) (2011) 77.

[15] Nerud F.; Baldrain P.; Gabriel J.; Ogbeifun D., Chemosphere 44 (2001) 957.

[16] Sopajaree K.; Procedings of the 6th international conference on environmental science and Technology, Greece 1999.

[17] Sarasa J.; Roche M. P.; Ormad M. P.; Gimeno E.; Puig A.; Ovelleiro J. L., Water Res. 32 (1998) 2721.

[18] Yibing X,; Chunwei Y.; Xiangzhong L., Colloids and surfaces A: Physiochem. Eng. Aspects 252 (2005).

[19] Konstantinou I. K.; Albanis T. A., A review, Appl. Catal. 49 (2004) 1.

[20] Galindo C.; Jacques P.; Kalt A., J. Photochem. Photobiol. A: Chem. 130 (2000) 35.

[21] Konitou K.; Maeda S.; Hongyou S.; Mishima K., J. Chem. Eng. 80 (2002) 208.

[22] Arslan I.; Balcioglu I. A.; Tubkanen T., Environ. Tech. 20, 9 (1999) 921.

[23] Asahi R.; Morikawa T.; Ohwaki T.; Aoki K.; Taga Y., Science 293 (2001) 269.

[24] Fu X.; Zeltner W.A.; Anderson M. A., Abst. Paper Am. Chem. Soc. 210 (1995) 163.

[25] Tennakone K.; Kottegoda I.R.M., J. Photochem. Photobiol. A: Chem. 96 (1996) 79.

[26] Colon G.; Hidalgo M.C.; Navio J.A., J. Photochem. Photobiol. A: Chem. 138 (2001) 78.

[27] Fu H. X.; Lu G.; Li S. B.; J. Photochem. Photobiol. A: Chem. 114 (1998) 81.

[28] Fujishima A.; Rao T.N.; Tyrk D. A., J. Photochem. Photobiol. C 1 (2000) 1.

[29] Zhu Y.; Zhang L.; Yao W.; Cao L., Appl. Surf. Sci. 158 (2000) 32.

[30] Zhu Y.; Zhang L.; Wang L.; Fu Y.; Cao L., J. Mater. Chem. 11 (2001) 1864.

[31] Zheng S. K.; Wang T. M.; Hao W.C.; Shen R., Vaccum 65 (2002) 155.

[32] Hashimoto K., Thin solid films 352 (1999) 260.

[33] Zhang L.; Zhu Y.; He Y.; Li W.; Sun H., Appl. Catal. B: Environ 40 (2003) 287.

[34] Li X.; Yue P.L.; Kutal C., New J. Chem. 8 (2003) 1264.

[35] Jaeger C. D.; Bard A. J., J. Phys. Chem. 83 (1979) 3146.

[36] Legrini O.; Oliveros E.; Braun A. M., Chem. Rev. 93 (1993) 671.

[37] Herrmann J.; Disdier J.; Pichat P., J. Phys. Chem. 90 (1986) 6028.

[38] Henglein A., J. Phys. Chem. 83 (1979) 2209.

[39] Herrmann J. M.; Baker R. T. K.; Tauster S. J.; Dumesic J.A., ACS Symposium series 298 (1986) 200.

[40] http://stainsfile.info

[41] http://www.redwop.com

[42] Hinda L.; Eric P.; Ammar H.; Mohamed K.; Elimame E.; Chantal G.; Jean-Marie H., Appl. Catal. B: Environ. 39 (2002) 75.

[43] Poulios I.; Aetopoulou I., J. Chem. Technol. Biotechnol. 74 (1999) 349.

[44] Gonclaves M. S. T.; Oliveira-Campos A. M. F.; Pinto E. M.; Plasencia P. M. S.; Queiroz M. J., Chemosphere 39 (1999) 781.

[45] Neppolian B.; Choi H. C.; Sakthivel S.; Arabindoo B.; Murugesan V., Chemosphere (2002) 1173.

[46] Chen L. C.; Chou T. C., J. Mol. Catal. 85 (1993) 201.

[47] Chen F.; Xie Y.; Zhao J.; Lu G., Chemosphere 44 (2000) 1159.

[48] Jin Kai Z.; Lu L.; Jianqiang Y.; Hong Liang L.; Pei-Zhi G.; Hong S.; Zhao X. S., J. Phys. Chem. C 112 (2008) 5316.

[49] Studies on catalysis by titania, PhD thesis, Joyes Jacob 2009.

[50] http://en.wikipedia.org

[51] http://www.osha.gov

[52] Bayati M. R.; Golestani-Fard F.; Moshfegh A.Z., Catal. Lett. 134 (2010) 162.

Chapter 5

Photocatalytic Degradation of Pesticides

Contents

Recent decades have witnessed increased contamination of drinking water. A wide variety of organics are introduced into the water system from various sources such as industrial effluents, agricultural runoffs and chemical spills. In recent years there is an increasing awareness for protection of the environment from hazardous wastes and effluents from the industries. Among the various technologies and materials available for waste water treatment, the advanced oxidation processes photocatalytic degradation (PCD) technique over semiconductors has shown to be one of the most promising processes for the wastewater treatment. Photocatalytic reactions using titanium dioxide (TiO_2) and its modified forms have shown to be useful for destroying a wide range of environmental contaminants. In this section we discuss the photocatalytic degradation of organic pollutants (we collectively called as pesticides) in aqueous medium using modified N and N S co-doped titania, and pure titania by visible light irradiation.

5.1 Introduction

The presence of organic pollutants in water sources indicates that the most of these compounds are recalcitrant and/or non-biodegradable and can persist for long periods in the environment representing a risk to mammalian and aquatic life (1,2). The possibility of entry of pesticides into water sources are follows: (i) industrial waste or effluents discharged directly into water (ii) seepage from buried toxic wastes into water supplies and (iii) contamination of surface and groundwater directly or from runoff during spraying operations (3). The water rinsate solutions produced during the formulation, dilution, mixing, transfer and application of commercial pesticides may pollute the waste water lines and may reach the sources of fresh water. They are also major sources for water pollution(4). The amount of pesticides routinely applied to agricultural commodities has dramatically increased in recent years which have led to serious concerns about the increasing risks to human health. The use and production of several organic pesticides has continuously increased since introduction of DDT in the early 1940s, giving as a result a great family of organo chlorine pesticides (5,6). The ineluctable consequence of the widespread use and availability of pesticides is the problem of accidental or intentional poisoning. While the annual number of deaths from pesticide poisoning is relatively small, accidental poisoning by pesticides is a seasonal hazard faced by many workers in respective fields.

Thus the need and addresses of various technologies and materials to prevent and mitigate the pesticide contamination in natural environment is essential. The technologies involve chemical, physical, microbiological, integrated practices including bioremediation, chemical remediation, phytoremediation, ultrasonic radiation, mercury promoted hydrolysis, adsorption, coagulation, reverse osmosis, pyrolysis, high-temperature oxidation,

advance oxidation process etc. To use these technologies safely, it is essential to find appropriate remediation reagents and conditions (7-15).

The traditional physical–chemical treatment such as nanofiltration, ozonation, combustion, and others, are efficient but have inherent limitations in applicability, effectiveness, and cost. Each method has its own limitations and disadvantages. For example the adsorption onto clays or carbon filters cannot degrade pollutants, which just transfer their phase and require further treatment. In the case of high concentration of organic priority pollutants, the activated sludge formation can be substantially intoxicated and suppressed. The conventional treatment processes using biological species are very slow or non-destructive for some kinds of compounds. Ozonation alone is less effective, since its reaction with organic contaminants is selective and generation of free radicals from its decomposition takes place only at elevated pH conditions. Nowadays, the main disposal method of pesticide stocks is incineration, which is expensive and not available in developing countries. Thus the possible use of the technique for the removal of persistent organic pollutants, such as pesticides in water, started receiving attention in the field of research (1,5,8,16-21).

Among the various process mentioned above, the advanced oxidation processes (AOP) by semiconducting photocatalyst materials, have been considered as promising for the remediation of contaminated water (1, 22-26). The photocatalyst materials generate the photo excited species such as holes and electron in valence band and conduction band respectively on semiconductors upon irradiation with light energy greater than or equal to its bandgap. The reaction of this activated pair with the adsorbed water, and/or with O_2, and/or with hydroxyl groups at the semiconductor surface produces highly reactive oxygen species such as hydroxyl radicals, peroxide radicals, superoxide anions etc. These highly reactive oxygen species, transferred across

the interface are capable of destructive removal of adsorbed organic species on the semiconducting surface. Among the semiconductors used, titanium dioxide has been demonstrated to be a very efficient catalyst and especially suitable to work by solar UV light (2, 27-33). The advantages and the necessity for its modification are already discussed in the previous chapters.

This chapter discusses the photocatalytic efficiency of the modified titania catalysts such as nitrogen doped titania, nitrogen sulphur co doped titania and the pure titania for the degradation of different organic pollutants in aqueous media under visible light irradiation. The organic pollutants used in these studies are 2,4-dichlorophenoxy acetic acid, 2,4,5-trichlorophenoxy acetic acid, monolinuron and aldicarb(these are collectively called pesticides in our study). The selection of these organic compounds on the basis of their application as water soluble pesticides and herbicides and their concentration can be monitored using a HPLC methods. Studies were carried out to demonstrate the effect of catalyst amount, effect of time, effect of light source, effect of dopant concentration, effect of various catalysts, effect lamp intensity and reusability. However the qualitative and quantitative analysis of individual by-products is often incomplete, due to technical and financial limitations. Thus in present studies we ignore the mechanical pathway behind the degradation of each pesticide and reports are purely based on the percent degradation calculated from data obtained from the HPLC analysis. We use a dichoric mirror of wavelength range in between 420-630 nm for visible and 280-400 nm for UV light irradiation. The experimental setup and conditions are explained in chapter 2.

After the irradiation the sample is centrifuged and filtered through a 0.2 micro pore membrane filter to ensure the removal of all the solid particles in order to inject the sample in HPLC instrument. A Dionex model Ultimate 3000

HPLC system with gradient pump, auto sampler of 20 micro liter injection loop and photo diode array UV detector was used. The column used for this purpose was a Thermo Hypersil reverse phase of ODS C-18 with dimension of (150 x 4.6 mm) having particle size of 5μm.

5.2 Activity studies

5.2.1 2,4-Dichlorophenoxyaceticacid

2,4-dichlorophenoxy acetic is commonly called 2,4-D. It is one of the most commonly used herbicides in controlling broadleaf weeds and other vegetation. 2,4-D and its derivatives are used to control broadleaf weeds in a variety of places including home lawns, cereal and grain crops, commercial areas, commercial turf, rights-of-way, and forests. Depending on the climatic conditions, types of formulation used and the nature of soil, 2,4-D causes certain environmental impact because of its widespread usage. It is a pollutant of great environmental concern because of its relatively high solubility in water. After its application to crops, the unused portions can leach below the root zone or be washed out during precipitation and contaminate nearby water sources. In addition, various amounts of 2,4-D have been detected in surface water and groundwater not only during application of the herbicide but also after a long period of use. 2,4-D has a mean lifetime of about 20 days, and its degradation products accumulate. Because of the toxicity of 2,4-D and its products, a conventional treatment method is not suitable for wastewaters containing 2,4-D, as they can destroy the microbial population of the treatment plants. Most microbial organisms lack enzyme systems to degrade these substances. Thus, these compounds tend to accumulate in water and soil, which is a reason they are termed recalcitrant or refractory compounds. Therefore, the development of an effective degradation process for this herbicide is very important (6, 34-38).

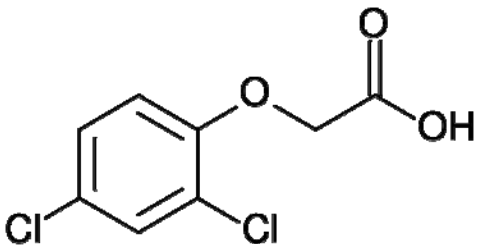

Fig. 5.1. Structure of 2,4-dichlorophenoxyacetic acid

a. Effect of Catalyst amount

Studies involve a 10^{-4} molar aqueous solution of 2,4-D. About 10 ml of solution was taken and catalyst of amount of 1g/L to 5 g/L with an increment of 1g was used. Before irradiation the system was magnetically stirred for 30 minutes under dark to establish the adsorption-desorption equilibrium between the catalytic surface and the pesticide. The irradiation time was limited to one hour based on the lamp life. The dichoric mirror of 420-630 nm was used as source for visible light. After the irradiation the sample was centrifuged and filtered through micro pore membrane filter using syringe pump. The concentration of the filtered sample was analyzed using HPLC. The mobile phase used in this study was a 1.0ml/min solution of methanol/water/trifluoroacetic acid in the ratio of 60:40:0.08 with UV detection at 230 nm. The concentration of sample before the irradiation was measured. The percent degradation was calculated using the relation, {Co – C} X 100 / Co., where Co and C are the concentration of pesticide before and after irradiation.

Photocatalytic degradation 2,4-D against the amount of catalyst is shown in Fig. 5.2. From the results it is clear that the photocatalytic degradation increases with increase of catalyst amount and reaches an optimum value and above this not much change is observed. The optimum value in this case is 3 g/L. The increase of photocatalytic activity with increase of catalyst amount is

assigned to the increase of active surface for the formation of activated photo excited species.

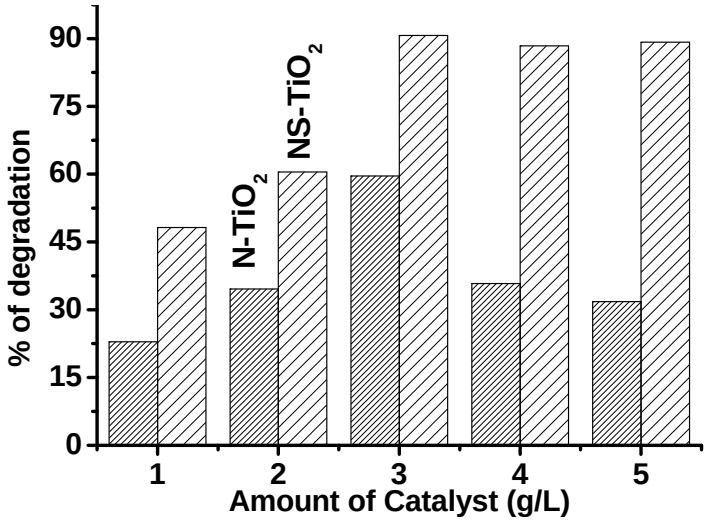

Fig. 5.2. % Degradation of 2,4-D against amount of catalyst
Irradiation time: 1 hour; 2,4-D con. 10 ml of 10^{-4} M

The observation of lower activity at a higher catalyst dosage can be explained as follows. When the titania loading exceeds the optimum dosage, the presence of excess photocatalyst in the aqueous solution increases the turbidity in the solution, which reduces the penetration of light, leading to the generation of a less photo catalytically activated species which inhibit or retard the further degradation of the pesticide compounds (39).

b. Effect of time.

A 50 ml of 10^{-4} molar aqueous solution of 2,4-D was used in this study. The catalyst amount of 3 g/L was added, which was optimized by the above experiment. Before irradiation the system was magnetically stirred for 30 minutes under dark to establish the adsorption-desorption equilibrium between the catalytic surface and the pollutant. The irradiation time was limited to one hour based on the lamp life. The dichoric mirror of 420-630 nm was used as source for visible light. After the lamp was switch on, around 10ml of the

suspension was pipetted out from the solution at an interval of 15 minutes each up to one hour. The pipetted sample was centrifuged and filtered through micro pore membrane filter using syringe pump. The concentration of the filtered sample is analyzed using HPLC which is explained in earlier section

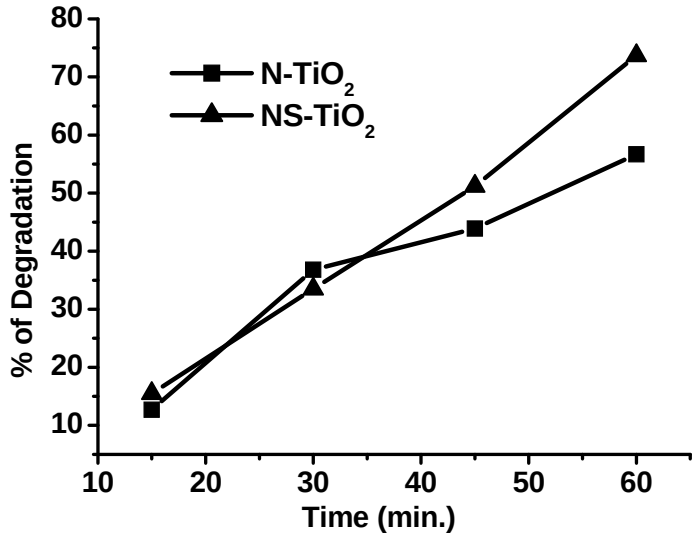

Fig. 5.3. % Degradation of 2,4-D against time
Amount of Catalyst: 3 g/L; 2,4-D con. 10 ml of 10^{-4} M

Fig. 5.3 shows the percent degradation of 2,4-D against time. The result shows almost a linear relationship with percent degradation and time. That is the percent degradation increases with increase in the irradiation time. Here we are limited to the irradiation time up to one hour (based on the life of lamp). As time of irradiation increases more and more light energy fall on the catalyst surfaces which increases the formation of photo excited species and enhance the photocatalytic activity.

c. Effect of light source

In this study a10 ml 10^{-4} molar aqueous solution of 2,4-D was used with a catalyst amount of 3 g/L and light illumination of one hour. The dichoric mirror of 280-400 nm and 420-630 nm was used for the source of UV light and visible light respectively. The experiment was also conducted without catalyst

in visible light and a control without light source. Study involves a comparison of the percent degradation by both modified catalysts with pure titania prepared in our laboratory and a commercially available 100% anatase titania in UV and visible light irradiation. The rest of them are same in above cases.

Table 5.1. % of degradation of 2,4-D against light source
Irradiation time: 1 hour; 2,4-D con. : 10 ml of 10^{-4} M;
Catalyst amount: 3 g/L

Studies	% of Degradation				
	N-TiO_2	**NS-TiO_2**	**L-TiO_2**	**A-TiO_2**	**Without Catalyst**
Visible light (420-630 nm)	59.6	90.7	30.0	29.3	0.0
UV light (280- 400nm)	30.6	40.8	63.9	93.3	---
Adsorption	1.0	1.0	1.0	1.0	---

Table 5.1 represent the percent degradation of 2,4-D against both the modified catalysts and pure titania in UV and visible light irradiation. Results shows that both the modified catalysts give better activity for the degradation of 2,4-D in visible light irradiation when compared with pure and commercial titania whereas activity decreased in UV light irradiation. The examination of dark reaction (i.e., without exposure to visible light) show that no significant variations in 2,4-D concentrations was observed after one hour of mixing. This indicates that no chemical or physical changes are involved between the two chemicals. The higher activity of modified catalysts in visible light is attributed to the presence of dopant elements, which helps in narrow the band gap of titania by introducing an energy levels between the bandgap or by mixing with valence bands of pure titania. The two key properties of dopants in the titania are the nature of dopant and the effect of dopants on the electronic structure of titania, which can intrinsically determine the photon absorption, redox power, and transport of photo induced carriers (40). The presence of both the dopants attributed to the higher

activity of NS-TiO_2 compared to the others. Moreover the higher surface area and small particle size of the modified catalyst also contribute to the higher activity.

The higher activity of pure and commercial titania in UV irradiation is attributed to its bandgap. It can be noted that pure titania exhibits a noticeable activity in visible region is explained as follows. The actual absorption spectrum of a photocatalyst is an overlapping result of intrinsic and extrinsic absorption bands. The photoexcitation of extrinsic absorption bands of a photocatalyst can also lead to surface photoreactions. The extrinsic absorption originates from the photoionization of original or newly formed defects and the excitation of surface states. Such extrinsic absorption requires less energy to activate. Therefore, it is possible to generate free charge carriers to induce surface chemical reactions by using visible light (41).

d. Effect of dopant concentration

In this section we evaluate the percent of degradation of 2,4-D against various catalysts including modified catalyst with different dopant concentration and pure titania. Studies involve 10 ml 10^{-4} molar aqueous solution of 2,4-D with a catalyst amount of 3 g/L and a visible light illumination of one hour.

Table 5.2. % Degradation of 2,4-D against various catalyst
Irradiation time: 1 hour; 2,4-D con. : 10 ml of 10^{-4} M,
Catalyst amount: 3 g/L

Catalyst	% of degradation
N-TiO_2 (l)	51.4
N-TiO_2	**59.6**
N-TiO_2 (h)	54.9
NS-TiO_2 (l)	36.9
NS-TiO_2	**90.7**
NS-TiO_2 (h)	45.6
L-TiO_2	30.0
A-TiO_2	29.3

The percent degradation of 2,4-D against all the prepared catalysts are shown in Table 5.2. It is noted that the activity of modified catalyst increases with increase of dopant concentration and reaches an optimum value. When the concentration of dopant is excessively high, the space charge region became very narrow and the penetration depth of light into titania greatly exceed the space charge layer. Therefore, the recombination of the photo generated electron-hole pairs became easier. Thus it is clear from the results that both N-TiO_2 and NS-TiO_2 give higher activity compared to others. To sum up, there is an optimum concentration of dopant in titania for the most efficient separation of photo generated carriers. The higher activity of modified titania compared to pure titania is due to the effect of dopants which reduce the bandgap and enhance the activity in visible light region.

5.2.2 2,4,5-Trichlorophenoxyacetic acid(2,4,5-T)

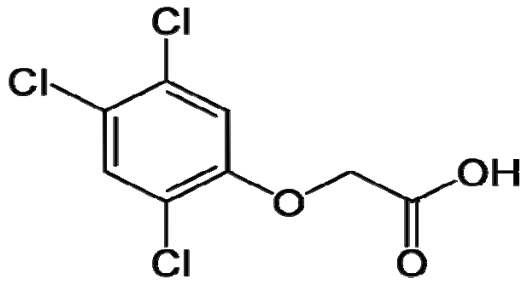

Fig. 5.4. Structure of 2,4,5-Trichlorophenoxyacetic acid

2,4,5-Trichlorophenoxyacetic acid (2,4,5-T), a synthetic auxin, is a chlorophenoxy acetic acid herbicide used to defoliate broad-leafed plants. It was developed in the late 1940s and was widely used in the agricultural industry until being phased out, starting in the late 1970s due to toxicity concerns. It is closely related to a number of other herbicides, such as 2,4-dichlorophenoxyacetic acid (2,4-D) and 2-methyl-4-chlorophenoxyacetic acid (MCPA), which are plant growth stimulants which cannot be metabolized by plants. It is considered to be less readily biodegradable than the analogous herbicide 2,4-D. The greater

resistance to microbial metabolism likely stems from the additional chlorine substituent in the aromatic ring. At low levels, these herbicides can enhance plant growth, but higher levels are herbicidal. Therefore if they are applied in high concentrations they cause lethal, uncontrollable and grossly distorted growth. The half-life of 2,4,5-T in soil varies with conditions, ranging from several weeks to many months. 2,4,5-T degrades to 2,4,5-trichlorophenol and other degradates. 2,4,5-T considerably irritates the eyes, and the skin. Chronic exposure causes impairment of the liver function, changes in behaviour and nerve damage. Intentional overdoses and unintentional high dose occupational exposures to chlorophenoxy acid herbicides have resulted in weakness, headache, dizziness, nausea, abdominal pain, myotonia, hypotension, renal and hepatic injury, and delayed neuropathy (42-46).

a. Effect of catalyst amount.

In this study a 10^{-4} molar aqueous solution of 2,4,5-T was used. About 10 ml of solution was taken and catalyst of amount of 0.5g/L to 1.5 g/L was added. Before irradiation the system was magnetically stirred for 30 minutes under dark to establish the adsorption-desorption equilibrium between the catalytic surface and the pesticide. The dichoric mirror of 420-630 nm was used as source for visible light. After the irradiation the sample was centrifuged and filtered through micro pore membrane filter using syringe pump. The concentration of the filtered sample was analyzed using HPLC. The mobile Phase used in this study was a 1.0ml/min solution of methanol /water/tri-fluoroacetic acid in the ratio 70:30:0.064 with UV detection at 208nm. The concentration of sample before the irradiation was measured. The percent degradation was calculated using the relation as {Co – C} X 100 / Co., where Co and C are the concentration of pesticide before and after irradiation.

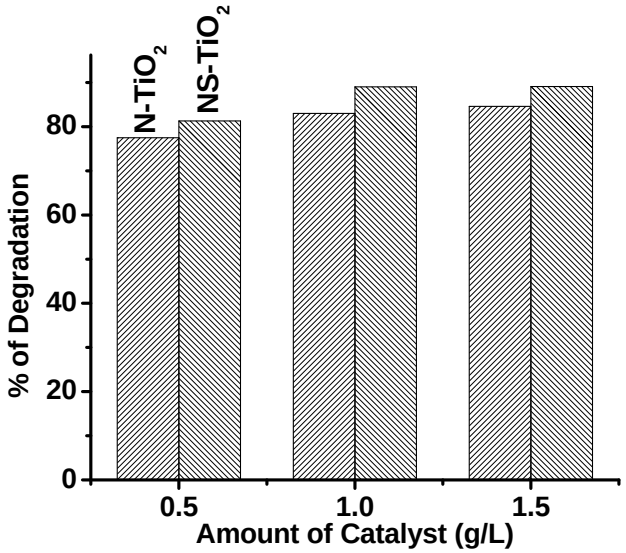

Fig.5.5. % Degradation of 2,4,5-T against amount of catalyst
Irradiation time: 45 min.; 2,4,5-T con. 10 ml of 10^{-4} M

Fig. 5.5. shows the percent degradation of 2,4,5-T against catalyst amount.

It is observed that the initial degradation rate increases proportionally to catalyst concentration. And it reaches a plateau, indicating a progressive saturation of the photonic absorption by the catalyst for a given incident radiation flux. Above this amount, the rate of decrease of 2,4,5-T concentration is not affected further by a progressive increase in catalyst concentration. This phenomenon may be due to the aggregation of catalyst particles at high concentrations, causing a decrease in the number of surface active sites. The optimized catalyst amount in this case is 1.0 g/L.

b. Effect of time

In this experiment a total of 60 ml 10^{-4} molar aqueous solution of 2,4,5-T was taken and catalyst amount of 1.0 g/L was added. Before irradiation the system was magnetically stirred for 30 minutes under dark to establish the adsorption-desorption equilibrium between the catalytic surface and the pollutant. The dichoric mirror of 420-630 nm was used as source for visible

light. After the lamp was switched on, around 10ml of the suspension was pipetted out from the solution at an interval of 10 minutes up to one hour. The concentration of samples collected at each interval was measured using HPLC and analysis details were explained in the previous section.

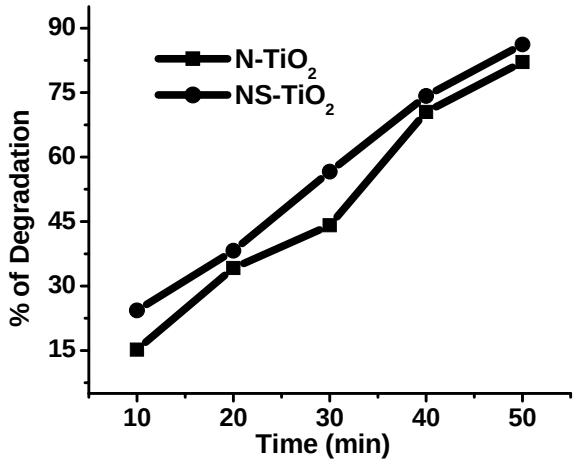

Fig. 5.6. % Degradation of 2,4,5-T against time
Amount of Catalyst: 1 g/L; 2,4,5-T con. 10^{-4} M

The photocatalytic degradation of 2,4,5-T against irradiation time is shown in Fig. 5.6. It is noted from the results that the percent of degradation increases with increase of irradiation and it reaches more than 80% with an irradiation time of 45 minutes. When time of irradiation increases more and more light energy falls on the catalyst surface which causes the generation of higher amount of photo excited species. As the number of photo excited species increases, it causes an increase in the reactive oxygen species responsible for the degradation of the adsorbed species.

c. Effect of light source

In this study a10 ml 10^{-4} molar aqueous solution of 2,4,5-T was used with a catalyst amount of 1 g/L and light illumination of 45 minutes. The dichoric mirror of 280-400 nm and 420-630 nm was used for the source of UV light and visible light respectively. The experiment was also conducted without

catalyst in visible light and a control without light source. Study involves a comparison of the percent degradation of both modified catalyst with pure titania prepared in our laboratory and commercially available 100% anatase titania in UV and visible light irradiation. The remaining part of the experiments is same in previous cases.

Table 5.3. % of degradation of 2,4,5-T against light source
Irradiation time: 45 min.; 2,4,5-T con. : 10 ml of 10^{-4} M;
Catalyst amount: 1 g/L

Studies	% of Degradation				
	N-TiO_2	**NS-TiO_2**	**L-TiO_2**	**A-TiO_2**	**Without Catalyst**
Visible light (420-630 nm)	83.0	89.1	68.7	62.4	12.8
UV light (280- 400nm)	74.6	76.8	93.1	95.5	---
Adsorption	3.9	18.1	9.2	16.5	---

The percentage of photocatalytic degradation of 2,4,5-T against the modified catalyst and pure titania in both UV and visible light are shown in Table 5.3. Results show that both the modified catalysts give higher activity in visible and lower activity in UV light for the degradation of 2,4,5-T when compared with pure and commercial titania. The dark reaction shows a significant change in the concentration of catalyst which is attributed to the adsorption property of the catalysts. The significant change in the concentration of 2,4,5-T without catalyst addition is due to leaching property of the material under light. The higher activity of modified catalysts in visible light was attributed to the presence of dopant elements, which significantly reduce the crystallite size, reduce the band gap and control the surface property through increase in the surface area. The presence of both the dopants attributed to the higher activity of NS-TiO_2 compared to the other catalysts.

d. Effect of dopant concentration

In this section we evaluate the percent of degradation of 2,4,5-T against various catalysts including modified catalyst with different dopant concentration and pure titania. Studies involve 10 ml 10^{-4} molar aqueous solution of 2,4,5-T with a catalyst amount of 3 g/L and a visible light illumination of one hour

Table 5.4. % Degradation of 2,4,5-T against various catalyst
Irradiation time: 45 min.; 2,4,5-T con. : 10 ml of 10^{-4} M,
Catalyst amount: 1 g/L

Catalyst	% of degradation
N-TiO_2 (l)	60.1
N-TiO_2	**83.0**
N-TiO_2 (h)	83.0
NS-TiO_2 (l)	69.0
NS-TiO_2	**89.1**
NS-TiO_2 (h)	86.7
L-TiO_2	68.7
A-TiO_2	62.4

Table 5.4 exhibits the results of all the catalyst for the photocatalytic removal of 2,4,5-T using visible light irradiation. The results show that the optimized catalyst labeled as N-TiO_2 and NS-TiO_2 give better results. Different loading of the dopants in titania reveals that at higher loading, the space charge region narrows and the efficiency of charge separation is reduced which results in the lower activities of the catalyst. An optimum concentration of dopants make the thickness of space charge layer substantially equal to the light penetration depth, because the space charge region becomes very narrow when the concentration of doping ions is too high, and the penetration depth of light into titania greatly exceeds the space charge layer, which will make the recombination of the photo generated carriers easier (47). To sum up, there is

an optimum concentration of dopant in titania for the most efficient separation of photo generated carriers and photocatalytic activity. The higher activity of modified titania compared to pure titania, results from the effect of dopants which enhance the activity in visible light region by narrows the bandgap of the titania semiconductor.

5.2.3 Aldicarb

Aldicarb a member of the N-methyl carbamate class of pesticides is commonly used in agriculture and can be naturally degraded to its carbamate metabolites, resulting in their occurrence in drinking water supplies. In its pure form, the chemical takes on the appearance of a white crystalline solid, which is scientifically known as 2-methyl-2-(methylthio)propionaldehyde O-methyl-carbamoyloxime. Aldicarb does not degrade in groundwater under aerobic conditions unless a relatively high pH exists, such as at pH 7.7. Carbamate insecticide poisoning has signs and symptoms similar to organophosphate poisoning, although the symptoms of the former are not as prolonged.

It is an active ingredient in the pesticide TEMIK®, a soil pesticide used in the agricultural sector worldwide for over 30 years for the control of insects, mites, and nematodes. On the contrary, aldicarb is not only acutely toxic, but also can cause liver damage, changes in blood cells, and increase in cholesterol levels. A variety of symptoms including weakness, blurred vision, headache, nausea, tearing, sweating, and tremors are caused by aldicarb usage. Very high doses can result in death due to paralysis of the respiratory system. The primary route of human exposure to aldicarb comes from the consumption of contaminated food and drinking water. This pesticide is highly toxic to birds and moderately toxic to fish and aquatic invertebrates. Run-off from treated areas may be hazardous to fish in neighboring areas. However, because of aldicarb's acute toxicity, this pesticide must always be formulated as a granular mix that contains only 10 to 15 percent of this active chemical ingredient (48-50).

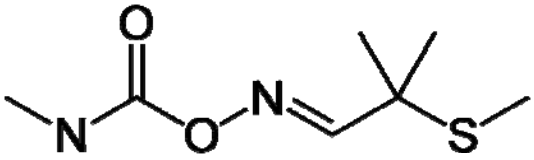

Fig. 5.7. Structure of aldicarb

a. Effect of catalyst amount

A 10 ml of 10^{-4} molar aqueous solution of aldicarb and catalyst amount of 1.0 g/L to 2.0 g/L with an increment of 0.5 g was taken for this study. Before irradiation the system was magnetically stirred for 30 minutes under dark to establish the adsorption-desorption equilibrium between the catalytic surface and the pesticide. The sample was then irradiated for 30 minutes using dichoric mirror of 420-630 nm as source for visible light. After the irradiation the sample was analyzed through HPLC with mobile phase of acetonitrile/water in the ratio of 30:70 (1.0ml/min) and UV detection at 246nm.

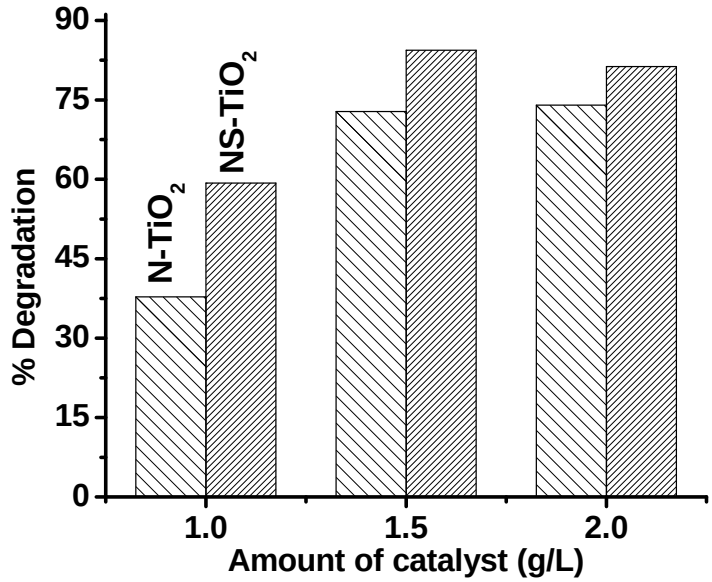

Fig. 5.8. % Degradation of aldicarb against amount of catalyst
Irradiation time: 30 min.; Aldicarb con. 10 ml of 10^{-4} M

Photocatalytic degradation of aldicarb against the amount of catalyst is shown in Fig.5.8. From the results it is clear that the photocatalytic degradation increases with increase of catalyst amount and reaches an optimum value. The optimum value in this case is 1.5 g/L. The increase of photocatalytic activity with increase of catalyst amount is assigned to the increase of active surface for the formation of activated photo excited species.

This optimum limit depends on the geometry and working conditions of the photo reactor and for a definite amount of catalyst in which all the particles, i.e. surface exposed are totally illuminated. When the catalyst concentration increases beyond the optimum value, it causes turbidity in solution. This turbidity prevents the penetration of light to the catalyst surface. Thus in any given application, the optimum catalyst concentration must be determined, in order to avoid excess catalyst and ensure total absorption of efficient photons.

b. Effect of time

Add 1.5 g/L of the catalyst to 60 ml of 10^{-4} molar aqueous solution of aldicarb. Before irradiation the system was magnetically stirred for 30 minutes under dark to establish the adsorption-desorption equilibrium between the catalytic surface and the pesticide. The dichoric mirror of 420-630nm was used as source for visible light. After the lamp was switched on, around 10ml of the suspension was pipetted out from the solution at an interval of 7 minutes each up to 35 minutes and analyzed using HPLC.

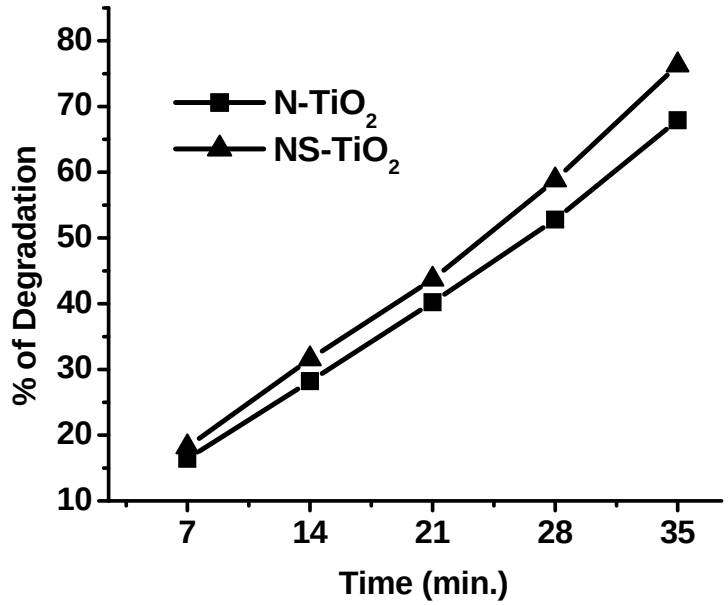

Fig. 5.9. % Degradation of aldicarb against time
Amount of Catalyst: 1.5 g/L; Aldicarb con. 60 ml of 10^{-4} M

Fig. 5.9 shows the percent degradation of aldicarb against time. The result shows a linear relation ship with percent degradation and time. That is the percent of degradation increases with increase in the irradiation time. As time of irradiation increases more and more light energy falls on the catalyst surface which increases the formation of photo excited species and enhances the photocatalytic activity.

c. Effect of light source

Studies involve the usage of 10 ml 10^{-4} molar aqueous solution of aldicarb with a catalyst amount of 1.5 g/L and light illumination of 30minutes. The dichoric mirror of 280-400nm and 420-630nm was used for the source of UV light and visible light respectively. Blank experiment was also conducted without using catalyst in visible light and also an experiment without light source. Study involves a comparison of the percent of degradation of both modified catalysts with pure titania prepared in our laboratory and commercially

available 100% anatase titania in UV and visible light irradiation. Remaining part of the experiment is same in above cases.

T able 5.5. % of degradation of Aldicarb against light source
Irradiation time: 30 min.; Aldicarb con. : 10 ml of 10^{-4} M;
Catalyst amount: 1.5 g/L

Studies	% of Degradation				
	N-TiO_2	**NS-TiO_2**	**L-TiO_2**	**A-TiO_2**	**Without Catalyst**
Visible light (420-630 nm)	72.8	84.4	35.9	42.0	8.2
UV light (280- 400nm)	42.0	50.8	72.0	95.6	---
Adsorption	8.9	12.6	11.2	32.2	---

Table 5.5 represents the percent of degradation of aldicarb against both the modified and pure titania in UV and visible light irradiation. Results shows that both the modified catalysts give better activity for the degradation of aldicarb in visible light irradiation when compared with pure and commercial titania whereas activity decreased in UV light irradiation. The adsorption studies show that the commercial anatase sample gives very good adsorption relationship with the aldicarb. The higher activity of modified catalysts in visible light was attributed to the presence of dopant elements. The dopants could lower the band gap of titania by the presence of an impurity state on the upper edge of the valence band. Thus the mixing the N2p and/or S3p states with O2p states could narrow the band gap of modified titania powders and lead to a stronger absorption in the visible light region. The higher activity of pure and commercial titania in UV irradiation is attributed to its bandgap.

d. Effect of dopant concentration

In this section we can evaluate the percent of degradation of aldicarb against various catalysts including modified catalysts with different dopant

concentrations and pure titania. Studies involve 10 ml 10^{-4} molar aqueous solution of aldicarb with a catalyst amount of 1.5 g/L and a visible light illumination of 30 minutes.

Table 5.6. % Degradation of aldicarb against various catalyst
Irradiation time: 30 min.; Aldicarb con. : 10 ml of 10^{-4} M,
Catalyst: 1.5 g/L

Catalyst	% of degradation
N-TiO_2 (l)	42.0
N-TiO_2	**72.8**
N-TiO_2 (h)	70.3
NS-TiO_2 (l)	38.8
NS-TiO_2	**84.4**
NS-TiO_2 (h)	80.9
L-TiO_2	35.9
A-TiO_2	42.0

The percent of degradation of aldicarb against all the prepared catalysts are shown in Table 5.6. The results showed that the optimized catalyst labeled as N-TiO_2 and NS-TiO_2 gives better results. Different loading of the dopants on titania reveals that at higher loading, the space charge region narrows and the efficiency of charge separation is reduced which results in the lower activities of the catalyst. An optimum concentration of dopants makes the thickness of space charge layer substantially equal to the light penetration depth, because the space charge region becomes very narrow when the concentration of doping ions is too high, and the penetration depth of light into titania greatly exceeds the space charge layer, which will make in the recombination of the photo generated carriers easier (47). To sum up, there iss an optimum concentration of dopant in titania for the most efficient separation of photo generated carriers and thus photocatalytic activity. The higher activity of modified titania compared to pure titania, results from the effect of dopants which enhance the activity in visible light region by narrows the bandgap of the titania semiconductor.

5.2.4 Monolinuron

Monolinuron belongs to the family of phenylurea herbicide. The IUPAC name of the compound is 3-(4-chlorophenyl)-1-methoxy-1-methylurea. It is used to control broad-leaved weeds and vegetable crops such as leeks and potatoes. They inhibit photosynthesis. However, they may also damage non-target aquatic primary producers such as phytoplankton, periphyton and macrophytes, and in turn alter the ecosystem equilibrium. In aquatic ecosystems, molecular transformations result from biotic or abiotic processes. Some of the phenylurea by-products are known to show phytotoxicity equivalent to or even higher than that of the starting compounds. They cause irritation to eyes, skin and mucous membranes, coughing and shortness of breath, nausea, vomiting, diarrhea, headache etc. (47,51,52).

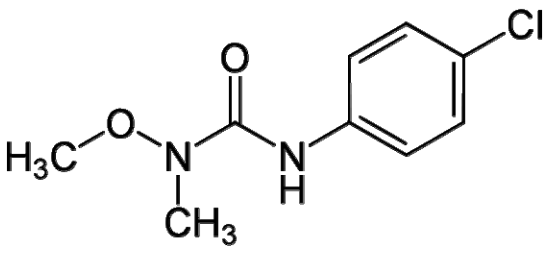

Fig. 5.10. Structure of monolinuron

a. Effect of catalyst amount

In this study a 10^{-4} molar aqueous solution of monolinuron was used. About 10 ml of solution was taken and catalyst of amount of 1.0 g/L to 5.0 g/L added. Before irradiation the system was magnetically stirred for 30 minutes under dark to establish the adsorption-desorption equilibrium between the catalytic surface and the pesticide. The dichoric mirror of 420-630 nm was used as source for visible light. After the irradiation the sample was centrifuged and filtered through micro pore membrane filter using syringe pump. The concentration of the filtered sample was analyzed using HPLC. The mobile Phase used in this study was a (0.7 ml/min) acetonitrile/water in the

ratio of 40:60 and UV detection at 240 nm. Then the percent of degradation was calculated using the relation, {Co – C} X 100 / Co., where Co and C are the concentration of pesticide before and after irradiation.

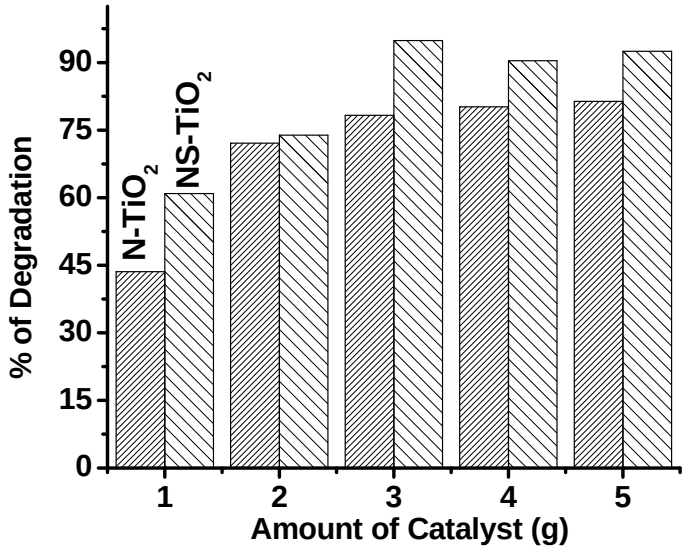

Fig.5.11. % Degradation of monolinuron against amount of catalyst Irradiation time: 1 hour; Monolinuron con. 10 ml of 10^{-4} M

Fig. 5.11 shows the percent of photocatalytic degradation of monolinuron against catalyst amount. The initial reaction rate of a photocatalytic reaction is directly proportional to the titania concentration. This behaviour is a consequence of the increase in the number of illuminated particle surface, which produce a larger amount of reactive electron-hole pairs. Nevertheless, there is a limit for the mass of catalyst to be introduced into the reactor corresponding to the total absorption of the photons coming from the light source. Higher amounts of titania results in a lower efficiency of the reaction since screening effects become predominant. Assuming that the optimal amount of the photocatalyst depends on the reaction condition, this value has to be determined for each experimental condition. The optimized catalyst amount in this case is 3.0 g/L.

b. Effect of time

A total of 70 ml 10^{-4} molar aqueous solution of monolinuron was taken and added catalyst amount of 3.0 g/L was added for this experiment. Before irradiation the system was magnetically stirred for 30 minutes under dark to establish the adsorption-desorption equilibrium between the catalytic surface and the dye. The dichoric mirror of 420-630 nm was used as source for visible light. After the lamp was switch on, around 10ml of the suspension was pipetted out from the solution at an interval of 10 minutes up to one hour. The concentration of samples collected at each interval was measured using HPLC and analysis details are explained in the previous section.

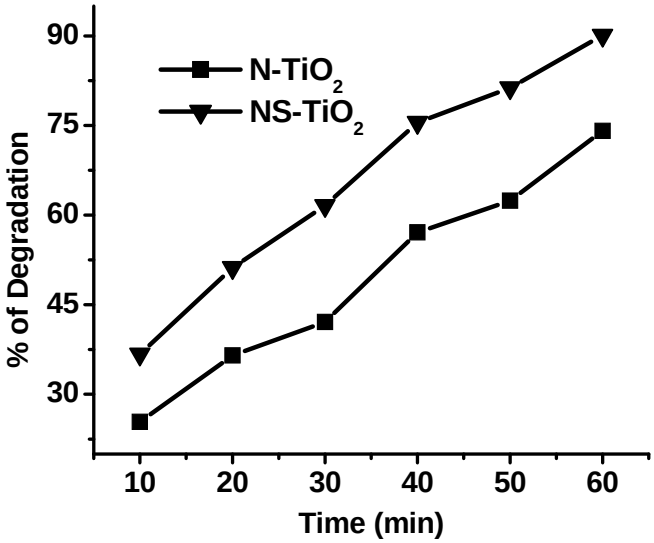

Fig. 5.12. % Degradation of monolinuron against time
Amount of Catalyst: 3 g/L; Monolinuron con. 10 ml of 10^{-4} M

The photocatalytic degradation of monolinuron against irradiation time is shown in Fig. 5.12. It was noted from the results that the percent of degradation increases almost linearly with increase of irradiation time. When time of irradiation increases more and more light energy falls on the catalyst surface which causes the generation of higher amount of photo excited species.

As the number of photo excited species increases, the reactive oxygen species increases which is responsible for the degradation of the adsorbed species.

c. **Effect of light source**

In this study a10 ml 10^{-4} molar aqueous solution of monolinuron was used with a catalyst amount of 3 g/L and light illumination of one hour. The dichoric mirror of 280-400 nm and 420-630 nm was used for the source of UV light and visible light respectively. The experiment was also conducted without catalyst in visible light and a control without light source. Study involves a comparison of the percent of degradation of both modified catalyst with pure titania prepared in our laboratory and commercially available 100% anatase titania in UV and visible light irradiation. Remaining part of experiments is the same in all cases.

Table 5.7. % of degradation of monolinuron against light source
Irradiation time: 1 hour; Monolinuron con. : 10 ml of 10^{-4} M;
Catalyst amount: 3 g/L

Studies	% of Degradation				
	N-TiO_2	**NS-TiO_2**	**L-TiO_2**	**A-TiO_2**	**Without Catalyst**
Visible light (420-630 nm)	78.3	94.9	36.5	57.9	20.1
UV light (280- 400nm)	53.3.	69.7	90.2	98.3	---
Adsorption	21.8	27.4	14.0	21.6	---

The percent of photocatalytic degradation of monolinuron against the modified catalyst and pure titania in both UV and visible light are shown in Table 5.7. Results shows that both the modified catalysts give higher activity in visible and lower activity in UV light for the degradation of monolinuron when compared with pure and commercial titania. The dark reaction shows a significant change in the concentration of catalyst which is attributed to the adsorption property of the catalysts. The significant change in the

concentration of monolinuron without catalyst addition is due to leaching property of the material under light. The higher activity of modified catalysts in visible light is attributed to the presence of dopant elements, which significantly reduce the crystallite size and the band gap and control the surface property through increase in the surface area. The presence of both the dopants attributed to the higher activity of NS-TiO_2 compared to the others.

d. Effect of dopant concentration

In this section we evaluated the percent of degradation of monolinuron against various catalysts including modified catalyst with different dopant concentrations and pure titania. Studies involve 10 ml 10^{-4} molar aqueous solution of monlinuron with a catalyst amount of 3 g/L and a visible light illumination of one hour

Table 5.8. % Degradation of monolinuron against various catalysts
Irradiation time: 1 hour; Monolinuron con. : 10 ml of 10^{-4} M,
Catalyst: 3 g/L

Catalyst	% of degradation
N-TiO_2 (l)	50.1
N-TiO_2	**78.3**
N-TiO_2 (h)	76.2
NS-TiO_2 (l)	61.2
NS-TiO_2	**94.9**
NS-TiO_2 (h)	90.8
L-TiO_2	36.5
A-TiO_2	57.9

Table 5.8 gives the results of all the catalysts for the photocatalytic removal of monolinuron using visible light irradiation. It is noted from the results that the activity of modified catalyst increases with increase of dopant concentration and reaches an optimum value. When the concentration of

dopant is excessively high, the space charge region became very narrow and the penetration depth of light into titania greatly exceed the space charge layer. Therefore, the recombination of the photo generated electron-hole pairs became easier. Thus it is clear from the results that both N-TiO_2 and NS-TiO_2 gives higher activity compared to others. To sum up, there is an optimum concentration of dopant in titania for the most efficient separation of photo generated carriers and thus photocatalytic activity. The higher activity of modified titania compared to pure titania is due to the effect of dopants which reduce the bandgap and enhance the activity in visible light region.

e. Reusability test

The reusability of the modified catalyst was evaluated by conducting a second cycle of degradation of the compounds 2, 4-D and monolinuron. For this purpose, the catalysts obtained after the first cycle was washed and activated by heating half an hour of its calcination temperature. A 10 ml of 10^{-4} molar aqueous solution of each compound with 3 g/L of catalyst was irradiated with visible light for one hour. After the irradiation the sample was collected, centrifuged, filtered and measured its concentration using HPLC. The HPLC conditions were already explained in the respective sections of each compounds.

Table 5.9. Reusability test of 2,4-D and Monolinuron.
2,4-D: Irradiation time- 1hour, Catalyst amount- 3 g/L
Monolinuron: Irradiation time- 1hour, Catalyst amount- 3 g/L

Studies [Visible light (420-630 nm)]	% of Degradation			
	2,4-D		Monolinuron	
	N-TiO_2	NS-TiO_2	N-TiO_2	NS-TiO_2
1st Cycle	59.6	90.7	78.3	94.9
2nd cycle	58.6	90.5	77.1	93.8

Table 5.9 represent the reusability result of modified catalyst against the degradation studies of 2, 4-D and monolinuron respectively. It is clear from the

results that both the modified catalysts give almost same percent degradation in each cycle of studies. The relative error stands within 1%. This indicates that the catalyst does not photo corrode, is not leached, is stable and exhibit high photocatalytic efficiency in repeated cycles.

f. Effect of lamp power

In this section we evaluated the effect of light intensity for the degradation of pesticides. For this purpose we used two different lamp systems of -150 W Xe lamp with light irradiation intensity of 96.8 mW/cm^2 and 100 W Xe lamp with light irradiation intensity of 64.7 mW/cm^2 respectively. A 10 ml of 10 $^{-4}$ molar aqueous solution of 2,4-D and monolinuron wer used with a catalyst amount of 3 g/L and visible light irradiation on 45 minutes.

Table 5.10. Effect of lamp power on 2,4-D and Monolinuron degradation
2,4-D: Irradiation time- 45 min., Catalyst amount- 3 g/L
Monolinuron: Irradiation time- 45 min., Catalyst amount- 3 g/L

Studies [Visible light (420-630 nm)]	**% of Degradation**			
	2,4-D		**Monolinuron**	
	N-TiO_2	**NS-TiO_2**	**N-TiO_2**	**NS-TiO_2**
150 W Xe lamp (96.8 mW/cm2)	68.2	94.6	74.9	98.9
100 W Xe lamp (64.7 mW/cm2)	45.2	74.2	59.1	79.2

Table 5.10 represents the percent of photocatalytic degradation of 2,4-D and monolinuron against the visible light source with different lamp power. Results clearly indicate that in both cases the percent of degradation increases with increase of lamp power. When the lamp power increases, its light intensity also increases which enhance the production of more photo excited species on catalyst surface. As number of photo excited species increases it causes degradation of more pollutants adsorbed on the catalytic material and enhances the activity.

References

[1] Parraa S.; Olivero J.; Pulgarin C., Appl. Catal. B: Environ. 36 (2002) 75 .

[2] Nikos L. S.; Despina R.; Eleftheria K.; Dionissios M.; Nikolaos P. X., Desalination 250 (2010) 351.

[3] Branko D.; Matej S., Intern. J. Environ. Anal. Chem. 87 (2007) 1079.

[4] Moctezuma. E.; Leyva E.; Monreal E.; ViUegas N.; Infante D., Chemosphere, 39 (1999) 511.

[5] Carlosa M-H.; Achilledebattisti ; Sergioferro ; Silviareyna ; Monicacerro-Lopez; Marcoa Q., Environ. Sci. Technol. 42 (2008) 6929.

[6] Sanjay P. K.; Sudhir P. D.; Sudhir B. S.; Jacob A. M.; Vishwas G. P., Ind. Eng. Chem. Res. 43 (2004) 8178.

[7] Weizheng.; Scottr Y.; Sharonk P.; Mingxin G., Environ. Sci. Technol. 38 (2004) 6855.

[8] Margarita H. P.; Gustavo P.; Manuel I.M.; Octavio M.; Pilar F.; Isabel O.; Wolfgang G.; Sixto M., Appl. Catal. B: Environ. 64 (2006) 272.

[9] Stein, M. W.; Sansone, E. B.; Degradation of Chemical Carcinogens; Van Nostrand Reinhold: New York, 1980.

[10] Muller, K. R., Ed. Chemical Waste. Handling and Treatment; Springer Verlag: Berlin, 1986.

[11] Clark R. M.; Fronk C. A,; Lykins B. W., Jr. Enuiron. Sci. Technol. 22 (1988) 1126.

[12] Ramalho R. S., Introduction to Wastewater Treatment Processes; Academic Press: New York, 1983.

[13] Rubin A. J., Ed., Chemistry of Wastewater Technology; Ann Arbor Science: Ann Arbor, MI, 1978.

[14] Staelin J.; Hoigne J. Enuiron. Sci. Technol. 19 (1985) 1206.

[15] Glaze W. H., Enuiron. Sci. Technol. 21 (1987) 224.

[16] Hapeman-Somich,C. J., ACS Symposium Series 459 (1991) 133.

[17] Slade P., Nature 207 (1965) 515.

[18] Kearney P. C.; Ruth J. M.; Zeng Q.; Mazzochi P., J. Agric. Food. Chem., 33 (5) (1985) 953.

[19] Kearney P.C.; Muldoon M. T.; Somich C. J., Chemosphere 16 (1987) 2321.

[20] Clapes P.; Soley J.; Vicente M. ; Rivera J.; Caixach J.; Ventura F., Chemosphere, 15 (1986) 395.

[21] Giri R. R.; Ozaki H.; Taniguchi S.; Takanami R., Int. J. Environ. Sci. Tech. 5 (1) (2008) 17.

[22] Devipriya S.; Yesodharan S., Solar Energy Mater. Solar Cells 86 (2005) 309.

[23] Gogate P. R.; Pandit A. B., Adv. Environ. Res. 8 (2004) 501.

[24] Konstantinou J. K.; Albanis T. A., Appl. Catal. B: Environ. 49 (2004) 1.

[25] Ioannisk K.; Theophanism S.; Vasilisa S.; Triantafyllosa A., Environ. Sci. Technol. 35 (2001) 398.

[26] McMurray T. A.; Dunlop P. S. M.; Byrne J. A., J. Photochem. Photobiol, A: Chem.182 (2006) 43.

[27] Pelizzetti E.; Pramauro E.; Minero C.; Serpone N.; Borgarello E. In Photocatalysis and Environment-Trends and applications; NATO ASI Series, Schiavello, M., Eds.; Kluwer: Dordrecht, The Netherlands, (1988) 469.

[28] Ollis D. F.; Pelizzetti E.; Serpone N., In Photocatalysis: Fundamental and Applications; Serpone, N., Pelizzetti, E., Eds.; Wiley: New York, (1989) 603

[29] Turchi C. S.; Ollis D. F., J. Catal. 119 (1989) 483.

[30] Childs L. P.; Ollis D. F., J. Catal. 66 (1980) 383.

[31] Hoffmann M. R.; Martin S. T.; Choi W.Y.; Bahnemann D. W., Chem. Rev. 95 (1995) 69.

[32] Mills A.; LeHunte S., J. Photochem. Photobiol, A: Chem. 108 (1997) 1.

[33] Hemant K. S.; Mohd S.; Malik M. H.; Mohammad M.; Detlef W. B., J. Mole. Catal. A: Chem. 264 (2007) 66.

[34] Trillas M.; Peral J.; Domknech X., Appl. Catal. B: Environ. 5 (1995) 377.

[35] Muller T. S.; Sun Z.; Gireesh Kumar M. P.; Murabayashi K. M., Chemosphere 36 (9) (1998) 2043

[36] Kwan C. Y.; Chu W., Water Res. 37 (18) (2003) 4405.

[37] Trillas M..; Peral J.; Domenech X.,J. Chem. Technol. Biotechnol. 67 (1996) 237.

[38] Zepp R. G.; Wolfe N. L.; Gordon N. L.; Baughman G. L. Environ. Sci. Technol. 9 (1975) 1144.

[39] Shuai-WenZ.; Choon-Wai H.; Paul Chen J., Ind. Eng. Chem. Res. 46 (2007) 6566.

[40] Gang L.; Lianzhou W.; Chenghua S.; Xiaoxia Y.; Xuewen W.; Zhigang C.; Sean C. S.; Hui-Ming C.; Gao Q. L., Chem. Mater. 21 (2009) 1266.

[41] Jin Kai Z.; Lu L.; Jianqiang Y.; Hong Liang L.; Pei-Zhi G.; Hong S.; Zhao X. S., J. Phys. Chem. C 112 (2008) 5316.

[42] http://en.wikipedia.org

[43] http://ces.iisc.ernet.in

[44] http://umbbd.msi.umn.edu

[45] http://www.cdc.gov

[46] http://www.ch.ic.ac.uk

[47] Pleskov Y. V., Sov. Electrochem. 17 (1981) 1.

[48] http://extoxnet.orst.edu

[49] http://toxipedia.org

[50] Tongwen W.,"Hyphenated HPLC-MS technique for analysis of compositional monosaccharides of transgenic corn glycoprotein and characterisation of degradation products of diazinon, fonofos and aldicarb in various oxidation system., Ph.D theisis

[51] N lieu S.; Kerhoas L.; Sarakha M.; Einhorn J., Environ Chem Lett 2 (2004) 83.

[52] http://www.pesticideinfo.org/

Chapter 6

Photocatalytic Water Splitting Reaction

Contents

In the development of new energy sources, hydrogen is one of the most attractive fuels for the 21st century. Hydrogen has considerable potential as an alternative fuel, especially if it can be generated inexpensively from an abundant raw material such as water. However, the efficient photocatalytic splitting of water to generate hydrogen using sunlight remains an as yet unachieved goal from a technological standpoint. A number of modification techniques and chemical additives have been developed in recent years to improve photocatalytic activity of TiO_2 under visible light irradiation. The development of better catalysts, tailoring of electronic structure and the reactivity as well as synthetic methods can be employed for controlling the morphology of catalysts. It is also going to benefited from recent progress in nano science. In this section we evaluate the efficiency of our modified catalyst and compare it with the unmodified titania for production of hydrogen through water splitting reaction.

6.1 Introduction

The modern society has been searching for a new form of energy that is clean renewable, cheap and a viable alternative to fossil fuel due to the drastic depletion of fossil fuels by their effective consumption and the serious environmental problems accompanying their combustion. Sunlight in the near IR, visible and UV region radiates a tremendous amount of energy and intensity to the earth so that harnessing this solar energy would contribute significantly to our electrical and chemical needs. Sustainable hydrogen production is a key target for the development of alternative future energy systems that will provide a clean and affordable energy supply. More over, it is carbon-free, facilitates use of more efficient power generation systems (e.g. fuel cells) and can be used to chemically reduce carbon oxides (CO, CO_2) to chemical fuels. But presently, 95% commercial hydrogen is produced from the non-renewal sources such as fossil fuels and the rest are obtained from other sources. Among them the major one is water splitting. Renewable hydrogen production is not popular yet because the cost is still high. Solar and wind are the two major sources of renewable energy and they are also the promising sources for renewable hydrogen production. The shifting to hydrogen based economy is based on various fundamental and organizational factors, mainly concerning production, storage and distribution. Among these, the production has received considerable attention. Hydrogen is also a versatile energy carrier that is currently produced from a variety of primary sources, such as fossil fuel, natural gas, naphtha, heavy oil, methanol, biomass, wastes, coal, solar energy, wind, nuclear power, water etc. There are various methods and technologies that haven been developed for the production of hydrogen from these materials and few of them have already been practiced. These technologies can be broadly classified as (1-11).

a) Thermo-chemical routes
b) Electrolytic

c) Photolytic
d) Biochemical pathway
e) Chemical(steam reforming of hydrocarbon)

Each of these technologies can be coupled with one another and one can generate further production methods. Among them photo-electrochemical and photo- micro biological methods have been receiving considerable attention in the last few decades. The term ‘‘photo electrochemical’’ refers to a scheme wherein light is used to introduce an electrochemical process which includes, Photoelectrolysis, Photocatalysis’ and Photo assisted splitting. The term photoelectrolysis is correctly applied to a case involving semiconductor photo electrode(s) in an electrochemical cell. Photocatalysis has been generally applied to the case of semiconductor suspensions. Photo assisted splitting’’ is recommended for cases wherein the excitation light energy only partially furnishes the voltage needed for the electrolysis process, the rest being accommodated by an applied external bias (12).

Among the various materials for the hydrogen production, water gets prominent role due to its large availability, easy to handle etc. Starting from water as the materials for the hydrogen production, the approaches include electrolysis, thermochemical water splitting, photoelectrolysis and photocatalyzed water splitting. Among these methods, photocatalytic production of hydrogen from water is the most attractive and rewarding work because water is abundant and renewable. And the process can occur at ambient conditions using only sunlight and a semiconductor photocatalyst (3).

Photocatalytic reactions are classified into two categories: uphill (Gibbs free energy being positive) and downhill (negative). Water splitting into H_2 and O_2 is accompanied by a large positive change in the Gibbs free energy i.e., it is an uphill reaction. In this reaction, photon energy is converted into

chemical energy, as seen in photosynthesis by green plants. Therefore, this reaction is termed as artificial photosynthesis. On the other hand, degradation reactions such as the photo-oxidation of organic compounds using oxygen molecules are generally downhill reactions. The reaction proceeds irreversibly. This type of reaction is regarded as a photo induced reaction and has been extensively studied using titanium dioxide photocatalysts (1,2,13).

There are two types of configuration adapted to a photo catalyst that can be used for photochemical water splitting: (i) photoelectrochemical cells (ii) particulate photo-catalytic systems. The photoelectrochemical cell for water decomposition involves two electrodes immersed in an aqueous electrolyte, one of which is a photocatalyst exposed to light. In particulate photocatalytic systems, the photocatalysts are in the form of particles or powders suspended in aqueous solution, in which each particle acts as micro photoelectrode that performs both the oxidation and reduction reactions of water on its surface. The particulate photocatalytic systems have the advantage of being much simpler and less expensive than photo electrochemical cell. But it has got some difficulty for the separation of stoichiometric products of hydrogen and oxygen due to the possibility of reverse reaction (2).

Historically the discovery of photo electrolysis of water directly into oxygen at a titania electrode and hydrogen at a Pt electrode by the illumination of light with energy greater than the band gap of titania is attributed to Fujishima and Honda through photocatalysis by titania. From this date, extensive work has been carried out to produce hydrogen from water by this novel oxidation reduction reaction using a variety of semiconductors (5, 14-17).

The water splitting process for H_2 generation has two major advantages namely the raw material is abundant and cheap and the combustion of H_2 in air produces water. This makes the whole process cyclic and non-polluting. From the

view point of large-scale hydrogen production, particulate photo catalyst systems are considered to be advantageous over more complex multilayer or tandem structure devices and have a wider range of potential applications (18-20).

6.2 Mechanism

The schematic representation of water splitting reaction by photo catalytic materials is shown in Fig. 6.1.

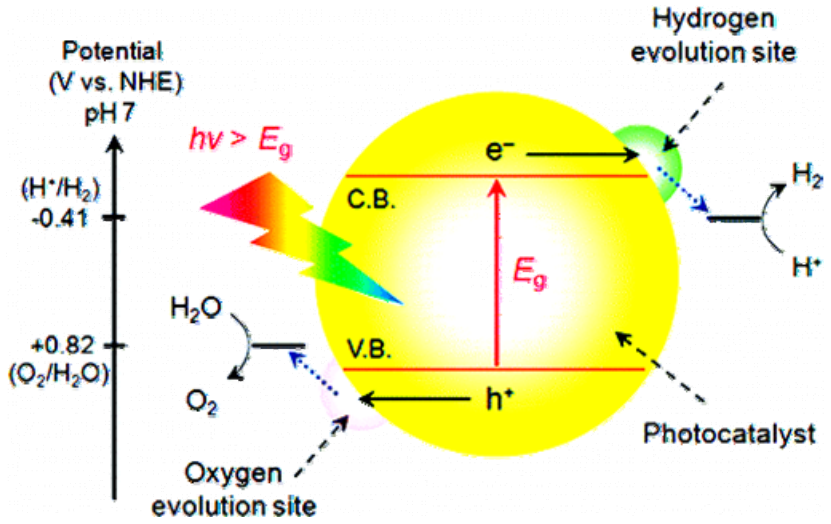

Fig. 6.1. Schematic representation of photocatalytic water splitting reaction over a semiconductor material.

Irradiation of light with energy greater than or equivalent to the band gap of semiconductor photo catalyst can generate electrons and holes in conduction band and valence band of photocatalyst. It causes reduction and oxidation of adsorbed species on semiconducting material. To achieve better overall water splitting, the bottom of the conduction band must be located at a more negative potential than the reduction potential of H^+ to H_2 (0 V at pH 0), while the top of the valence bands must be positioned more positively than the oxidation potential of H_2O to O_2 (1.23 V at pH 0). There fore, the minimum photon energy thermodynamically required to drive the reaction is 1.23 eV (6, 21).

$$TiO_2 \xrightarrow{h\nu} h^+ + e^-$$

Oxidation: $H_2O + 2\,h^+ \longrightarrow 2H^+ + 1/2\,O_2$

Reduction: $2H^+ + 2\,e^- \longrightarrow H_2$

Over all: $H_2O \xrightarrow{TiO_2/h\nu} H_2 + 1/2\,O_2$

In the last three decades, a large number of semiconductor materials have been investigated for photoelectochemical process. The semiconductor system which is efficient solar energy converter, should have optimized band gap so as to make maximum utilization of solar radiation, and should also have sufficient chemical stability against photo or other corrosion processes.

Many types of semiconductors with over 130 materials including oxides, nitrides, sulphides, carbides, and phosphides, have been reported to act as efficient photocatalyst for hydrogen evolution via water splitting with varying degree of both positive and negative results. A few of them are semiconductors containing elements such as Ga or In, compounds such as GaAs, CdTe and CdSe, metal oxides such as ZnO, TiO_2, ZrO_2, SnO_2, WO_3, Fe_2O_3, RuO_2, sulphide such as CdS, ZnS, GaS, metal (oxy)sulfide, metal (oxy)nitride, tantalates, niobates, Indates, Tungsten based materials, metal oxides with d^0 and d^{10} electronic configuration, Perovskite type materils, Inorganic complexes etc (12, 22-39).

Among these titania become a prominent one because of its favourable band gap, high chemical and photochemical stability, biological inertness, low cost, ease of method of preparation etc. A lot of studies with its modified forms are still in progress. One of the main drawbacks of titania material is its wide band gap energy which permits only its activity suitable by UV irradiation.

Although there has been extensive research during the last decades on titania photo catalyst. An efficient photo catalyst active in visible region with high quantum efficiency is still a dream today. Various methods for improving the efficiency includes: dye sensitization, doping with metals and non metals, coupled with other semiconductors etc (40-47). Among these the non-metal doping predominates over others due to its strong visible absorption by reducing the band gap by mixing their orbital with valence band of titania.

Titania exists mainly in two phases- anatase (band gap 3.2 eV) and rutile (3.0 eV). In most investigation it has been found that anatase is more active than rutile and this can be explained by considering its electronic band structure. The location of valence band of these two phases is almost same but their conduction bands are slightly different. The conduction band potential of rutile coincides almost with the NHE potential, whereas that of anatase is shifted cathodically by almost 0.2 V. Hence the driving force for water reduction is very small for rutile while the reduction takes place more easily in the anatase form. When comparing rutile and anatase, the poor light absorption capability of rutile causes lower mobility for photogenerated carriers which decrease photocatalytic activity for water splitting (3).

Water decomposition is a very difficult and complex reaction. The various intermediate chemical steps present a kinetic limitation that decreases the efficiency of the reaction. One possible way to overcome this problem is the use of sacrificial electron donors or acceptors. The introductions of sacrificial agent (electron donor or proton acceptor) increases the efficiency of hydrogen production through suppressing the recombination of electrons and holes by reaction irreversibly with photo induced species or by reverse reaction between O_2 and H_2 (48-53).

Organic compounds, such as alcohols (methanol, ethanol, isopropanol, etc.), acids (formic acid, acetic acid, etc.), and aldehydes (formaldehyde, acetaldehyde, etc.) have all been used as electron donors for photocatalytic hydrogen generation. Among them, methanol was most widely used for the hydrogen generation process. The suggested mechanic routes as follows (54, 55)

$$h^+ + H_2O \longrightarrow {}^{\bullet}OH + H^+$$

$$CH_3OH + {}^{\bullet}OH \longrightarrow {}^{\bullet}CH_2OH + H_2O$$

$${}^{\bullet}CH_2OH \longrightarrow HCHO + H^+ + e^-$$

$$2H_2O + e^- \longrightarrow H_2 + 2OH^-$$

$$\text{Overall rean.} \quad CH_3OH \xrightarrow{\text{Catalyst / h}\upsilon} HCHO + H_2$$

The product, formaldehyde (HCHO), could be further oxidized to methanoic acid (HCOOH) and subsequently to CO_2 together with hydrogen generation.

$$HCHO + H_2O \xrightarrow{\text{Catalyst / h}\upsilon} HCOOH + H_2$$

$$HCOOH \xrightarrow{\text{Catalyst / h}\upsilon} CO_2 + H_2$$

In metal doping process, most time the doping species itself act as recombination centre and reduce the photocatalytic efficiency. Whereas the presence of noble metals on titania surface results in the formation of a Schottky barrier at the metal/semiconductor interface, which leads to a decrease in electron-hole recombination rate. Decreasing the over potential for hydrogen evolution owing to a large over potential for the evolution of H_2 on the surface of TiO_2, the material alone becomes inactive. Usually, this problem can be solved by loading TiO_2 with co-catalysts of noble metals, such as Pt,

Pd, Au, Rh, and Ag. Loading these metals, which have a low over potential for hydrogen, can make it easier to generate hydrogen (1, 3).

The crystallite defects largely contribute to the efficiency of the photocatalyst. The defects itself promote as trapping and recombination centers between photogenerated electrons and holes, resulting in a decrease in the photocatalytic activity. The higher the crystalline quality, the smaller is the amount of defects. Therefore, a high degree of crystallinity, rather than a high surface area, is required for a photocatalyst, especially for an uphill reaction like water splitting (1,13).

The objective of the present study is to investigate the effect of N doped and N S co-doped titania for the production hydrogen through water splitting reaction in visible region. The studies involve the effect of catalyst amount, effect of time and also a comparison of modified catalysts with pure titania prepared in laboratory and a commercial one.

6.3 Experimental section

The photoactivity of all the samples were evaluated under a medium-pressure mercury lamp (Hg, Ace Glass Inc., 450W) irradiation in a closed rectangular quartz cell equipped with a sampling and evacuation ports. The samples were irradiated in an outer irradiation–type quartz cell where lamp was surrounded with water circulation jacket to absorb IR irradiation. The lamp exhibits broad range emission spectra with maxima at both UV and the visible range. The lamp radiates 16% of the radiation in UV and remaining in visible region. The catalytic activity experiments were conducted in static mode for water in methanol (2:1 v/v %) mixtures, in the presence of well dispersed catalyst. The reaction products were analysed over a period upto 6 h with an interval of 2h. A gas chromatograph (Netel (Michro-1100), India) equipped with a thermal conductivity detector (TCD), molecular sieve

column (4m length) with Ar as carrier was employed in the isothermal temperature mode at 50°C oven temperature. The number of photons falling on the reaction cell or flux of the light determined by light flux meter was observed to be 19 x 10^4 lux or 278.2 watts/m^2 in horizontal geometry irradiation of UV-visible photoirradiator.

6.4 Activity

a. Effect of catalyst amount

Studies involve a 10:5 by volume ratio of water to methanol solution and add catalyst amount of 0.05g, 0.1g and 0.15g respectively. After a four hour irradiation of visible light the sample was collected and analyzed using gas chromatography.

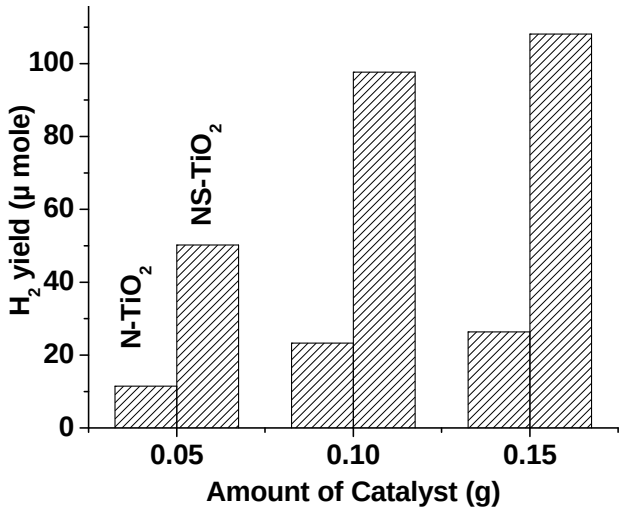

Fig. 6.2. Yield of hydrogen produced against amount of catalyst
Irradiation time: 4 hour; Water to methanol ratio 10:5

Fig. 6.2 shows the result of hydrogen obtained against the amount of catalyst. It is clear from the figure that the yield of hydrogen increases with increase catalyst amount. The active surface for the generation of photo excited species increases with increase of amount of catalyst. But above an optimized range there is no more higher activity.

b. Comparison study

In this study all the catalyst were used for evaluated for their activity in visible light for the water splitting reaction. Studies involve a 10:5 volume ratio of water to methanol with a catalyst amount of 0.1g. Sample was collected and analyzed at an interval of 2 hours up to 6 hours.

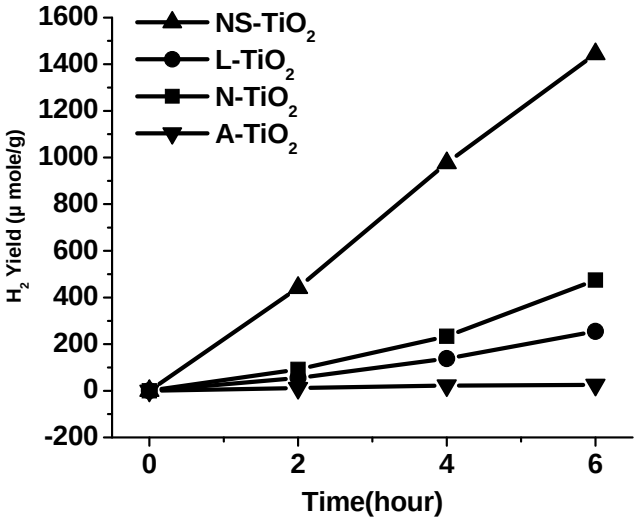

Fig. 6.3. Yield of hydrogen produced with time against different catalyst
Amount of catalyst: 1.0g; Water to methanol ratio 10:5

The comparison of results of the all the catalyst for the hydrogen production is shown in Fig. 6.3. The results showed that the yield of hydrogen increases with increase of time for all the catalyst except the commercial titania (A-TiO_2), which has a very low activity. It is also observed from the result that NS co-doped titania gives better result than others and this is due to the strong absorption band created by the dopants in visible region by mixing with the valence band of pure titania. Moreover other factors such crystallite nature, anatase phase, surface area, small particle size etc. also contribute to their higher activity.

References

[1] Akihiko K.; Yugo M., Chem. Soc. Rev. 38 (2009) 253.

[2] Rufino M. N. Y.; Consuelo _lvarez Galv_n M.; Del Valle F.; Jos A. V.; Jos L. G. F., Chem.Sus. Chem. 2 (2009) 471.

[3] Dennis Y. C. L.; Xianliang F.; Cuifang W.; Meng N.; Michael K. H. L.; XuxuW.; Xianzhi F., Chem. Sus.Chem. 3 (2010) 681.

[4] Bin Z.; Meghan S.; Lin H.Y.; Ismat Shah S.; Jiuhui Q.; Huang C.P.,Appl.Catal. B: Environ. 92 (2009) 41.

[5] Viswanathan B. A key notes on "Photoelectrochemical Production of Hydrogen-a dream or reality".

[6] Meng N.; Michael K. H. L.; Dennis Y. C.L.; Sumathy K., Renewable and Sustainable Energy Reviews 11 (2007) 401.

[7] Michael A. Henderson, "Fundamental Investigations of Water Splitting On Model TiO_2 Photocatalysts Doped for Visible Light Absorption".

[8] Armor J. N., Appl. Catal. A: Gen. 176 (1999) 159.

[9] Das D.; Veziroglu T. N., Int. J. Hydrogen Energy 26 (2001) 13.

[10] Stojic D. L.; Marceta M. P.; Sovilj S. P.; Miljanic S. S., J. Power Sources 118 (2003) 315.

[11] Weirich W.; Knoche K. F.; Behr F.; Barnert H., Nucl. Eng. Des./Fusion 78 (1984) 285.

[12] Krishnan R., J. Appl. Electrochem. 37 (2007) 765.

[13] Akihiko K.; Hideki K.; Issei T., Chem. Lett. 33 (2004).

[14] Fujishima A.; Honda K., Nature 37 (1972) 238.

[15] Markham M. C.; Hannan M. C.; Evans S. W., J. Am. Chem. Soc. 76 (1954) 820.

[16] Markham M. C.; Hannan M. C.; Paternostro R. M.; Rose C. B., J. Am. Chem. Soc. 80 (1958) 5394.

[17] Radwan A. Al-Rasheed., "Water Treatment by Heterogeneous Photocatalysis – An Overview". 2000.

[18] Sakai Y.; Sugahara S.; Matsumura M.; Nakato Y.; Tsubomura H., Can. J. Chem. 66 (1988) 1853.

[19] Bard A. J.; Fox M. A., Acc. Chem. Res. 28 (1995) 141.

[20] Jerina M., M. Tech. Dissertation "Hydrogen Generation via Photocatalytic Splitting of water using Modified Titanates" 2009.

[21] Yuzun F.; Dongmei L. I.; Minghui D.; Yanhong L.; Qingbo M., Front. Chem. China 4(4) (2009) 343.

[22] Akihiko K.; Isses T.; Hideki K., Chem. Commun. (2002) 1958.

[23] Akihiko K.; Masahiko S., Chem. Commun. (2000) 1371.

[24] Shuji O.; Mitsuru K.; Kazunori S.; Yasunobu I., J. Mater. Chem. 8 (11) (1998) 2335.

[25] Sang M. J.; Pramod H. B.; Hyum G. K.; Dong w. H.; Jum S> J.; Sang W. B.; Jae S. L., Phys. Chem. Chem. Phys. 7 (2005) 1315.

[26] Akihiko K., Pure Appl. Chem. 79 (2007) 1917.

[27] Kudo A.; Kato H., Chem. Lett. 26 (1997) 867.

[28] Machida M.; Yabunaka J.; Kijima T., Chem. Commun. (1999) 1939.

[29] Ikeda S.; Itani T.; Nango K.; Matsumura M., Catal. Lett. 98 (2004) 229.

[30] Hwang D. W.; Kim J.; Park T. J.; Lee J. S., Catal. Lett. 80 (2002) 53.

[31] Koca M.; Sahin M., Int. J. Hydrogen Energy 27 (2002) 363.

[32] Sato J.; Saito S.; Nishiyama H.; Inoue Y., J. Phys. Chem. 105 (2001) 6061.

[33] Sato J.; Saito S.; Nishiyama H.; Inoue Y., J. Phys. Chem. 107 (2003) 7970.

[34] Frank E. O., Chem. Mater. 20 (2008) 35.

[35] Zou Z.; Ye J.; Sayama K.; Arawa H., J. Photochem. Photobiol. A: Chem. 148 (2002) 65

[36] Abe R.; Higashi M.; Sayama K.; Abe Y.; Sugihara H., J. Phys. Chem. B 109 (2005) 16052.

[37] Yao W., J. Ye, Chem. Phys. Lett. 435 (2007) 96.

[38] Kato H.; Kudo A., Catal. Today 78 (2003) 561.

[39] Gian L. C.; Elena S.; Lucio F.,Appl. Catal. B: Environ. 84 (2008) 332.

[40] Carp O.; Huisman C. L.; Reller A., Prog. Solid State Chem. 32 (2004) 33.

[41] Gratzel M., Nature 414 (2001) 338.

[42] Karakitsou K. E.; Verykios X. E., J. Phys. Chem. 97 (1993) 1184.

[43] Choi W.; Termin A.; Hoffmann M. R., J. Phys. Chem. 98 (1994) 13669.

[44] Anpo M.; Takeuchi M.; Ikeue K.; Dohshi S., Curr. Opin. Solid State Mater. Sci. 6 (2002) 381.

[45] Asahi R.; Morikawa T.; Ohwaki T.; Aoki K.; Taga Y. Science 293 (2001) 269.

[46] [Khan S. U. M.; Sl-Shahry M.; Ingler W. B., Jr. Science 297 (2002) 2243.

[47] Regan B. O.; Gratzel M., Nature 353 (1991) 737.

[48] Bolton J. R., solar energy 57 (1996) 37.

[49] Linsebeigler A. L.; Lu G.; Yates Jr. J. T., Chem. Rev. 95 (1995) 735.

[50] Bard A. J., J. Phys. Chem. 86 (1982) 172.

[51] Hasimoto K.; Kawai T.; Sakata T., J. Phys. Chem. 88 (1984) 4083.

[52] Sakata T., J. Photochem. 29 (1985) 205.

[53] Gian L. C.; Elena S.; Lucio F.,Appl. Catal. B: Environ. 84 (2008) 332.

[54] Xiaobo C.; Shaohua S.; Liejin Guo.; Samuel S. M., Chem. Rev. 110 (2010) 6503.

[55] Akihiko K.; Isses T.; Hideki K., Chem. Commun. (2002) 1958.

…..ꕥ…..

Chapter 7

Photocatalytic Anti-bacterial Study

Contents

Urgent development of effective and low-cost disinfecting technologies is needed to address the problems caused by an outbreak of harmful microorganisms. Semiconductor photocatalysis, especially by titania and its modified forms has drawn much attention recently due to its promising application in chemical conversion and storage of solar energy for solar cells, hydrogen production, refractory pollutants elimination, self-cleaning surface. It has become the most important photocatalyst in environmental bio-decontamination for a large variety of organisms, bacteria, viruses, fungi and cancer cells, which can be totally degenerated and converted to CO_2, H_2O and harmless inorganic anions. This chapter evaluates the photocatalytic antibacterial efficiency of our modified titania, N-TiO_2 and NS-TiO_2 for the deactivation of Escherichia coli bacteria in aqueous medium using visible light irradiation.

7.1 Introduction

Water sources polluted by industrial wastes contain high percent of micro-organisms and organic compounds. Millions of deaths, many millions of cases of disease and disabilities are caused by harmful microorganisms every year. One of many reasons triggering off the deterioration of water quality and causing difficulties in making water drinkable are living organisms, namely bacteria, fungi etc. They influence many features of water quality, including its smell, colour, turbidity, pH, the content of organic substances, the content of nitrogen etc. Therefore, it is necessary to disinfect the polluted water, and thus the technology behind the disinfection increases with increase on its demand.

A high level of trihalomethanes (THMs) and other carcinogenic disinfection byproducts (DBPs) are resulted, when normal chlorination treatment of ground water contains high total organic carbon. But it fails in the deactivation of some pathogens, e.g. Cyptosporidium. In order to reduce the disinfection by-products formation, it may be desirable to inactivate organisms and decompose organic compounds prior to chlorine addition. Researchers are now focusing their efforts on production of durable, environmental friendly, cost-effective and safe antibacterial agents (1-5).

A lot of methods and materials are available for disinfection for water which includes, treatment of chlorine dioxide, ozone, ultraviolet (UV)-radiation, advanced filtration processes, photocatalytic oxidation, and materials such as metal oxides, silver, copper, poly(ethylene imine), alcohols, iodine etc. But the durability and life of such materials may be hindered by leaching of the active components out of the coating. This leaching effect is also likely to cause rapid development of resistance in bacteria. Among these the photocatalytic process is considered to be the most convenient and least expensive. This method follows a simultaneous treatment of photolytical

sterilization of microbial cells and photo catalytical decomposition of organic compound. (1, 2,6-18).

The antibacterial effect of heterogeneous titania semiconductor photocatalyst was first demonstrated by Matsunaga et al. in 1985. Since this report, the photocatalytic property has been widely studied in a variety of micro organisms such as viruses, bacteria, fungi, algae, and also in cancer cells. A lot microorganism such as Streptococcus mutans, Streptococcus natuss, Streptococcus cricetus, Escherichia coli, scaccharomyces cerevisisas, Lactobacillus acidophilus, poliovirus1etc.were destructed effectively using heterogeneous photocatalyst. Subsequently there have been a number of papers reporting disinfection of bacteria, viruses and other pathogens by photoactive titania and its modified forms (9, 19-23).

The advantages of photocatalytic disinfection are (3, 24).

a) No need of expensive chemicals

b) consumption of atmospheric oxygen as one of the reagent

c) Catalysts are reusable, inexpensive, non-hazardous

d) Solar light is used for the activation process

e) No need of any maintenance, power supply etc

f) It gives almost complete mineralization and deactivation of micro organism

g) The technology can be applicable in remote and rural areas.

Among the various photocatalytic materials, titania becomes a prominent one. The advantages and drawbacks of titania and its modification are already discussed in previous chapters.

The common existing bacteria in water such as Escherichia coli (Gram-negative bacteria) species is taken as model for this study. Escherichia coli (E.coli), classified as part of the Enterobacteriaceae family of gamma-proteobacteria. E.coli mainly lives in the lower intestine of warm-blooded animals (including birds and mammals), is one of the main species in bacterial family. It causes diarrhea, gastroenteritis, urinary tract infection, pyrogenic infection and septicemia. Its presence in groundwater is a common indicator of fecal contamination. Thus the detection of E.coli in drinking water is taken as evidence of recent pollution with human or animal feces, and is commonly used as a model organism for bacteria in general.

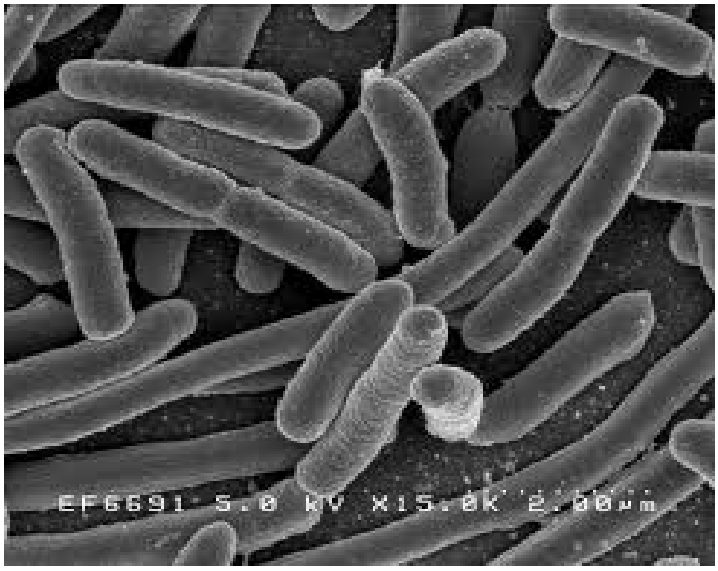

Fig. 7.1. A rod like image of Escherichia coli

The exact mechanism behind the deactivation of E.coli by photocatalyst material is not yet known clearly. Some research groups suggested that the free radicals that have been responsible for the cell DNA replication and the modification of cellular membranes and others suggested the direct oxidation of intracellular coenzyme. It cannot be ruled out by the possibility of deactivation of E.coli by H_2O_2 formed in the reaction system. The anti

bacterial property of H_2O_2 is well known and evidence of its formation in irradiated semiconductor suspension is already reported in various groups.

The outer membrane of E. coli is composed of lipopolysaccharide (LPS, a phospholipid layer) and peptidoglycan (periplasm). The strength of the cell wall is mainly based on LPS and peptidoglycan, whose structure is mechanically a strong network. Thus, the firm and resilient outer membrane of the cell plays an important role in the maintenance of cell morphology. Without a mechanically strong network, the cell will become elliptical or round. But the inner membrane of the cell still existed; otherwise the cell would break apart (24-26).

The pairs of free electrons and holes are formed in the conduction and valence band region of titania under light irradiation, which react with oxygen and adsorbed hydroxyl group to produce further reactive oxygen species such as superoxide ($O_2^{\bullet -}$) ,hydroxyl radicals ($OH^{\bullet}$), H_2O_2 etc, can cause fatal damage to microorganisms. These species could decompose outer membranes which consist of lipopolysaccharide (LPS) and peptidoglycan. The damage of peptidoglycan will change the morphology of E. coli. Without the protection of peptidoglycan and phospholipid layer, the leakage of the interior substances would occur and the cells eventually die (25-43).

In this chapter, we have discussing the application of modified titania and pure titania photocatalyst for its antibacterial effect on the species E.coli in aqueous media using visible light irradiation. Studies involve the effect of catalyst amount, effect of time, comparison with pure and modified catalyst, catalyst with different amount of dopant loading etc.

7.2 Experimental conditions

Escherichia coli were obtained from the Department of Marine Biology, Microbiology and Biochemistry, Cochin University of Science and

Technology. A sub culture was prepared using nutrient broth and it was incubated at 37^0C for 24 hr with 200 rpm in a rotary shaker. 10 ml of the culture was washed with a 0.9% saline solution by centrifugation at 12000 rpm for 15 minutes. The supernatant was discarded and the cells were suspended in 10 ml normal saline. The cell suspension was serially diluted to get proper concentration which was reported as number of colonies forming unit/ml (cfu/ml).

7.3 Activity Studies

A fixed amount of the photocatalyst was added to 9 ml 0.9% saline solution in a reagent bottle and it was sterilized by autoclaving at 120 ^{0}C and 15 lbs for 30 minutes and mixed with 1ml of the prepared cell suspension after cooling. The reaction mixture was stirred with a magnetic stirrer to prevent settling of the photocatalyst. The reaction mixture was irradiated with visible light obtained from a 100 W ozone free Xe lamp with a dichoric mirror of 420-630 nm. A bacterial suspension without photocatalyst was irradiated as a control, and the reaction mixture with no visible light irradiation was used as a dark control. After irradiation, 1 ml of the sample was spread on petridish contained nutrient agar and incubated for 48 hours at 37 ^{0}C and then it was taken out for counting. A triplicate of each experiment was conducted and its average was taken. Anti bacterial efficiency (in percent) was reported using the equation, {Co – C} X 100 / Co, where Co and C are the number of colonies formed before and after irradiation.

a. Effect of amount of catalyst

In this study a series of catalyst amount from 2.5, 5.0 and 7.5 mg was added to the cell suspension solution and allowed to irradiation. Both the modified catalysts such as N-TiO_2 and NS-TiO_2 were used for this purpose.

After the irradiation, the number of colonies formed in each experiment was calculated, which was explained.

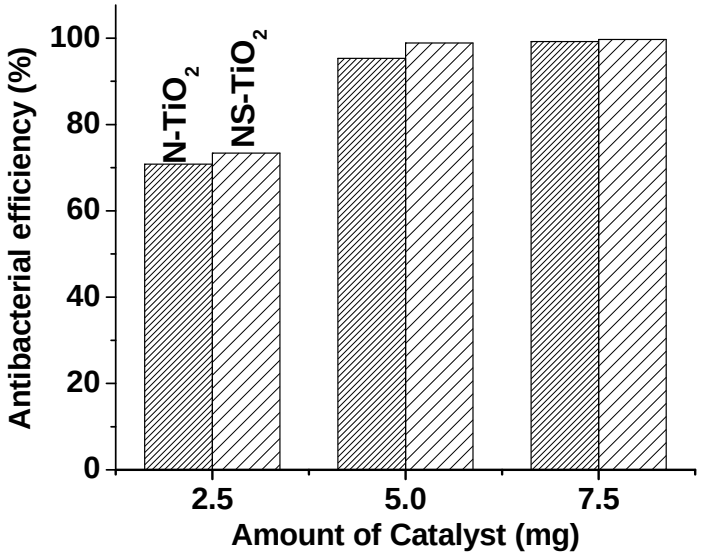

Fig. 7.2. Antibacterial efficiency against amount of catalyst.
Irradiation time: 1 hour.

The antibacterial efficiency of both the modified catalysts is shown in Fig. 7.2. The result shows that the antibacterial efficiency increases with increase in catalyst amount and reaches an optimum value and above this there is no noticeable change. The optimum efficiency is reported in this case with a catalyst dosage of 5.0 mg. The increase of activity with increase of catalyst dosage is attributed to the increase in catalyst surface area, increase of light absorption and consequently the creation of a higher number of active species. However at higher loadings, beyond the optimum, parts of the catalyst were in the dark and there was a decrease in the light penetration. Variation in the degree of settling influences the consistency of the sampling process, total amount of light absorption and scattering of the incident light by the catalyst. These factors together contribute to a decrease in the efficiency of the catalyst at loadings above the optimum level.

b. Effect of time

Studies involve both the modified catalysts with an amount of 5.0 mg and irradiation time of 20, 40 and 60 minutes. After the irradiation, the number of colonies formed in each experiment was calculated.

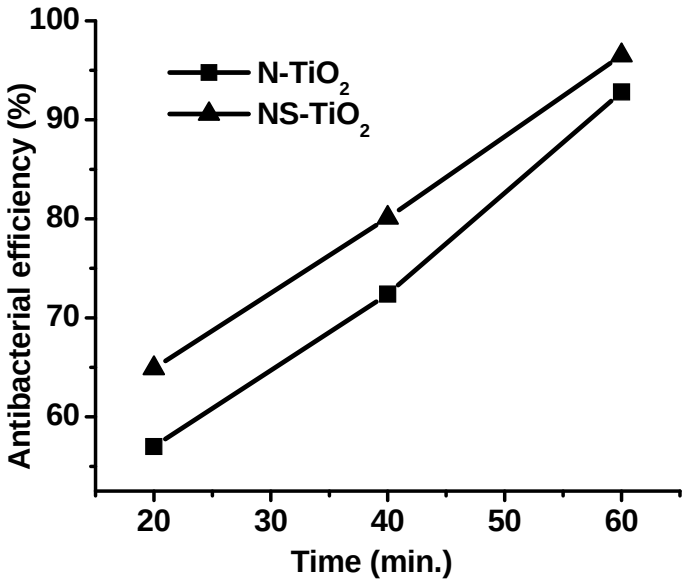

Fig. 7.3. Antibacterial efficiency against irradiation time. Catalyst amount: 5.0mg

Fig 7.3 shows the antibacterial efficiency of both the modified catalysts against irradiation time. The antibacterial efficiency of the both modified catalysts increase with increase in light irradiation. As time of irradiation increases, more and more photo excited species are formed. It causes increase of reactive oxygen species and the deactivation of bacterial cell.

c. Effect of dopant concentration

Here we conduct the antibacterial efficiency of both the modified catalysts with different amount of dopant source (details are shown in chapter 2 and 3). A 5.0 mg of each catalyst was taken for this experiment with one hour irradiation of visible light. The antibacterial efficiency was calculated as explained earlier.

Table 7.1. Antibacterial efficiency against effect of dopant concentration . Catalyst amount: 5.0 mg; Irradiation time: 1hour

Catalyst	Anti bacterial efficiency(%)
N-TiO_2 (l)	86.2
N-TiO_2	**95.3**
N-TiO_2 (h)	96.2
NS-TiO_2 (l)	89.5
NS-TiO_2	**98.8**
NS-TiO_2 (h)	99.1

Table 7.1 shows the antibacterial efficiency of the modified catalysts against the amount of dopant source. The results reveal that both the optimized catalyst (N-TiO_2 and NS-TiO_2) give better results. The presence of dopants (impurities such as N and S) shows a higher degree of visible light activity and it increases with increase of the dopant concentration. But it can be noted that an optimized quantity of dopants in the catalyst that gives a better result. Beyond that there is no noticeable change in the activity. The overdose of dopants may cover the surface or exist in the interface of titania crystallites, which can accelerate the aggregation of titania particles and result in the growth of titania crystallites because of the function of the bridge connection.

d. A comparison study

In this section we have discussed the results obtained by conducting the experiments in dark and controlled conditions with modified titania, pure titania prepared in the laboratory and commercial titania. In this experiment about 5.0 mg of catalyst was taken, that was optimized in earlier studies with visible light irradiation of one hour.

Table 7.2. A comparison study.
Catalyst amount: 5.0 mg; Irradiation time: 1hour

Catalyst	Anti bacterial efficiency (%)
N-TiO_2	95.3
NS-TiO_2	99.2
L-TiO_2	53.1
A-TiO_2	27.1
Without irradiation	6.5
Without Catalyst	10.0

Table 7.2 shows a comparison study of the antibacterial efficiency of the modified catalyst against pure titania with a controlled and dark conditions. The interaction between bacteria and the catalyst in the dark revealed that there was a very little antibacterial efficiency. This indicates that the toxicity of the applied photocatalyst to bacteria is not appreciable under the experimental condition of this study. But a controlled experiment without catalyst shows a little significant antibacterial activity which is attributed to the effect of light intensity which causes the damage of cell wall under irradiation. It is interesting to note that both the modified catalysts give more than 95% antibacterial efficiency in visible light compared to pure samples which has a maximum of 54% antibacterial efficiency (Fig. 7.4 and 7.5). The visible light activity in non-metal doped titania may be caused by band-gap narrowing from mixing the N 2p or S 3p states with O 2p states. It also provides an alternative explanation that a localized N 2p or/and S 3p state formed above the valence band is responsible for the visible light activity of the doped titania. More detailed studies are required to conclude whether our S^{6+} doping can indeed create intra-band-gap states close to the conduction band edges and thus induce visible light absorption at the sub-band-gap energy. This would be similar to the situation of conventional transition-metal ion doping.

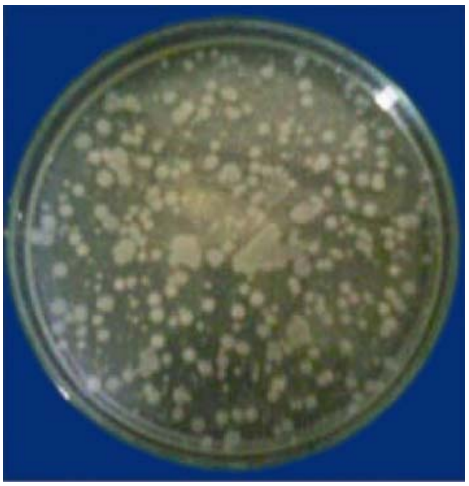

Fig. 7.4. Formation bacteria before light irradiation (dark control)

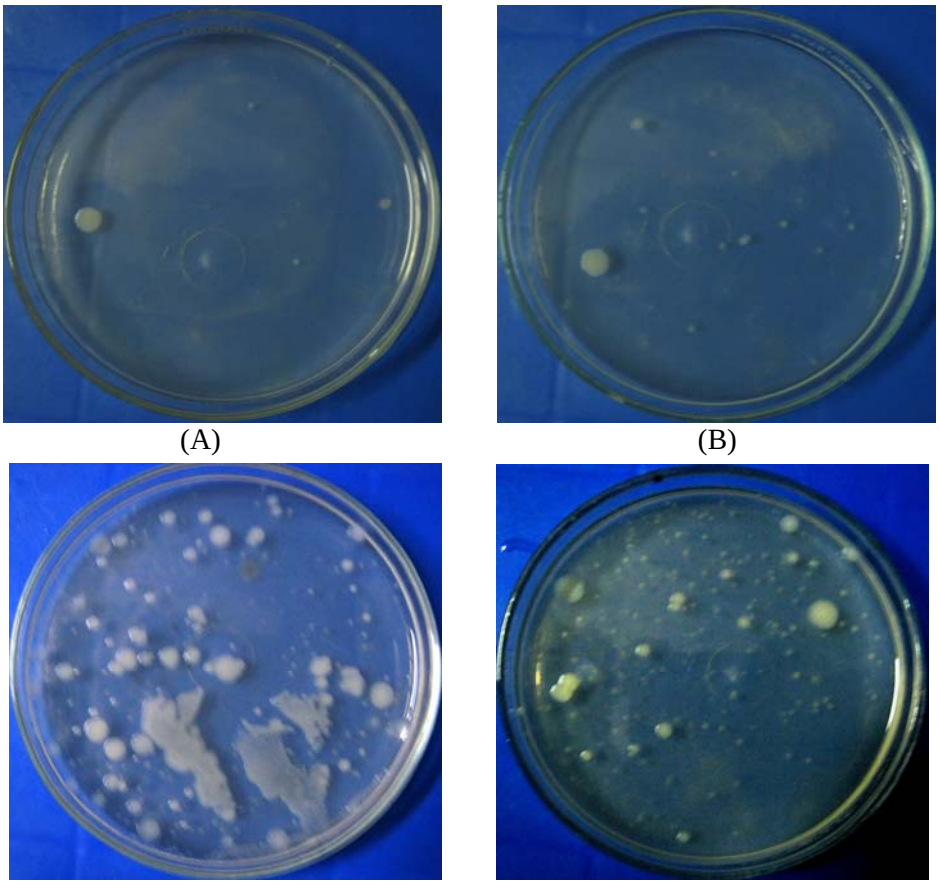

(A) (B)

(C) (D)

Fig. 7.5. Formation of bacteria after visible light irradiation of one hour. (A) NS-TiO_2, (B) N-TiO_2, (C) L-TiO_2 and (D) A-TiO_2

References

[1] Hsuan-Liang L.; Thomas C. K. Y., Process Biochemistry 39 (2003) 475.

[2] Shiraishi F.; Toyoda K.; Fukinbara S., Chem. Eng. Sci. 54 (1999) 1547.

[3] Chang W.; Wen-Yuan L.; Zulkarnain Z.; Nathan E. W.; Kat Z.; Andrew P. K.; Russell L. S.; Krishnan R., Environ. Sci. Technol. 28 (1994) 934.

[4] Dunlop P. S. M.; Byrne J. A.; Manga N.; Eggins B. R., J. Photochem. Photobiol. A: Chem. 148 (2002) 355.

[5] Andrzej M.; Wladyslaw W., Current Topics in Biophysics 25(1) (2001) 19.

[6] Stoimenov P. K.; Klinger R. L.; Marchin G. L.; Klabunde K.J., Langmuir 18 (2002) 6679.

[7] Morones J. R.; Elechiguerra J. L.; Camacho A.; Holt K.; Kouri J. B.; Ramírez J.T.; Yacaman M. J., Nanotechnology 16 (2005) 2346.

[8] Messaouda M.; Chadeaub E.,; Brunonc C.; Balleta T.; Rappennea L.; Rousseld F.; Leonardc D.; Oulahalb N.; Langleta M., J. Photochem. Photobiol. A: Chem. 215 (2010) 147.

[9] Ame´zaga-Madrida P.; Silveyra-Moralesa R.; Co´rdoba-Fierrob L.; Neva´rez-Moorillo´nc G. V.; Miki-Yoshidaa M.; Orrantia-Borundaa E.; Sol´ısb F. J., J. Photochem. Photobiol. B: Bio.70 (2003) 45.

[10] Hyett G.; Blackman C. S.; Parkin I. P., Faraday Discuss. 136 (2007) 329.

[11] http://www.agion-tech., Agion Technology Overview (2006).

[12] BioCote Silver Technology, BioCote Ltd. (2007).

[13] Cooney T. E., Infect. Control Hosp. Epidemiol. 16 (1995) 444.

[14] Rutala W. A.; Weber D. J.; Infect. Control Hosp. Epidemiol. 16 (1995) 442.

[15] Noyce J. O.; Michels H.; Keevil C. W., J. Hosp. Infect. 63 (2006) 289.

[16] Pasquier N.; Keul H.; Heine E.; Moeller M.; Biomacromolecules 8 (2007) 2874.

[17] Ming-Show W.; Wen-Chen C.; Der-Shan S.; Hsuan-Shun H.; Jiann-Hwa C.; Pei-Jane T.; Nien-Tsung L.; Mei-Shiuan Y.; Shang-Feng H.; Shih-Lien W.; Hsin-Hou C., Appl. Environ. Microbiol. 72 (2006) 6111.

[18] McDonnell G.; Russell A. D.,. Clin. Microbiol. Rev. 12 (1999) 147.

[19] Evans P.; Sheel D. W., Surface & Coatings Technology 201 (2007) 9319.

[20] Matsunaga T.; Tomada R.; Nakajima T.; Wake H., FEMS Microbiol. Lett. 29 (1985) 211.

[21] Zheng H .; Pin-Ching M.; Blake D. M.; Wolfrum J.; Edward J.; J. Photochem. Photobiol. A: Chem. 130 (2000) 163.

[22] Blake D. M.; Pin-Ching M.; Zheng H.; Jacoby E. J.; Wolfrum J.; Huang J., Sep. Purif. Methods 28 (1999) 1.

[23] Jimmyc Y.; Wingkeiho J.; Hoyinyip; Pokeungwong; Jincaizhao, Environ. Sci. Technol. 39 (2005) 1175.

[24] Suja Devipriya " Semiconductor oxide mediated photocatalytic removal of chemical and bacterial pollutants from wastewater" Ph.D thesis (2006).

[25] Yang Y. S.; Wang G.; Shen Y. H., Microbial Physiology, Chemical Industry (2007) 10.

[26] Shan Q.; Shanwen X.; Fang M.; Jixian Y., Powder Technology (2011) doi:10.1016/j.powtec.2010.12.032.

[27] Xuefeng J.; Lu Y.; Peng L.; Xi L.; Jian S., Colloids and Surfaces B: Biointerfaces 79 (2010) 69.

[28] Fu G. F.; Vary P. S.; Lin C. T., J. Phys. Chem. B 109 (2005) 8889.

[29] Sunada K.; Kikuchi Y.; Hashimoto K.; Fujishima A., Environ. Sci. Technol. 32 (1998) 726.

[30] Richard P. H. H.; Anton I. P. M. K.; Ben Biochim K., Biophys. Acta. 1469 (2000) 43.

[31] Deyong W.; Mingce L.; Jiangya Z.; Weimin C.; Xiehao Z.; Chao C.; Yahui W., Surface & Coatings Technology 203 (2009) 3728.

[32] Hoffmann M. R.; Martin S. T.; Choi W.; Bahnemannt D. W., Chem. Rev. 95 (1995) 69.

[33] Choi W., Catal. Surv. Asia 10 (2006) 16.

[34] Yang L.; Jin L.; Xiaofeng Q.; Clemens B., J. Photochem. Photobiol. A: Chem. 190 (2007) 94.

[35] Sunada K.; Watanabe T.; Hashimoto K., J. Photochem. Photobiol. A: Chem.156 (2003) 227.

[36] Watts R. J.; Kong S.; Orr M. P.; Miller G.C.; Henry B.E., Wat. Res. 29 (1995) 95.

[37] Cho M.; Chung H.; Choi W.; Yoon J., Appl. Environ. Microbiol. 71 (2005) 270.

[38] Gogniat G.; Thyssen M.; Denis M.; Pulgarin C.; Dukan S., FEMS Microbiol. Lett. 258 (2006) 18.

[39] Weng Y.; Wang Y.; Asbury J. B.; Ghosh H. N.; Lian T., J. Phys. Chem. B 104 (2000) 93.

[40] Rincon A. G.; Pulgarin C., Appl. Catal. B: Environ. 49 (2004) 99.

[41] Nadtochenko V.; Denisov N.; Sarkisov O.; Gumy D.; Pulgarin C.; Kiwi J., J. Photochem. Photobiol. A: Chem. 181 (2006) 401.

[42] Chia-Liang C.; Der-Shan S.; Wen-Chen C.; Yao-Hsuan T.; Han-Chen H.; Jia-Bin W.; Pei-Hua C.; Jiann-Hwa C.; Pei-Jane T.; Nien-Tsung L.; Mei-Shiuan Y.; Hsin-Hou C., J. Biomed. Sci. 16:7 (2009).

[43] Maness, P. C.; Smolinski S.; Blake D. M.; Huang Z.; Wolfrum E. J.:Jacoby W. A.,. Appl. Environ. Microbiol. 65 (1999) 4094.

…..ஜ۞ஜ…..

Chapter 8

Summary and Conclusions

Contents

8.1 Summary

Catalysis is a phenomenon which enhances the rate of reaction by a substance without itself undergoing any change after the completion of the reaction. The substance behind the process is called catalyst. Photocatalysis is the process in which the catalytic reaction is activated by absorption of light energy by the catalyst. Semiconductor materials become a very good photocatalyst based on its bandgap. Among the various semiconductor materials, titania becomes the prominent one. The high photocatalytic efficiency, eco friendliness, chemical inertness, low cost of preparation, thermal stability etc are the advantages of titania compared to others. In photocatalytic process, titania catalyst absorb light energy and create photo excited species such as holes and electrons in valence band and conduction band respectively. These photo excited species are very good oxidants and reductants (i.e., act as redox system) and also they create more powerful oxidant and reductant by reaction with adsorbed water, hydroxyl and oxygen species, which help for the degradation of adsorbed species on their surfaces.

Band gap, surface area, crystallite size, morphology, phase purity, method of preparation etc are other of the factors which affect the activity of photocatalyst. Titania exists mainly in three crystallite phases such as anatase, rutile and brookite. Among which anatase phase exhibits better photocatalytic activity than others with band gap of 3.2 eV. Even though titania is a very good photocatalyst, its activity is limited to UV irradiation based on its band gap. In order to bring its activity in visible region, we modify the titania by doping non-metals such as nitrogen and co-doping with nitrogen and sulphur. The prepared catalysts are characterized by various techniques such as XRD, UV-Visible DRS, Surface area, SEM, TEM, XPS, Raman and TG analysis and the results are correlated to their activities.

One of the major applications of this technology is the degradation of organic pollutants in water and air streams which is considered as one of the so-called advance oxidation processes (AOP). In AOP methods the driving material for the degradation of pollutants is the powerful oxidizing agent such as hydroxyl radical obtained by the oxidation of photo excited holes with adsorbed water or surface hydroxyl groups on titania materials. This research work includes degradation of some selected dyes such as crystal violet, rhodamine B, methylene blue and acid red1 and pesticides such 2,4-D, 2,4,5-T, aldicarb and monolinuron etc in aqueous media which produces harmful effects on aquatic life. The research also contributes the antibacterial study of E-coli and the generation of hydrogen through photocatalytic splitting of water.

8.2 Conclusions

Chapter 1 This chapter contains a general introduction about photocatalysis by semiconductors. This includes a brief history of catalysis, photocatalysis, and the mechanism behind the photocatalysis. It also explains the importance of titania as photocatalyst with its structure, different methods of preparation, advantages, drawback etc. The advantages and limitations of sol-gel method are described briefly. The necessity for modification and different methods available for the modification with its merits and demerits are also highlighted. An outline of present research work was also incorporated.

Chapter 2 This chapter contains a detailed description about the experimental conditions, chemicals and technologies used for the preparation of catalysts with its notation using sol-gel method. We also discussed the theory and experimental basis behind various techniques adopted for the characterisation of prepared catalysts such as XRD, UV-Visible DRS, SEM-EDX, TEM, XPS, Elemental analysis,

Raman spectra, TG etc. The instrument with its specification and the experimental set up for the measure of photocatalytic activity are well discussed.

Chapter 3 We have successfully synthesized pure titania, nitrogen doped titania and nitrogen, sulphur co-doped titania through sol-gel methods using titanium tetraisopropoxide, urea and thiourea as the main chemicals. The phase purity and the crystalline nature of the prepared catalysts are obtained from XRD analysis. All the prepared catalysts give purely anatase phase. It is also confirmed by HRTEM, SAED and Raman analysis. The crystallite size calculated using Scherrer equation from the XRD data. It gives very good correlation of particle size obtained from TEM. Particle size histogram showed that they are in nano scale with average size of 8-13 nm. The band gap reductions of the modified catalysts are calculated from UV-Vis.DRS spectrum. The visible light absorption of the modified catalysts is correlated to their bandgap. The presence of dopant impurities such as nitrogen and sulphur are qualitatively confirmed from the C, H, N, S elemental analysis and EDX analysis. The physical colour change of the modified catalyst also reinforces the presence of the dopant impurities in the modified catalysts. The chemical composition and oxidation states of elements are obtained from XPS analysis. Surface area is measured using BET method. The surface morphologies of the catalysts are obtained from SEM and TEM images, which show spherical and rectangular particles. HRTEM and SAED images showed particles to be crystalline and highly ordered in nature. Finally the thermal stability of the samples are confirmed from the TG analysis and the calcination temperature of catalysts are fixed to 400 ^{0}C.

Chapter 4 This chapter is mainly discussing the photocatalytic degradation of dyes materials in aqueous solution using visible light irradiation. We have reported the efficiency of the modified catalyst with high percent photocatalytic degradation of dyes such as Crystal violet, Rhodamine B, Methylene blue and Acid red1. The optimum catalyst amount for this study is 3 g/L. The synergic effect of the dopants N and S confirms the better activity of NS-TiO_2 compared to others in visible light. Around 75% of dyes are degraded with visible light irradiation of one hour. The effect of catalyst amount, effect of time, effect light sources and effect of dopant concentration are successfully explained. Thus the application of modified titania photocatalyst proves better efficiency in the degradation of dyes using visible light irradiation which is correlated to its bandgap.

Chapter 5 In this chapter we are discussing the photocatalytic degradation of few organic pollutants (collectively called pesticides) in aqueous medium. Compounds such 2,4-dichlorophenoxyacetic acid, 2,4,5-trichlorophenoxyacetic acid, aldicarb and monolinuron are selected and their photocatalytic degradation using the modified and pure titania are studied well. More than 80% of all the pollutants are photo catalytically degraded using modified catalyst with a visible light irradiation with time less than one hour. Factors affecting photocatalytic degradation such as catalyst amount, irradiation time, light source, dopant concentration, lamp power and reusability of the catalysts are well studied and discussed successfully. The photocatalytic activity of the catalyst also tested for reusability. The high correlation between the activity and lamp power also observed. The phase purity, smaller particle size, high surface area etc contribute to higher activity.

Chapter 6 In this chapter we discuss the brief history about the hydrogen production through photocatalytic water splitting reaction. This includes the different materials and technologies for the production of hydrogen, the general mechanism behind the photocatalytic water splitting reaction on semiconductor materials. The advantages of titania as photocatalyst with its drawbacks and modifications are also discussed. The results indicated that 0.1 g of NS-TiO_2 catalyst gives a good yield of hydrogen with visible light irradiation of 4 hours when compared with the same quantity and time of irradiation of others catalysts. The higher surface area, high purity anatase crystalline nature, small band gap etc. contributes the higher activity of the modified catalysts.

Chapter 7 One of the major advantageous of photo catalytic disinfection is that it completely ensures the deactivation of bacteria and inhibits its re-emergence. This has a crucial role in commercial application of disinfection process. Thus the application of photocatalytic process is an effective substitute for normal disinfection method to prevent the reappearance of bacteria in treated water. In this section we have successfully deactivated the Escherichia coli bacteria by irradiation of visible light using both N and N S co-doped titania. Increasing the photocatalyst concentration and time of irradiation provided more rapid deactivation and it is optimized with catalyst dosage of 5.0 mg

Disinfection by titania photocatalyst with its modified forms become a promising technology which has proven to be very effective for the treatment of a wide range of biological species in potable water. The technique can be used for the disinfection

of water and wastewater even in areas which lack electricity and other infrastructures. Concurrent removal of organic, inorganic and bacterial pollutants from water is an added advantage of titania photocatalysts. Its application is not limited its still on continue.

8.3 Future Outlook

- The present photocatalytic degradation studies are limited to few dyes, pesticides and bacteria species based on the duration of course. A lot of systems are still pending to be evaluated.
- Moreover this study is limited only to the percent degradation; their mechanical pathway for the degradation and existence of any intermediate products is still not understood.
- This study is limited to doping with nonmetals. Nowadays the co-doping with metal and non-metal, multi elemental doping are the hot topics.
- This study is limited to sol-gel method for the preparation of catalysts. Other methods are still opens for comparison of the activity of catalysts.
- This thesis discusses the photocatalytic applications of powdered catalyst which lacks a complete recovery of catalyst after its application. Thus new technologies are needed for complete recovery of the catalyst without any loss of activity.
- Thoroughly detailed mechanisms behind the photocatalytic application with pure and modified catalyst are still a debate among the researchers.

…..ꕥ…..